



ARIZONA DEPARTMENT OF TRANSPORTATION

REPORT NUMBER: FHWA-AZ91-264-I

# EVALUATION OF CONCRETE PAVEMENTS IN THE PHOENIX URBAN CORRIDOR

**Volume I  
Final Report**

**Prepared by:**

K.D. Smith  
D.G. Peshkin  
A.L. Mueller  
E. Owusu-Antwi  
M.I. Darter  
ERES Consultants, Inc.  
8 Dunlap Court  
Savoy, Illinois 61874

**September 1991**

**Prepared for:**

Arizona Department of Transportation  
206 South 17th Avenue  
Phoenix, Arizona 85007  
in cooperation with  
U.S. Department of Transportation  
Federal Highway Administration

## Technical Report Documentation Page

<b>1. Report No.</b> FHWA-AZ91-264-I	<b>2. Government Accession No.</b>	<b>3. Recipient's Catalog No.</b>	
<b>4. Title and Subtitle</b> EVALUATION OF CONCRETE PAVEMENTS IN THE PHOENIX URBAN CORRIDOR Volume I - Final Report	<b>5. Report Date</b> September 1991		<b>6. Performing Organization Code</b>
	<b>7. Author(s)</b> K. D. Smith, D. G. Peshkin, A. L. Mueller, E. Owusu-Antwi, M. I. Darter		
<b>9. Performing Organization Name and Address</b> ERES Consultants, Inc. 8 Dunlap Court Savoy, Illinois 61874-9501	<b>8. Performing Organization Report No.</b>		
	<b>10. Work Unit No.</b>		
<b>12. Sponsoring Agency Name and Address</b> ARIZONA DEPARTMENT OF TRANSPORTATION 206 S. 17TH AVENUE PHOENIX, ARIZONA 85007	<b>11. Contact or Grant No.</b> HPR-PL-1(31)264		
	<b>13. Type of Report &amp; Period Covered</b> Final Report 3/88 - 9/91		
<b>14. Sponsoring Agency Code</b>			
<b>15. Supplementary Notes</b> <p style="text-align: center;">                     ADOT Contract Manager: Larry Scofield                      Prepared in cooperation with the U.S. Department of Transportation, Federal Highway Administration                 </p>			
<b>16. Abstract</b>  <p>                     Arizona has been building portland cement concrete (PCC) pavements since the 1950's and now has approximately 400 lane miles of PCC pavements. Overall, these pavements have performed exceptionally well and have carried large traffic volumes. However, these pavements have experienced a range of distresses, including faulting, cracking, spalling, and, consequently, roughness. Since ADOT is considering the construction of approximately 230 lane miles of PCC in the next 20 years, a comprehensive evaluation of the 36 concrete pavements in the Phoenix Urban Corridor was conducted to identify the performance trends of the different designs and to aid in the recommendation of appropriate rehabilitation strategies. The field testing and evaluation consisted of condition surveys, drainage survey, nondestructive deflection testing, coring and subsurface boring investigations, a roughness survey, and Weigh-in-Motion (WIM) studies on selected sites.                 </p> <p>                     This volume summarizes the performance of the various concrete pavements in the Phoenix Urban Corridor. That performance data is then used in the evaluation of various concrete pavement design models to assess their applicability to Arizona conditions. Attempts at the development of new models from the performance data were not successful due to the limited number of sections and the large number of confounding factors. The performance data was also used in the development of design recommendations and in the determination of suggested rehabilitation activities for each section.                 </p> <p>                     This volume is the first in a series of two. Volume II contains appendices with the project summary tables, project strip maps, data base description, WIM data, rehabilitation selection guidelines, and an overview of rehabilitation methods.                 </p>			
<b>17. Key Words</b> concrete, concrete pavement, pavement performance, pavement evaluation, pavement design, pavement rehabilitation		<b>18. Distribution Statement</b> Document is available to the U.S. public through the National Technical Information Service, Springfield, Virginia 22161	
<b>19. Security Classification (of this report)</b> Unclassified		<b>20. Security Classification (of this page)</b> Unclassified	<b>21. No. of Pages</b> 176
<b>22. Price</b>		<b>23. Registrant's Seal</b>  	

# SI\* (MODERN METRIC) CONVERSION FACTORS

## APPROXIMATE CONVERSIONS TO SI UNITS

Symbol	When You Know	Multiply By	To Find	Symbol
--------	---------------	-------------	---------	--------

### LENGTH

in	inches	25.4	millimetres	mm
ft	feet	0.305	metres	m
yd	yards	0.914	metres	m
mi	miles	1.61	kilometres	km

### AREA

in <sup>2</sup>	square inches	645.2	millimetres squared	mm <sup>2</sup>
ft <sup>2</sup>	square feet	0.093	metres squared	m <sup>2</sup>
yd <sup>2</sup>	square yards	0.836	metres squared	m <sup>2</sup>
ac	acres	0.405	hectares	ha
mi <sup>2</sup>	square miles	2.59	kilometres squared	km <sup>2</sup>

### VOLUME

fl oz	fluid ounces	29.57	millilitres	mL
gal	gallons	3.785	litres	L
ft <sup>3</sup>	cubic feet	0.028	metres cubed	m <sup>3</sup>
yd <sup>3</sup>	cubic yards	0.765	metres cubed	m <sup>3</sup>

NOTE: Volumes greater than 1000 L shall be shown in m<sup>3</sup>.

### MASS

oz	ounces	28.35	grams	g
lb	pounds	0.454	kilograms	kg
T	short tons (2000 lb)	0.907	megagrams	Mg

### TEMPERATURE (exact)

°F	Fahrenheit temperature	$5(F-32)/9$	Celsius temperature	°C
----	------------------------	-------------	---------------------	----

## APPROXIMATE CONVERSIONS FROM SI UNITS

Symbol	When You Know	Multiply By	To Find	Symbol
--------	---------------	-------------	---------	--------

### LENGTH

mm	millimetres	0.039	inches	in
m	metres	3.28	feet	ft
m	metres	1.09	yards	yd
km	kilometres	0.621	miles	mi

### AREA

mm <sup>2</sup>	millimetres squared	0.0016	square inches	in <sup>2</sup>
m <sup>2</sup>	metres squared	10.764	square feet	ft <sup>2</sup>
ha	hectares	2.47	acres	ac
km <sup>2</sup>	kilometres squared	0.386	square miles	mi <sup>2</sup>

### VOLUME

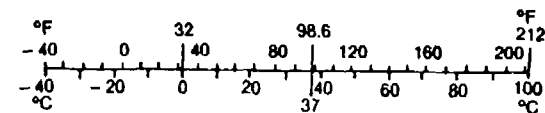
mL	millilitres	0.034	fluid ounces	fl oz
L	litres	0.264	gallons	gal
m <sup>3</sup>	metres cubed	35.315	cubic feet	ft <sup>3</sup>
m <sup>3</sup>	metres cubed	1.308	cubic yards	yd <sup>3</sup>

### MASS

g	grams	0.035	ounces	oz
kg	kilograms	2.205	pounds	lb
Mg	megagrams	1.102	short tons (2000 lb)	T

### TEMPERATURE (exact)

°C	Celsius temperature	$1.8C + 32$	Fahrenheit temperature	°F
----	---------------------	-------------	------------------------	----



\* SI is the symbol for the International System of Measurement

(Revised April 1989)

# TABLE OF CONTENTS

<b>CHAPTER 1 INTRODUCTION .....</b>	<b>1</b>
1. BACKGROUND AND PROBLEM STATEMENT .....	1
2. OBJECTIVES OF STUDY .....	1
3. STUDY APPROACH .....	2
4. SEQUENCE OF REPORT .....	2
 <b>CHAPTER 2 STUDY SECTIONS AND DATA COLLECTION .....</b>	 <b>4</b>
1. INTRODUCTION .....	4
2. CONCRETE PAVEMENT STUDY SECTIONS .....	4
3. DATA COLLECTION ACTIVITIES .....	15
4. DATA BASE DESCRIPTION .....	22
 <b>CHAPTER 3 PERFORMANCE EVALUATION OF SECTIONS .....</b>	 <b>25</b>
1. INTRODUCTION .....	25
2. PERFORMANCE EVALUATIONS .....	25
3. OVERALL PERFORMANCE SUMMARY OF DESIGN TYPES ..	38
4. PRELIMINARY EVALUATION .....	45
 <b>CHAPTER 4 EVALUATION OF CONCRETE PAVEMENT DESIGN AND ANALYSIS MODELS .....</b>	 <b>49</b>
1. INTRODUCTION .....	49
2. ANALYSIS MODELS .....	49
3. THE CMS PROGRAM .....	52
4. THE ILLI-SLAB PROGRAM .....	60
5. ANALYSIS OF PAVEMENT PREDICTION MODELS .....	75
6. MODEL DEVELOPMENT EFFORTS .....	105
7. SUMMARY .....	113

# TABLE OF CONTENTS

## (continued)

<b>CHAPTER 5 DESIGN STRATEGIES FOR PCC PAVEMENTS IN THE PHOENIX URBAN CORRIDOR .....</b>	<b>115</b>
1. INTRODUCTION .....	115
2. PERFORMANCE OF SELECTED DESIGN STRATEGIES .....	117
3. RECOMMENDED DESIGN STRATEGIES .....	119
4. ADDITIONAL DESIGN/ CONSTRUCTION CONSIDERATIONS .....	120
5. SUMMARY .....	132
<b>CHAPTER 6 RECOMMENDED REHABILITATION MEASURES FOR STUDY SECTIONS .....</b>	<b>133</b>
1. INTRODUCTION .....	133
2. S.R. 360 (SUPERSTITION FREEWAY) .....	133
3. INTERSTATE 10 .....	143
4. INTERSTATE 17 .....	149
5. SUMMARY .....	155
<b>CHAPTER 7 SUMMARY AND CONCLUSIONS ...</b>	<b>160</b>
<b>REFERENCES .....</b>	<b>163</b>

# LIST OF FIGURES

Figure 1.	Location of three primary highways comprising the Phoenix Urban Corridor .....	5
Figure 2.	Location of study sections on I-10 .....	8
Figure 3.	Location of study sections on I-17 .....	11
Figure 4.	Location of study sections on S.R. 360 .....	14
Figure 5.	Example strip map prepared for each section .....	18
Figure 6.	FWD testing pattern for study sections with tied PCC shoulders ..	21
Figure 7.	Pavement rideability and roughness measurements for I-10 .....	27
Figure 8.	Transverse joint spalling on I-10 .....	27
Figure 9.	Transverse joint faulting and joint spalling on I-17 .....	33
Figure 10.	Pavement rideability and roughness measurements for I-17 .....	33
Figure 11.	Transverse joint faulting on S.R. 360 .....	37
Figure 12.	Pavement rideability and roughness measurements for S.R. 360 ...	37
Figure 13.	Roughness history for I-10 sections .....	43
Figure 14.	Roughness history for I-17 sections .....	43
Figure 15.	Roughness history for S.R. 360 sections .....	44
Figure 16.	Roughness history by pavement design type .....	44
Figure 17.	Percent slab corners with voids as a function of loaded corner deflection .....	46
Figure 18.	Use of CMS in the design process .....	54
Figure 19.	Temperature profile for AZ 2 on July 15, 1987 .....	57
Figure 20.	Variation in 6 a.m. thermal gradient for AZ 2, January through June 1987 .....	58
Figure 21.	Variation in 6 a.m. thermal gradient for AZ 2, July through December 1987 .....	58
Figure 22.	Variation in 3 p.m. thermal gradient for AZ 2, January through June 1987 .....	59
Figure 23.	Variation in 3 p.m. thermal gradient for AZ 2, July through December 1987 .....	59
Figure 24.	Example finite element mesh for edge loading condition .....	63
Figure 25.	Variation in edge stress as a function of slab thickness and shoulder type .....	66
Figure 26.	Variation in stress ratio as a function of slab thickness and shoulder type .....	66
Figure 27.	Variation in edge stress as a function of PCC shoulder load transfer efficiency and slab thickness .....	67
Figure 28.	Variation in thermal edge stress as a function of $k$ -value and slab thickness .....	71
Figure 29.	Variation in thermal edge stress as a function of $t$ -value and joint spacing .....	71

# LIST OF FIGURES (continued)

Figure 30.	Thermal edge stress vs. $L/\ell$ (stabilized bases) . . . . .	74
Figure 31.	Thermal edge stress vs. $L/\ell$ (aggregate base/no base) . . . . .	74
Figure 32.	AASHTO predicted ESALs vs. actual ESALs for 17 sections in dry-nonfreeze region . . . . .	79
Figure 33.	PEARДАРP predicted PSI vs. actual PSR for 17 sections in dry-nonfreeze region . . . . .	79
Figure 34.	PEARДАРP predicted roughness vs. actual roughness for 17 sections in dry-nonfreeze region . . . . .	81
Figure 35.	PEARДАРP predicted spalling vs. actual spalling for 17 sections in dry-nonfreeze region . . . . .	81
Figure 36.	PEARДАРP predicted faulting vs. actual faulting for 17 sections in dry-nonfreeze region . . . . .	85
Figure 37.	PEARДАРP predicted cracking vs. actual cracking for 17 sections in dry-nonfreeze region . . . . .	85
Figure 38.	COPEs predicted pumping vs. actual pumping for 17 sections in dry-nonfreeze region . . . . .	88
Figure 39.	COPEs predicted faulting vs. actual faulting for 17 sections in dry-nonfreeze region . . . . .	88
Figure 40.	COPEs predicted joint deterioration vs. actual joint deterioration for 17 sections in dry-nonfreeze region . . . . .	90
Figure 41.	COPEs predicted cracking vs. actual cracking for 17 sections in dry-nonfreeze region . . . . .	90
Figure 42.	COPEs predicted PSR vs. actual PSR for 17 sections in dry-nonfreeze region . . . . .	92
Figure 43.	PFAULT predicted faulting vs. actual faulting for 17 sections in dry-nonfreeze region . . . . .	92
Figure 44.	Predicted PSR using new FHWA model vs. actual PSR for ADOT study sections . . . . .	97
Figure 45.	Predicted spalling using new FHWA model vs. actual spalling for ADOT study sections . . . . .	97
Figure 46.	Predicted faulting using new FHWA model vs. actual faulting for ADOT study sections . . . . .	104
Figure 47.	Predicted cracking using new FHWA model vs. actual cracking for ADOT study sections . . . . .	104
Figure 48.	Roughness regression equations for 360-04 and 360-09 . . . . .	110
Figure 49.	Roughness regression equation for 10-03 . . . . .	110
Figure 50.	Roughness regression equations for selected sections on I-17 . . . . .	112
Figure 51.	Effect of diamond grinding on 17-10 pavement roughness . . . . .	112

# LIST OF FIGURES

## (continued)

Figure 52.	Accumulated ESAL's by design group and slab thickness . . . . .	118
Figure 53.	Typical cross-section of JPCP on a stabilized base. . . . .	121
Figure 54.	Typical cross-section of full-depth JPCP on subgrade. . . . .	122
Figure 55.	Typical cross-section of CRCP on a base. . . . .	123
Figure 56.	Typical transverse joint details. . . . .	127

# LIST OF TABLES

Table 1.	Study sections on I-10 .....	7
Table 2.	Study sections on I-17 .....	10
Table 3.	Study sections on S.R. 360 .....	13
Table 4.	Overall design matrix of study sections .....	16
Table 5.	Drainage coefficients ( $C_d$ ) for study sections .....	19
Table 6.	Listing of major data items contained in the data base .....	23
Table 7.	Distress indicators for primary survey lane of I-10 sections .....	26
Table 8.	Average joint faulting between random-spaced slabs .....	28
Table 9.	Summary of results of field testing for I-10 sections .....	30
Table 10.	Distress indicators for primary survey lane of I-17 sections .....	31
Table 11.	Summary of results of field testing for I-17 sections .....	34
Table 12.	Summary of pavement designs on S.R. 360 .....	34
Table 13.	Distress indicators for primary survey lane of S.R. 360 sections ...	36
Table 14.	Summary of results of field testing for S.R. 360 sections .....	38
Table 15.	CMS inputs for use with concrete pavements .....	53
Table 16.	Summary of slab response to edge loading condition (14.4 kip dual wheel load with a tire pressure of 120 psi) .....	64
Table 17.	Summary of slab response to corner loading condition (14.4 kip dual wheel load with a tire pressure of 120 psi) .....	69
Table 18.	Summary of maximum thermal stresses for each section due to daytime thermal gradient of 3.22 °F .....	72
Table 19.	Summary of the statistical analysis of the selected prediction models using sections from the dry-nonfreeze climatic region (adapted from reference 12) .....	77
Table 20.	Predicted and actual PSR values for new FHWA PSR prediction model .....	96
Table 21.	Predicted and actual percent joint spalling for new FHWA spalling prediction model .....	99
Table 22.	Predicted and actual joint faulting for new FHWA faulting prediction model .....	103
Table 23.	Predicted and actual percent slab cracking for new FHWA slab cracking prediction model .....	106
Table 24.	Summary of project sections by design strategy .....	116
Table 25.	Additional design and construction considerations for the JPCP and CRCP design strategies .....	120
Table 26.	Recommended gradations for permeable bases <sup>(39)</sup> .....	125

# LIST OF TABLES

## (continued)

Table 27.	Summary of recommended rehabilitation actions for pavement sections on S.R. 360 . . . . .	156
Table 28.	Summary of recommended rehabilitation actions for pavement sections on I-10 . . . . .	157
Table 29.	Summary of recommended rehabilitation actions for pavement sections on I-17 . . . . .	158

# CHAPTER 1 INTRODUCTION

## 1. BACKGROUND AND PROBLEM STATEMENT

Arizona has been building portland cement concrete (PCC) pavements since the 1950's and now has approximately 400 lane miles of PCC pavements. Overall, these pavements have performed exceptionally well and have carried large traffic volumes. However, these pavements have experienced a range of distresses, including faulting, cracking, spalling, and, consequently, roughness. In an effort to address these distresses, a variety of different pavement designs have been constructed in the Phoenix area freeway system over the last 30 years.

The design of the 1960's was a 9 in nondoweled jointed plain concrete pavement (JPCP) constructed over an aggregate base. However, this design was susceptible to joint faulting, the occurrence of which was the driving force behind the construction of a number of different experimental designs built on State Route 360, the Superstition Freeway, in the 1970's.<sup>(1)</sup> These experimental pavements included a nondoweled JPCP on a cement-treated base (CTB), a nondoweled JPCP on a lean concrete base (LCB), a continuously reinforced concrete pavement (CRCP) constructed as an inner lane, a 6 in prestressed concrete pavement on a 4 in CTB, a nondoweled JPCP on an LCB, and thick, nondoweled JPCP slabs (11 in and 13 in) placed directly on subgrade.<sup>(1,2,3)</sup> In the mid-1980's, the new standard concrete pavement design adopted by ADOT was a doweled JPCP with skewed joints constructed over an LCB.

Each design strategy has unique features which incur an associated performance level and cost. For example, there is a significant difference between the initial construction costs of a nondoweled JPCP placed on subgrade and a doweled JPCP placed on an LCB. There are also differences in the cost of maintaining each strategy. And, perhaps most importantly, there are differences in pavement performance for each design strategy and therefore pavement life.

In the next 20 years, ADOT plans to build approximately 230 lane miles of new PCCP in the Phoenix urban area. In order to select both optimum design strategies for the new concrete construction and optimum rehabilitation methods for existing concrete pavements, ADOT desires an evaluation of their various concrete pavement designs and rehabilitation methods.

## 2. OBJECTIVES OF STUDY

The objectives of the study may be summarized as follows:

- To document the performance of Arizona's existing portland cement concrete pavements and to recommend a course of action for the Arizona Department of Transportation to consider for future designs and rehabilitation of the urban corridor freeway system.
- To review various pavement management systems and to recommend one which is appropriate to Arizona's concrete pavement network.

This report and the accompanying appendix specifically address the first objective. The second objective has been addressed in a separate report entitled *A Pavement Management System for the Concrete Pavements in the Phoenix Urban Corridor*.

### **3. STUDY APPROACH**

In order to determine which strategy is most effective for new construction on the Phoenix-area freeway system, the differences in the performance of the existing strategies was analyzed. This was accomplished first through an evaluation of the performance of existing pavements in Arizona, followed by an analytical and life-cycle cost analysis of those pavements and other designs.

In conjunction with the evaluation of the designs, an analysis was made of various concrete rehabilitation techniques to determine which are most effective for the existing distresses and types of pavements. Not only must the rehabilitation of the existing PCCP be considered, but the future rehabilitation of the newly-constructed designs must be considered as well.

From these analyses, a comprehensive master plan can be developed for the urban freeway system that addresses not only future concrete pavement designs, but also recommended rehabilitation measures for the existing system.

### **4. SEQUENCE OF REPORT**

Chapter 2 of this report provides background information (design and construction) on the sections included in the study. It also briefly describes the field testing procedures and the data base established for the study. Chapter 3 provides a performance evaluation of each section and identifies performance trends and possible causes of distress. Chapter 4 presents an evaluation of various models for their applicability to concrete pavements in the Phoenix Urban Corridor (PUC). Based upon the findings of chapters 3 and 4, chapter 5 provides the recommended design strategies and for the Phoenix Urban Corridor. Chapter 6 provides recommended rehabilitation strategies for each section included in the study. Finally, chapter 7 provides overall summary and conclusions for the project.

Under separate cover, several appendices are included with the report as supporting documentation. Appendix A provides summary tables that contain all of the design, construction, and performance data for each section. Appendix B contains detailed strip maps that were prepared directly from the field surveys. Appendix C contains a more detailed description of the project data base. Appendix D provides a summary of the data collected from the Weigh-in-Motion (WIM) studies performed on selected sections. Appendix E provides rehabilitation strategy selection guidelines, while appendix F gives a summary of concrete rehabilitation methods and their applicability to Arizona conditions.

# CHAPTER 2 STUDY SECTIONS AND DATA COLLECTION

## 1. INTRODUCTION

In order to complete the objectives of the contract listed in chapter 1, an intensive office and field data collection effort was undertaken. This process involved the identification of candidate sections, the selection of specific sections for evaluation, extensive field testing, interviews with knowledgeable ADOT personnel, and data storage and data analysis procedures.

This chapter describes the sections that were included in the study and provides background information on the data collection work that was done. Information is also provided on the data base that was established for the study.

## 2. CONCRETE PAVEMENT STUDY SECTIONS

ADOT has constructed a myriad of concrete pavement designs in the Phoenix Urban Corridor. In selecting sections for inclusion in this study, at least one of each of the various types of designs that had been constructed was included. However, where possible, two or more of each design were preferred since this would provide a stronger statistical basis from which to draw conclusions.

At about the same time that this study was being initiated, the research team was conducting a similar study evaluating the performance of concrete pavements nationwide for the Federal Highway Administration (FHWA). That study included 7 sections from the Phoenix Urban Corridor that were ultimately included into the ADOT study. Details of that study, including results of the analysis of the Arizona sections, are provided in references 4, 5, and 6.

All told, a total of 35 concrete pavement sections were selected for evaluation (including the 7 from the FHWA study). These sections were located on the three primary freeways of Phoenix: Interstate 10, Interstate 17, and State Route 360—Superstition Freeway (see figure 1). These sections represent every concrete pavement construction that ADOT has undertaken in the Phoenix Urban Corridor (PUC) from 1961 to the early 1980's. Selection of these specific sections was based on traffic considerations, their rehabilitation history, and their overall ability to contribute to the objectives of the project. The selected sections for this study were given a numerical designation indicating the highway and a sequential identifier, whereas those sections from the FHWA study simply used a "AZ" prefix in front of the sequential identifier. A brief summary of the pavement sections follows.

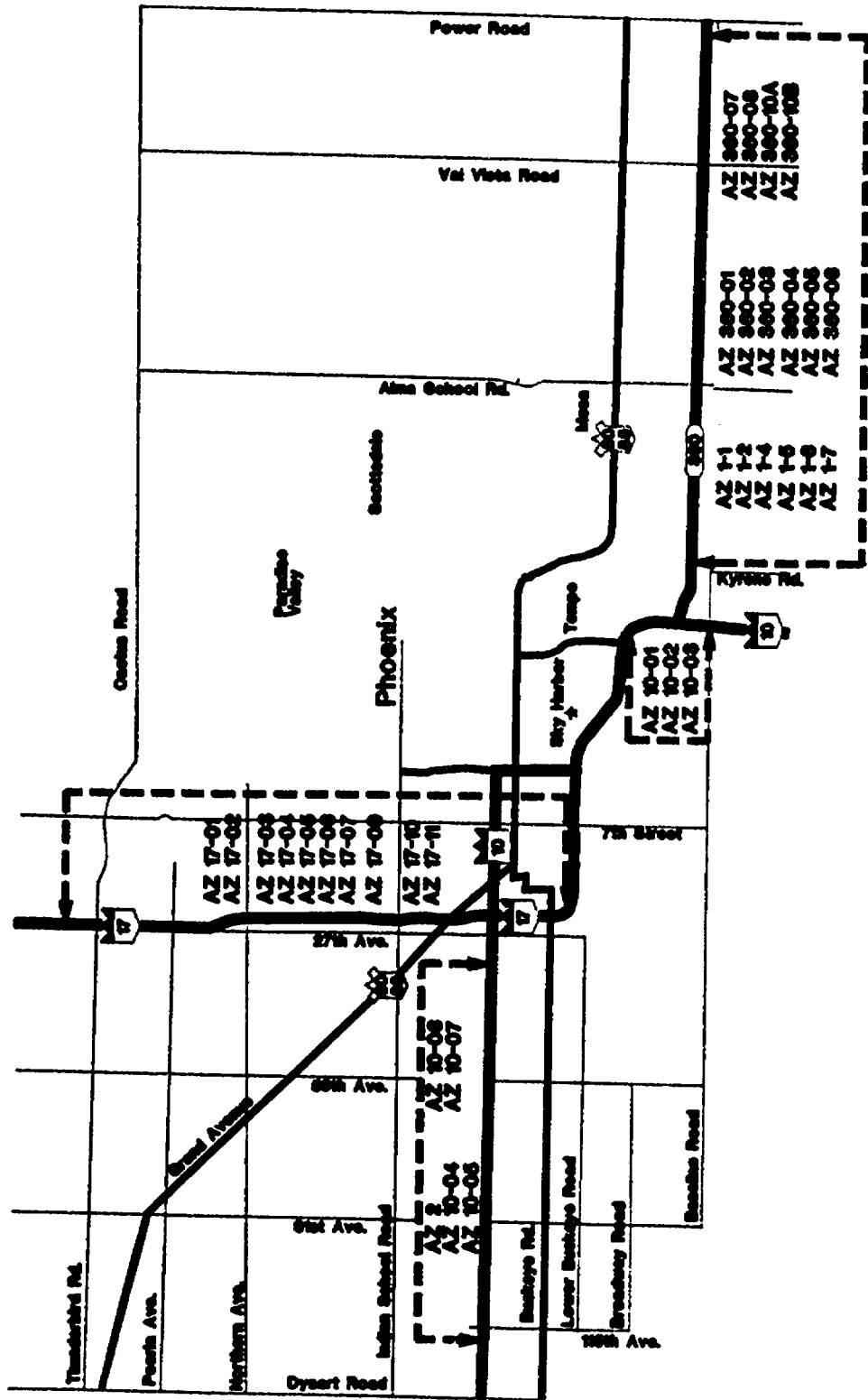


Figure 1. Location of the three primary highways comprising the Phoenix Urban Corridor.

## **Interstate 10**

Interstate 10 is the primary east-west route that runs through Phoenix. A total of eight jointed plain concrete pavement (JPCP) sections were evaluated on I-10. Three of the eight sections were constructed in 1968 and the rest were constructed between 1984 and 1986. Table 1 lists the sections included from I-10, along with relevant design features, and figure 2 indicates the location of each section within Phoenix.

The older sections on I-10, which were constructed in 1968, are 9 in JPCP slabs constructed on a dense-graded aggregate base. Transverse joints are skewed, nondoweled, and placed at a spacing of 13-15-17-15 ft. These sections represented the first use of random joint spacing on Phoenix's interstate system.

The newer sections on I-10, all built after 1984, represent Arizona's current concrete pavement design. They consist of 10 in JPCP slabs constructed on a lean concrete base, a skewed, random joint spacing of 13-15-17-15 ft, and 1.25 in diameter dowel bars placed on 12-in centers at the transverse joints.

Traffic volumes on these sections vary considerably over their length. Sections 10-01 through 10-03 have a two-way average daily traffic (ADT) of approximately 125,000 to 150,000 vehicles per day (vpd), including 9.7 percent trucks. Sections 10-4 through 10-7 and AZ 2 have two-way ADT's of between 30,000 and 50,000 vpd, with truck volumes ranging from 3 to 9 percent of the ADT.

## **Interstate 17**

Interstate 17 is the major north-south route that serves the Phoenix urban area. It is the oldest of Phoenix's concrete urban corridor network, having been constructed in the early 1960's. Table 2 provides a listing of the sections from I-17 that were included in the study, along with pertinent design feature information. Figure 3 illustrates the location of the study sections within the city of Phoenix.

The design of each of the I-17 sections all consist of 9 in JPCP slabs on an aggregate base, 15-ft joint spacing (either perpendicular or skewed), and no dowels. While the transverse joints were generally created by sawing, it should be noted that every fourth joint was formed using a metal insert during initial construction. As will be discussed, this resulted in severe spalling problems at those joints.

Sections 17-07 and 17-09, located on the Durango Curve, were overlaid in 1979 with an asphalt rubber membrane called a 3-layer system. The 3-layer system was placed to restore rideability to the pavement sections. These sections were included as part of this study because ADOT was interested in an evaluation of the performance of the 3-layer system.

Table 1. Study sections on I-10.

SECTION ID	LOCATION	YEAR BUILT	SLAB THICK, in	BASE TYPE	JOINT SPACE, ft	DOWELS
AZ 10-01	Broadway - Superstition MP 154.05 - 154.25 EB	1968	9	AGG	13-15-17-15	No
AZ 10-02	Broadway - Superstition MP 154.40 - 154.60 EB	1968	9	AGG	13-15-17-15	No
AZ 10-03	Broadway - Superstition MP 153.87 - 153.67 WB	1968	9	AGG	13-15-17-15	No
AZ 10-04	43 <sup>rd</sup> - 51 <sup>st</sup> Avenue MP 140.67-140.47 WB	1986	10	LCB	13-15-17-15	Yes
AZ 10-05	67 <sup>th</sup> - 75 <sup>th</sup> Avenue MP 136.68 - 136.88 EB	1985	10	LCB	13-15-17-15	Yes
AZ 10-06	115 <sup>th</sup> Avenue - Agua Fria MP 130.88 - 130.68 WB	1984	10	LCB	13-15-17-15	Yes
AZ 10-07	Agua Fria - Dysart MP 130.50 - 130.30 WB	1984	10	LCB	13-15-17-15	Yes
AZ 2	East of 35 <sup>th</sup> Avenue MP 141.19 - 141.39 EB	1985	10	LCB	13-15-17-15	Yes

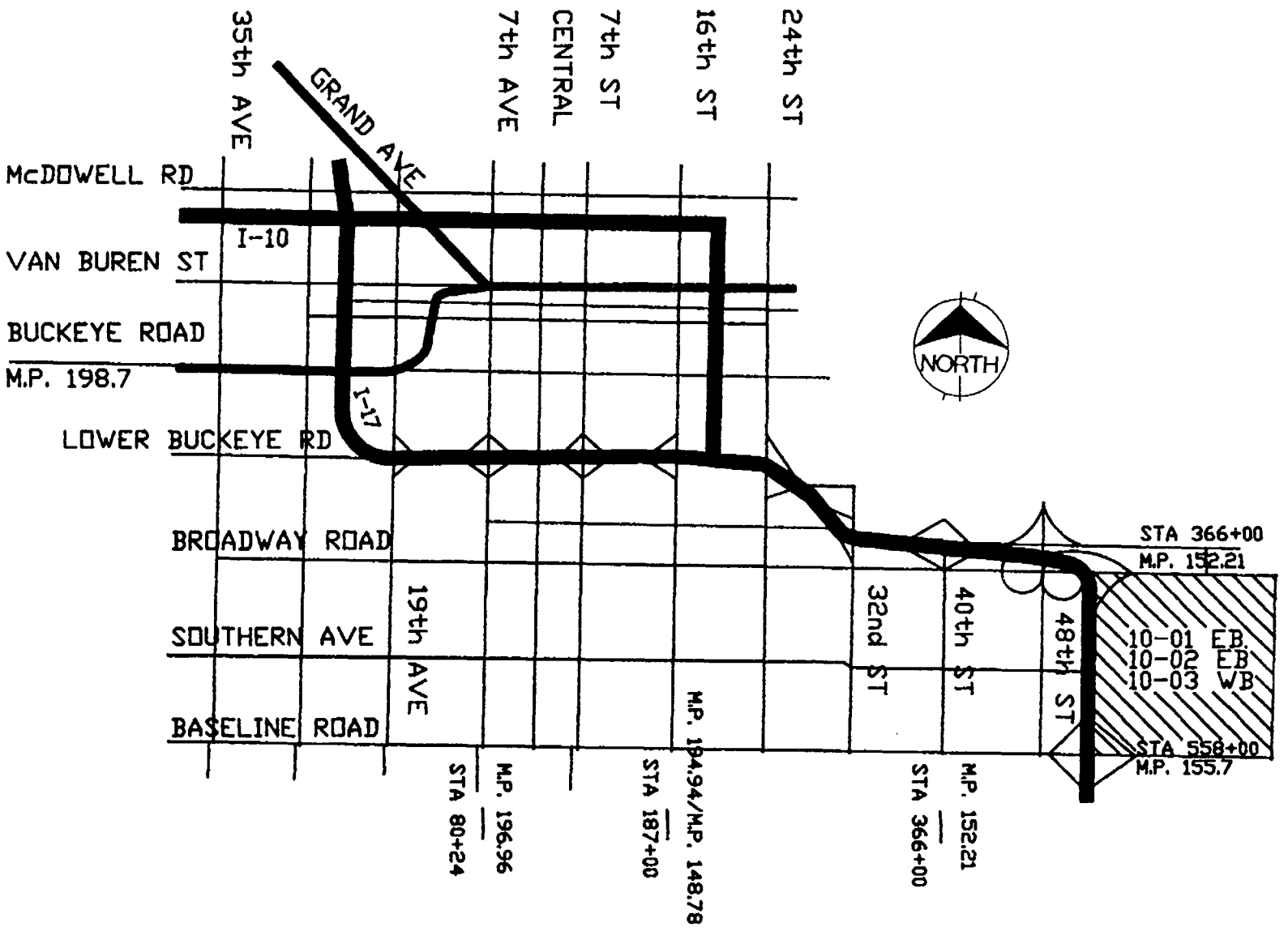


Figure 2. Location of study sections on I-10.

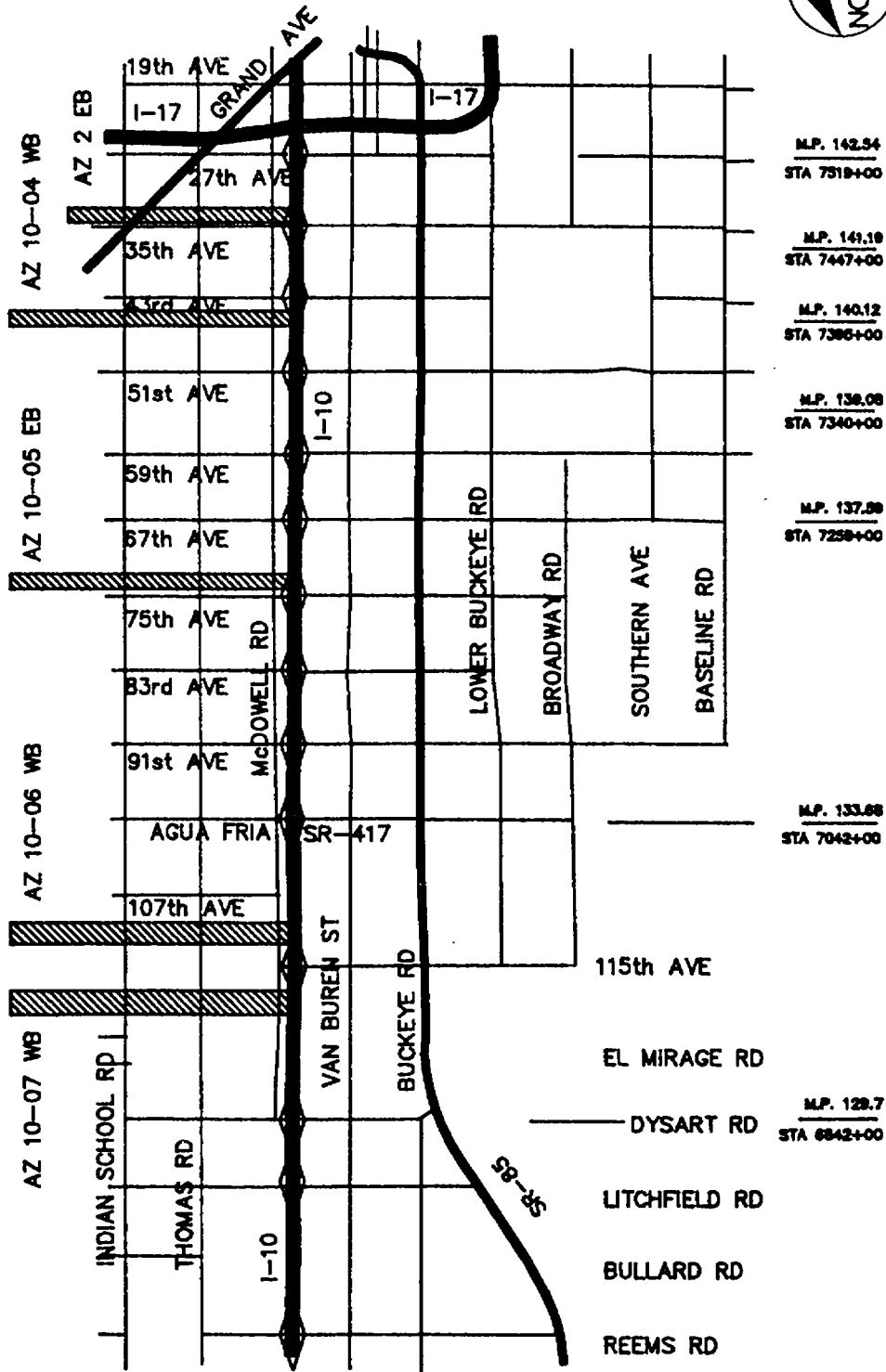


Figure 2. Location of study sections on I-10 (continued).

Table 2. Study sections on I-17.

SECTION ID	LOCATION	YEAR BUILT	SLAB THICK, in	BASE TYPE	JOINT SPACE, ft	DOWELS
AZ 17-01	Camelback - Indian School MP 203.50 - 203.30 SB	1961	9	AGG	15	No
AZ 17-02	Thomas - Indian School MP 202.30 - 202.50 NB	1961	9	AGG	15	No
AZ 17-03	Greenway - Thunderbird MP 211.89 - 211.69 SB	1965	9	AGG	15	No
AZ 17-04	Dunlap - Northern MP 208.20 - 208.00 SB	1965	9	AGG	15	No
AZ 17-05	Greenway - Thunderbird MP 211.40 - 211.60 NB	1965	9	AGG	15	No
AZ 17-06	Buckeye - Grant MP 198.70 - 198.90 NB	1963	9	AGG	15	No
AZ 17-07 <sup>1</sup>	19 <sup>th</sup> - Grant (Durango Curve) MP 198.10 - 197.90 SB	1979 1963	1.2 AC 9 PCC	AGG	--- (15)	No
AZ 17-09 <sup>1</sup>	19 <sup>th</sup> - Grant (Durango Curve) MP 197.80 - 197.60 SB	1979 1963	1.2 AC 9 PCC	AGG	--- (15)	No
AZ 17-10	Bethany Home - Glendale MP 205.20 - 205.35 NB	1961	9	AGG	15	No
AZ 17-11	Peoria - Cactus MP 208.70 - 208.90 NB	1965	9	AGG	15	No

<sup>1</sup> These sections were overlaid in 1979 with a 3-layer asphalt rubber overlay.

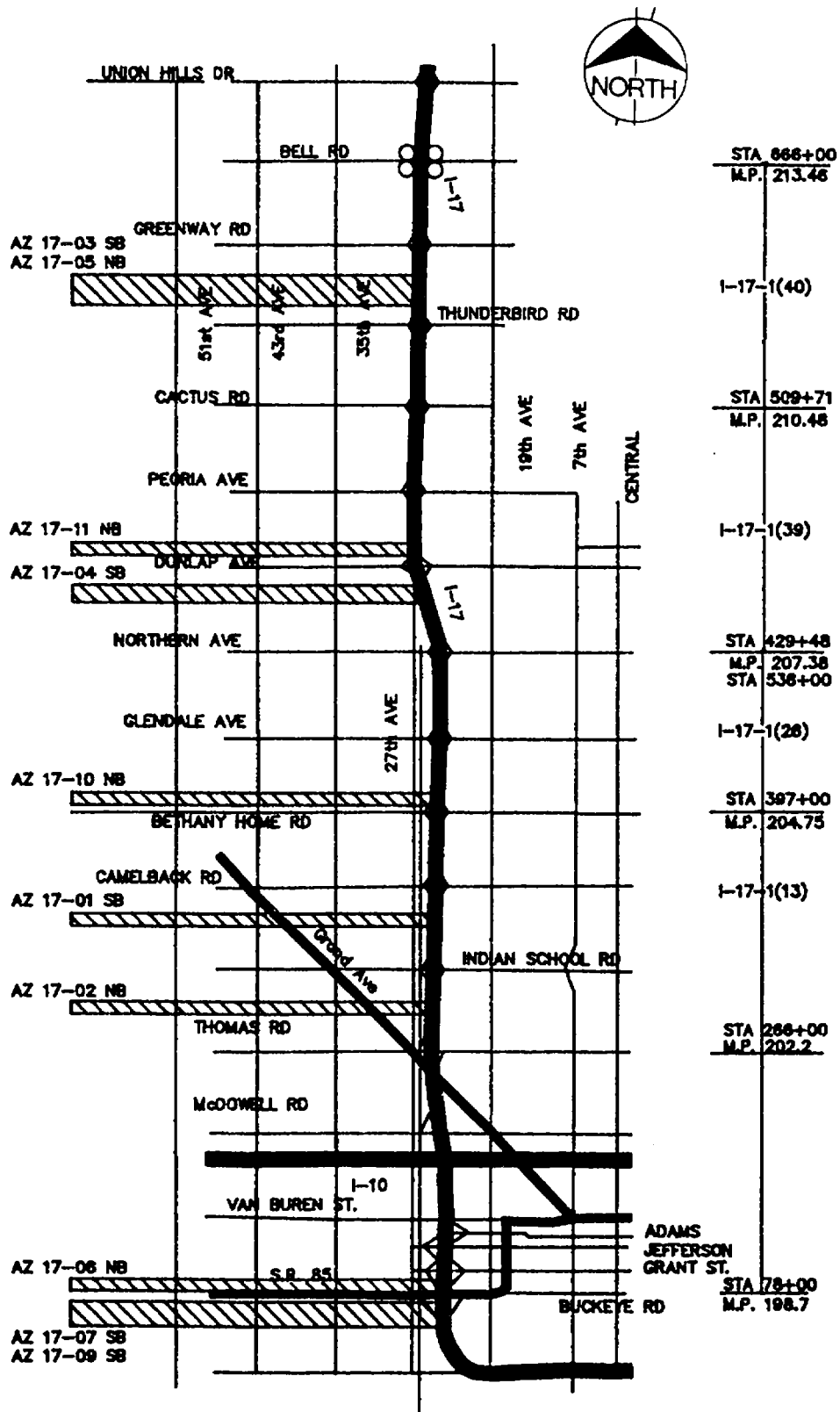


Figure 3. Location of study sections on I-17.

Traffic volumes on I-17 are extremely high. All of the sections are subjected to a two-way ADT of 110,000 to 135,000 vpd, including about 9.5 percent trucks.

### **S.R. 360 (Superstition Freeway)**

State Route 360, the Superstition Freeway, begins at Interstate 10 and extends to the east of Phoenix. The Superstition Freeway contains many different concrete pavement designs, the construction of which was an attempt by ADOT to evaluate the relative performance of the various design strategies. The first section of the Superstition Freeway was built in 1972 and construction still continues today as it stretches eastward to ultimately connect with U.S. 60.

Seventeen sections, listed in table 3, were included in the study from S.R. 360. This table indicates the varying pavement designs that were constructed on this freeway. The location of each of these sections is shown in figure 4.

It is interesting to trace the evolution of the various designs that were constructed on the Superstition Freeway. The first design, section AZ 1-1, was constructed in 1972 and consisted of a nondoweled 9-in JPCP slab on a cement-treated base with 13-15-17-15 ft random joint spacing. This design was followed with the construction of a nondoweled 13-in JPCP slab-on-grade design in 1975 (sections AZ 1-2 and AZ 360-09).

In 1977, ADOT constructed one of the few prestressed concrete pavements in the country. This was a 6 in prestressed slab over a lean concrete base. Gap slabs (areas originally left open to allow for the prestressing operations) were spaced at 200 to 500 ft intervals. The prestressed design is represented in this study as sections 360-05, 360-06, 360-10a, and 360-10b.

Concrete pavements in 1979 returned to the slab-on-grade design. A 13-in JPCP (section AZ 1-4) was constructed along with an 11-in JPCP (AZ 360-04 and AZ 1-5). Each of these designs employed skewed joints, randomly spaced at 13-15-17-15 ft intervals.

In 1981, the precursor to Arizona's current concrete pavement design was constructed. This design consisted of a 9 in concrete slab over a lean concrete base, skewed, random joints at 13-15-17-15 ft intervals, and no dowel bars (sections AZ 1-6 and AZ 1-7). This design was also used for sections constructed in 1983 (section 360-03) and in 1985 (sections 360-01 and 360-02).

In 1984, Arizona experimented with continuously reinforced concrete pavements (CRCP). These were 9 in concrete slabs placed over an aggregate base and were constructed as the innermost lanes of the widening of the existing two-lane prestressed pavement section (sections 360-07 and 360-08).

Table 3. Study sections on S.R. 360.

SECTION ID	LOCATION	YEAR BUILT	SLAB THICK, in	BASE TYPE	JOINT SPACE, ft	DOWELS
AZ 360-01	Higley - Power MP 15.54 - 15.74 EB	1985	9	LCB	13-15-17-15	No
AZ 360-02	Higley - Greenfield MP 13.50 - 13.70 EB	1985	9	LCB	13-15-17-15	No
AZ 360-03	Lindsay - Valvista MP 11.82 - 12.02 EB	1983	9	LCB	13-15-17-15	No
AZ 360-04	Alma School - Dobson MP 6.47 - 6.31 WB	1979	11	None	13-15-17-15	No
AZ 360-05	Price - Dobson MP 4.24 - 4.47 EB	1977	6	LCB	402 (prestress)	No
AZ 360-06	Price - Dobson MP 4.58 - 4.81 EB	1977	6	LCB	402 (prestress)	No
AZ 360-07	Price - Dobson MP 4.20 - 4.44 EB	1984	9	AGG	--- (CRCP)	No
AZ 360-08	Price - Dobson MP 4.74 - 5.01 EB	1984	9	AGG	--- (CRCP)	No
AZ 360-09	McClintock - Price MP 3.60 - 3.43 WB	1975	13	None	13-15-17-15	No
AZ 360-10a	Price - Dobson MP 5.01 - 5.05 EB	1977	6	LCB	207 (prestress)	No
AZ 360-10b	Price - Dobson MP 5.07 - 5.25 EB	1977	6	LCB	502 (prestress)	No
AZ 1-1	Mill Avenue - 1-10 MP 1.19 - 0.99 WB	1972	9	CTB	13-15-17-15	No
AZ 1-2	McClintock - Rural MP 4.34 - 4.14 WB	1975	13	None	13-15-17-15	No
AZ 1-4	Arizona - Alma School MP 7.42 - 7.22 WB	1979	13	None	13-15-17-15	No
AZ 1-5	Alma School - Dobson MP 6.50 - 6.30 WB	1979	11	None	13-15-17-15	No
AZ 1-6	Stapley - Arizona MP 9.40 - 9.20 WB	1981	9	LCB	13-15-17-15	No
AZ 1-7	Gilbert - Stapley MP 10.38 - 10.18 WB	1981	9	LCB	13-15-17-15	No

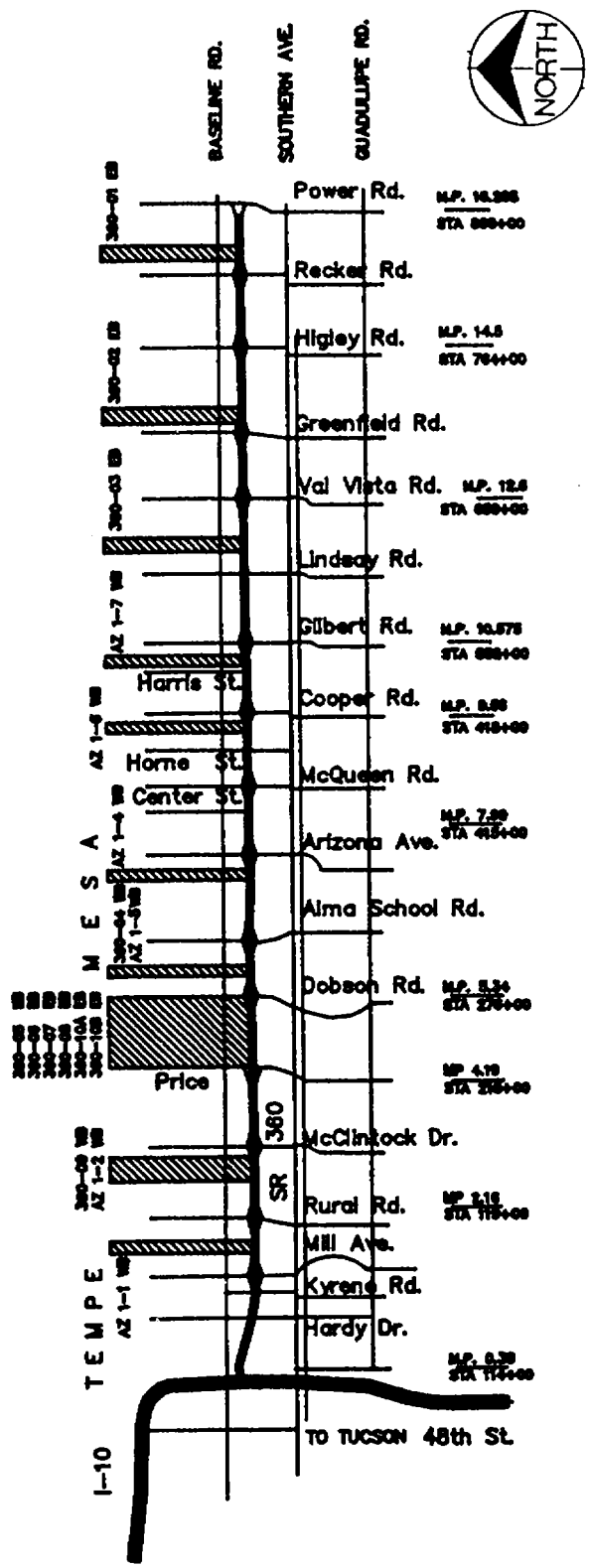


Figure 4. Location of study sections on S.R. 360.

The sections on the Superstition freeway carry a wide range of traffic volumes. Those sections closer to Phoenix (AZ 360-03, -04, -05, -06, -07, -08, -09, -10a, -10b, AZ 1-1, AZ 1-2, and AZ 1-5) all carry two-way ADT's of 105,000 to 120,000 vpd. Sections AZ 1-4 and AZ 1-6 are subjected to a two-way ADT of approximately 95,000 vpd. Section AZ 1-7 has a two-way ADT of about 75,000 vpd, and sections AZ 360-01, -02, and -03, which are located the furthest east, carry a two-way ADT of roughly 45,000 vpd. Truck traffic for all sections is about 3 to 3.5 percent of the ADT.

### **Overall Design Matrix**

The overall design matrix for the selected study sections is given in table 4. This table shows that there are a number of confounding variables that make it difficult to evaluate the impact that individual design features (such as slab thickness, base type, and presence of dowels) may have on concrete pavement performance. There still can be qualitative judgments made, however, regarding the relative performance of the various design types.

All of the design, construction, and performance data for the study sections have been tabulated into concise summary tables. These summary tables, furnished in appendix A, provide complete information on the design and performance of each pavement section included in the study.

### **3. DATA COLLECTION ACTIVITIES**

The field evaluations of the selected pavement sections represented an extensive data collection effort. Every attempt was made to collect information compatible with the Strategic Highway Research Program (SHRP) Long-Term Pavement Performance (LTPP) data base and to create as complete as possible a data record for each pavement section in this project.

To achieve a high level of reliability in the data collection process, the SHRP *Data Collection Guide for Long-Term Pavement Performance Studies* was followed to ensure the identification and collection of all key data elements.<sup>(7)</sup> In the field, pavement distresses were identified and quantified according to the *Distress Identification Manual for Long-Term Pavement Performance (LTPP) Studies*.<sup>(8)</sup> This manual provided a uniform basis for collecting distress data, and its use also ensured that the collected data was consistent with data collected for the LTPP studies.

The field work was performed over a four-week period during March and April of 1988. Due to the large traffic volumes, the testing had to be conducted between the hours of 9 p.m. and 5 a.m. Traffic control was provided by an independent subcontractor. The condition surveys were all conducted by the same survey crew (consisting of two experienced engineers), thereby ensuring consistency in the data collection activities.

Table 4. Overall design matrix of study sections.

		SLAB THICKNESS			
		9 in		10 - 13 in	
BASE TYPE	NONE			AZ 1-2 AZ 1-4 AZ 1-5	AZ 360-04 AZ 360-09
	AGG	AZ 10-01 AZ 10-02 AZ 10-03 AZ 17-01 AZ 17-02 AZ 17-03	AZ 17-04 AZ 17-05 AZ 17-06 AZ 17-10 AZ 17-11		
	LCB or CTB	AZ 1-1* AZ 1-6 AZ 1-7	AZ 360-01 AZ 360-02 AZ 360-03	AZ 2 AZ 10-04 AZ 10-05	AZ 10-06 AZ 10-07

\* Only section in the study with CTB.

Note: Shaded sections contain dowel bars.

The Arizona Department of Transportation (ADOT) provided extensive assistance in the data collection activities. ADOT furnished the use of their Falling Weight Deflectometer (FWD) to ensure consistency in the deflection data collected under this study with deflection data that they may have already collected. ADOT personnel were also on site to aid in the testing and to ensure that there were no problems encountered. ADOT also assisted in the collection of the Weigh-In-Motion (WIM) data. Finally, ADOT made exhaustive efforts to provide complete design and construction information for every pavement section.

### **Pavement Condition Survey**

A detailed pavement condition survey was conducted on each pavement section concurrently with the FWD testing and coring/boring operations. Although performed at night, sufficient lighting was available to determine the extent and severity of the various distresses. Data items collected included:

- Visible distress (cracking, joint spalling, etc.).
- Joint and crack faulting.
- Joint widths.
- Lane/shoulder drop-off and separation.
- Shoulder condition.

From the field survey sheets, comprehensive project strip maps were developed that clearly illustrate the condition of the pavement. These maps, provided in appendix B, also provide additional information on the results of the field testing as well as pavement design, rehabilitation, and traffic volumes. An example of the strip maps that were prepared for each section is depicted in figure 5.

### **Drainage Survey**

A comprehensive drainage survey was conducted in order to perform a rational drainage analysis of each section. This is in acknowledgement of the tremendous impact that drainage can have on pavement performance. The drainage survey consisted of the following:

- Depth and evaluation of condition of drainage ditches.
- Examination of transverse and longitudinal joint sealant.
- Examination of drainage outlets.
- Identification of visible signs of pumping.
- Measurement of transverse and longitudinal slopes.

This information, coupled with the analysis of the base, subbase, and subgrade materials retrieved from the boring operations, was used to assign an AASHTO drainage coefficient for each section. These coefficients are listed in table 5 and are

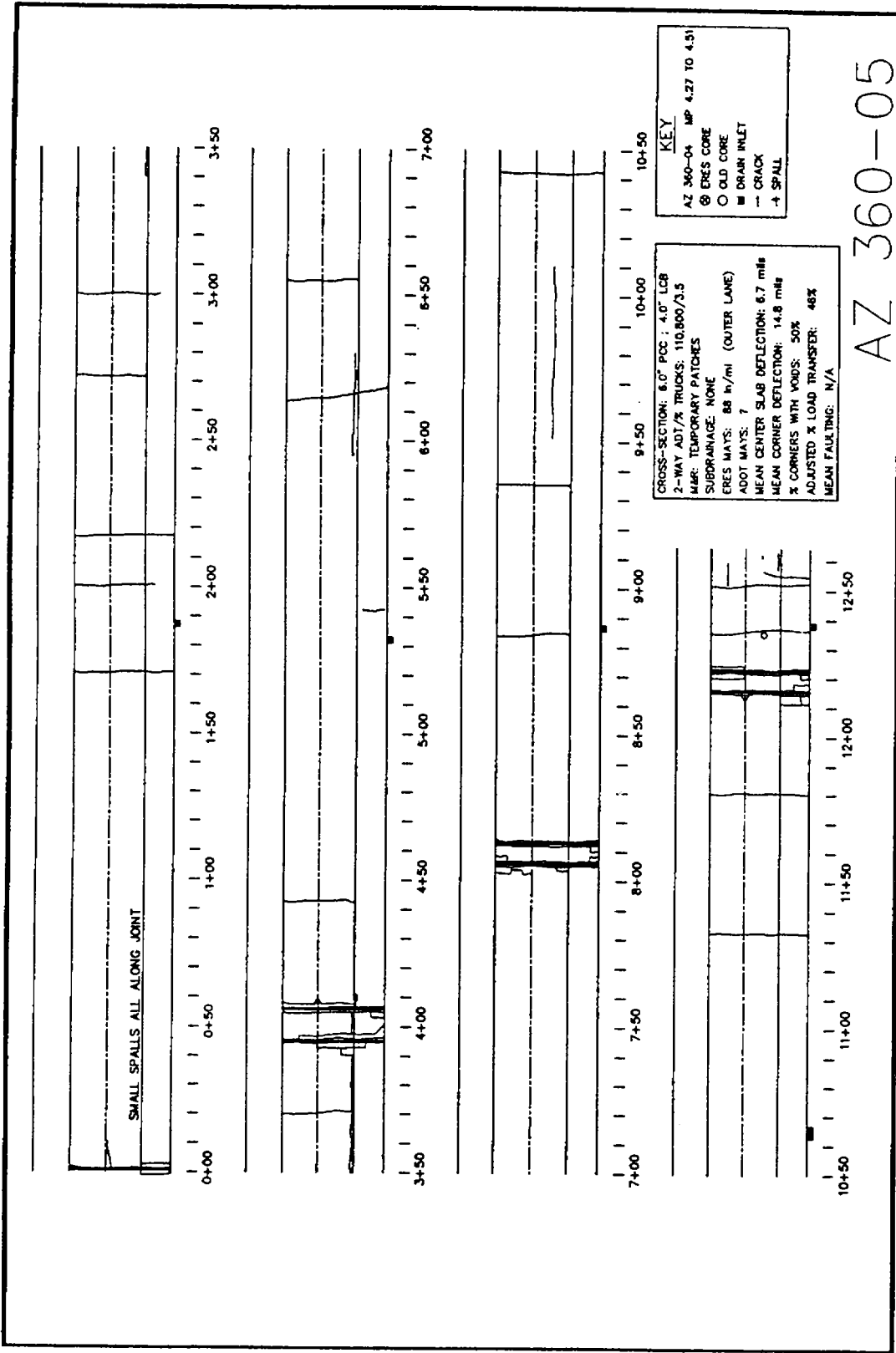


Figure 5. Example strip map prepared for each section.

Table 5. Drainage coefficients ( $C_d$ ) for study sections.

SECTION	$C_d$ VALUE
10-01	0.95
10-02	0.95
10-03	1.00
10-04	1.15
10-05	1.15
10-06	1.15
10-07	1.15
AZ 2	1.05
17-01	1.00
17-02	1.15
17-03	0.95
17-04	1.00
17-05	0.90
17-06	1.00
17-10	1.05
17-11	1.05
360-01	1.15
360-02	1.15
360-03	1.15
360-04	1.10
360-05	1.15
360-06	1.15
360-07	---
360-08	---
360-09	1.10
360-10a	1.15
360-10b	1.15
AZ 1-1	1.00
AZ 1-2	1.10
AZ 1-4	1.10
AZ 1-5	1.10
AZ 1-6	1.10
AZ 1-7	1.15

also provided in the summary tables of appendix A. For concrete pavements, the AASHTO drainage coefficient ranges from 0.7, indicating very poor drainage conditions, to 1.25, which indicates very good drainage conditions. Details of the procedure used to determine the AASHTO drainage coefficients are given in reference 9.

### **Photo Survey**

The paper record of the condition survey was supported by a 35-mm photographic record of each section. This photo survey consisted of an initial set of photographs taken to provide an overview of the section, and subsequent photos of typical section features (e.g., transverse joints, slab condition, drainage features, etc.).

### **Falling Weight Deflectometer (FWD) Testing**

Nondestructive deflection testing was performed with a Dynatest FWD. The deflection data collection effort was used to backcalculate layer moduli, to determine load transfer efficiencies, and to identify voids between the slab and the base at slab corners. Generally, 10 mid-slab center deflections and 20 joint corner deflections were taken, although 10 mid-slab edge deflections were also obtained if a tied concrete shoulder existed. The testing pattern used for sections with tied concrete shoulders is illustrated in figure 6.

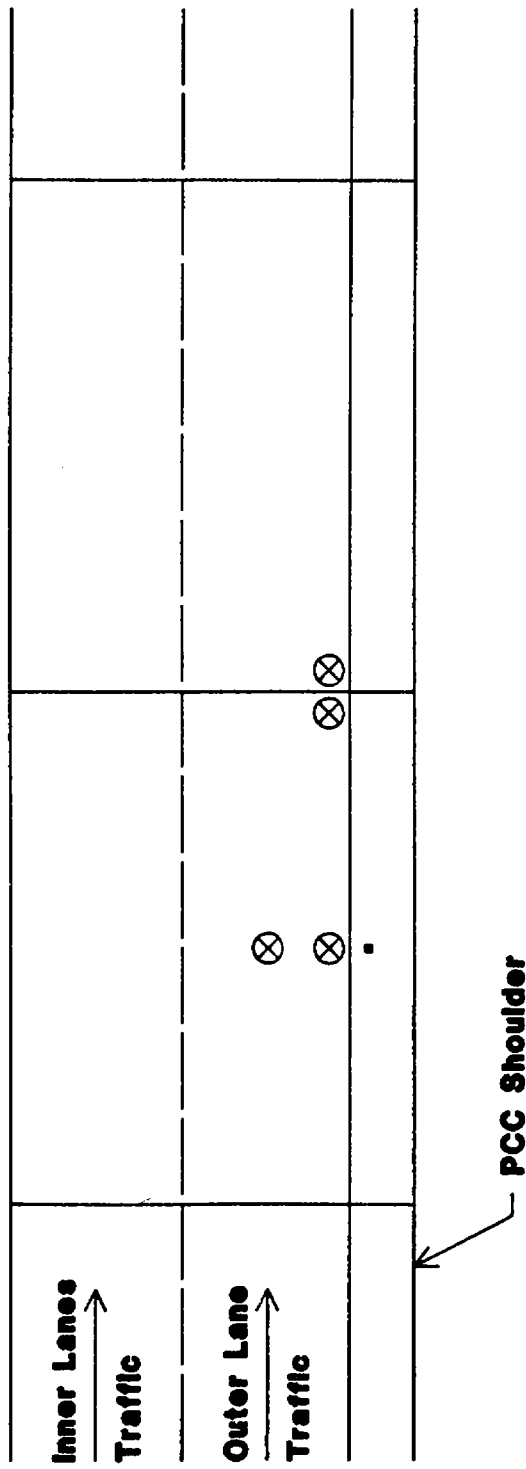
### **Coring/Boring**

Coring was performed with a portable drill equipped with a 6-in diameter bit. Center slab cores were retrieved from almost all of the sections and tested in split tensile according to AASHTO T-198 (ASTM C 496). Stabilized base samples of sufficient dimensions were also retrieved and tested similarly. Cores were retrieved from the transverse joints of most of the older sections and examined visually for any signs of deterioration along the underside of the joint core or for microcracking of the aggregate.

Base, subbase, and subgrade materials were retrieved from beneath the slab from core holes. The particle size distribution of granular materials was determined according to standard test methods. The liquid limit and plasticity index were also determined. This information was used to estimate a classification of the granular material according to procedures described in AASHTO M 145.

### **Pavement Roughness**

Pavement surface roughness data was collected on all of the sections. A 1985 Buick Le Sabre was fitted with a rear-axle-mounted Mays Roughness Meter, which was run over each lane of each section twice and the results averaged. The test was



**Required: 10 slab centers and 5 slab edges, including load transfer across shoulder joint. Also need 10 slab corners (20 dropel spread out over length of test section.**

Figure 6. FWD testing pattern for study sections with tied PCC shoulders.

run at a constant speed of 50 mi/h. During the first pass, the passengers in the car also assigned the section a present serviceability rating (PSR).

### **Weigh-In-Motion (WIM) Studies**

WIM data was collected on selected study sections for 48 continuous hours. The data collected included truck weight data and vehicle classification data. The WIM studies were performed at the following locations:

- Interstate 10 (MP 137.0, EB)
- Interstate 10 (MP 140.0, WB)
- Interstate 17 (MP 209.5, NB)
- State Route 360 (MP 3.0, EB)

The WIM equipment was calibrated by acquiring data from trucks of known weights and comparing those values to readings obtained for the same vehicles using the WIM equipment; adjustment factors were then developed and applied accordingly. Reduced data from the WIM studies is provided in appendix D.

### **Personnel Interviews**

In-depth interviews were conducted with knowledgeable individuals both within ADOT's staff and others in the Phoenix area. The intent of these interviews was to obtain more detailed information concerning ADOT's concrete pavement designs and their performance. This was accomplished through discussions with engineers involved in their design, construction, maintenance, and rehabilitation. Engineers in the research branch and materials section were also consulted. Transportation planners were consulted to discuss traffic counts. The information obtained provided valuable insights into both the history of concrete pavement design as well as current concerns for the maintenance and rehabilitation of those pavements.

## **4. DATA BASE DESCRIPTION**

A comprehensive data base was created for this research project to store the extensive design and performance data collected for each study section. The data base was created using the UNIFY Relational Data Base Management System.<sup>(10)</sup> The system resides on an IBM PC-AT with 640K RAM and a 30-Mb hard disk.

The data elements included in the data base were based on the LTPP data collection guide.<sup>(7)</sup> Two data bases were created to accommodate the large amount of data that was collected for this research project: the *Inventory* data base and the *Monitoring* data base. The type of information included in each data base is listed in table 6.

Table 6. Listing of major data items contained in the data base.

---

**INVENTORY DATA BASE**

---

Inventory Data

Geometric, Shoulder, and Drainage Information  
General Survey Information  
Layer Descriptions  
Longitudinal and Transverse Joint Data  
Concrete Mixture Data  
Base and Subbase Material Properties  
Subgrade Properties  
Age and Major Improvements

Maintenance Data

Historical Maintenance Information

Rehabilitation Data

Historical Rehabilitation Data

Environmental Data

General Environmental Data  
Annual Historical Environmental Data  
Average Monthly Historical Data

---

**MONITORING DATA BASE**

---

Monitoring Data

Deflection Testing Data  
Pavement Roughness Information  
Distress Survey Information

Traffic Data

Average Daily Traffic  
Percent Trucks  
Equivalent Single-Axle Load Applications

---

The data base contains an error checking routine that checks for invalid character input for the field parameters on the screens. Each data base has its own data listing procedure and will list information from that particular data base only. The error checking routine and the data listing procedure can be output to the screen, to a specified file, or to the printer.

In addition to the main UNIFY data base developed under this study, an additional data base was established for the execution of statistical analyses. This data base was developed for use with the personal computer (PC) version of SAS<sup>TM</sup> (11).

Appendix C to this report provides much more detailed information on the use and manipulation of the data base. It also provides a listing of all of the data sheets on which the data base is founded, along with a key for the various codes in the data base.

# CHAPTER 3 PERFORMANCE EVALUATION OF SECTIONS

## 1. INTRODUCTION

This chapter presents a synopsis of the overall performance of each concrete pavement design included in the study. Where possible, reasons for differences in performance are cited. At the end of the chapter, overall conclusions are offered regarding the performance of each design type. A complete listing of information pertaining to the design, construction, maintenance, rehabilitation, traffic, and performance of each section is provided in appendix A.

## 2. PERFORMANCE EVALUATIONS

### Interstate 10

The concrete pavement sections constructed on I-10 can be separated into two different designs: the 1968 design (AZ 10-01, -02, -03) and the 1980's design (AZ 10-04 through 10-07 and AZ 2). The 1968 design consists of a 9 in JPCP slab constructed over a 4 in aggregate base. The joint spacing is 13-15-17-15 ft and the transverse joints do not contain dowels. The 1980's design is a 10 in JPCP slab over a 5 in lean concrete base. The transverse joints are also spaced at 13-15-17-15 ft intervals and include 1.25 in diameter dowels.

### Results of Condition Survey

The performance of the individual sections on I-10 is summarized in table 7. This table shows that there is little difference in performance between the sections in terms of joint faulting (range 0.01 to 0.06 in), and transverse cracking (none). No visible signs of pumping were observed. It is interesting that, for either the old or the new sections, no transverse cracking existed. Two of the newer sections did, however, exhibit longitudinal cracking, although not at a significant level.

There was a discernible difference in the rideability of the two designs. The 1968 designs consistently had a lower PSR (and a corresponding higher roughness value) than the 1980's design. This is illustrated in figure 7. This difference in rideability may be explained by the fact that the older sections have sustained more traffic loading and aging cycles that caused settlements and roughness. It may also be a result of roughness built in to the slab during construction.

Figure 8 shows the difference in the amount of joint spalling exhibited by both designs. Again, as might be expected, the 1968 design exhibits much more medium-

Table 7. Distress indicators for primary survey lane of I-10 sections.

Section	Primary Survey Lane <sup>1</sup>	PSR	Mays Rough, in/mi	Avg. Fault, in	Trans. Crks/ mile <sup>2</sup>	Long. Crks, ft/mi <sup>2</sup>	Spalling, % Joints <sup>3</sup>	ESAL's, millions <sup>4</sup>
AZ 10-01	1	3.8	159	0.03	0.0	0.0	42	3.2
AZ 10-02	1	3.7	170	0.06	0.0	0.0	29	3.3
AZ 10-03	3	3.8	144	0.03	0.0	0.0	39	23.8
AZ 10-04	3	4.1	88	0.03	0.0	0.0	1	2.8
AZ 10-05	3	4.2	80	0.01	0.0	0.0	1	2.4
AZ 10-06	3	4.2	64	0.02	0.0	560.0	0	6.8
AZ 10-07	3	4.1	54	0.02	0.0	20.0	1	6.8
AZ 2	3	3.6	71	0.01	0.0	0.0	0	1.7

<sup>1</sup>Lane 1 is the inside (median-side) lane, lane 2 is the center lane, and lane 3 is the outermost lane.

<sup>2</sup>Transverse and longitudinal cracking include all severity levels of cracking.

<sup>3</sup>Transverse joint spalling includes only medium- and high-severity spalls.

<sup>4</sup>In indicated traffic lane, one direction.

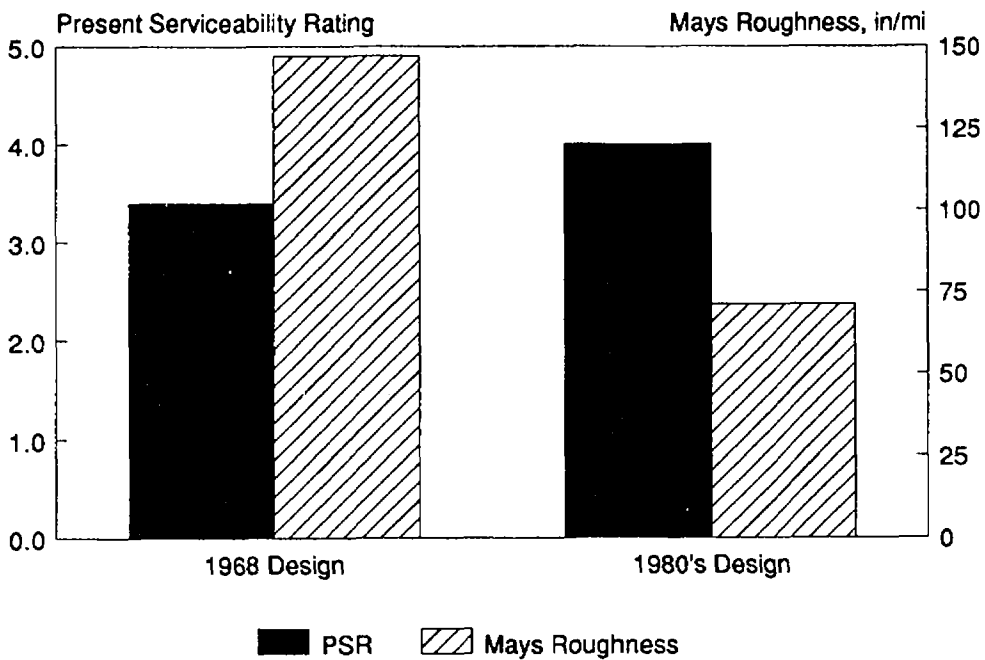


Figure 7. Pavement rideability and roughness measurements for I-10.

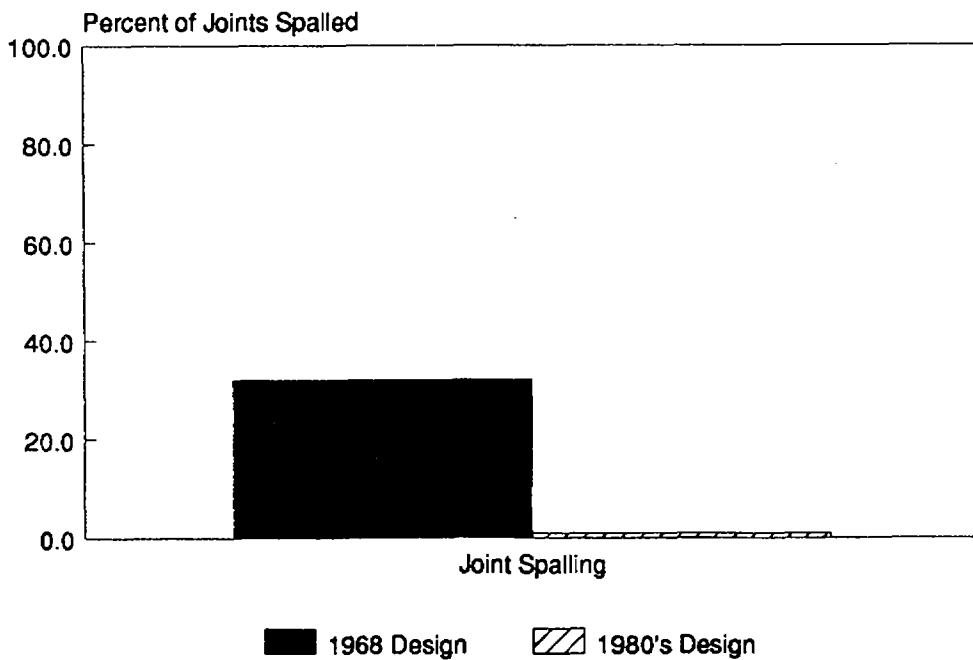


Figure 8. Transverse joint spalling on I-10.

and high-severity spalling than the newer sections. The older sections had an asphaltic-based sealant that was in very poor condition, thereby allowing incompressibles to infiltrate the joints.

The performance trends observed in the outer lanes (lane 3) of the I-10 sections also held true for the center (lane 2) and inner lanes (lane 1). The 1968 sections were rougher (lower PSR values and higher roughness values) and exhibit much more transverse joint spalling than the newer sections. It should be noted that the roughness for AZ 2 was obtained about six months before that obtained for the other sections. Different calibration techniques were used, which helps to explain why the roughness for AZ 2 is about one-half of that of 10-03, yet AZ 2 has a lower PSR.

A review of the faulting data on I-10 suggested that a closer examination be given to the relative faulting of the random-spaced joints. Only the older projects (10-01, 10-02, and 10-03) were examined because it was felt that the faulting trends exhibited by those sections would be more representative since they were older and had been subjected to more traffic loadings. The results of this investigation are shown in table 8.

Table 8. Average joint faulting between random-spaced slabs.

Section	Primary Survey Lane	ESAL's, millions	Average Joint Faulting Between Slabs, in			
			15 ft → 13 ft	13 ft → 15 ft	15 ft → 17 ft	17 ft → 15 ft
10-01	1	3.2	0.022	0.022	0.023	0.070
10-02	1	3.3	0.055	0.056	0.044	0.086
10-03	3	23.8	0.019	0.024	0.036	0.052
<b>Average</b>			0.032	0.034	0.034	0.068

This table shows that joints between the 15 ft and 13 ft slabs, joints between 13 and 15 ft slabs, and joints between 15 and 17 ft slabs all exhibited about the same amount of faulting. However, the faulting of joints between 17 and 15 slabs is about twice that of the other combinations. That is, when moving from a 17 ft slab to a 15 ft slab, the faulting of the transverse joint is greater. Furthermore, the development of this faulting appears to be independent of traffic loadings.

There are several factors that may be contributing to this phenomenon. First of all, the slabs are experiencing thermal contraction and expansion, and it takes an opening of only about 0.03 in for a joint to lose aggregate interlock. A larger opening will occur between the 17 and 15 ft slabs because they are the longest slabs in the pattern. At the same time, all of the slabs are undergoing thermal curling (due to a

difference in temperature between the top and bottom of the slab) and moisture warping (due to a difference in moisture content between the top and bottom of the slab). While thermal curling is cyclical, moisture warping will have the long-term effect of curving the slab edges up because of the dry climate. The relative amount of slab edge warping will be a function of the slab length, and differential movement under traffic loading can then occur because of the different amounts of warping occurring at each slab. The worst case occurs when moving from the 17 ft slab (which theoretically will have a greater amount of edge warping than the other slab lengths in the pattern) to a 15 ft slab. In this case, there will be impact loading in addition to the differential movement as the traffic loading strikes the 15 ft slab from the higher elevation of the 17 ft slab. This phenomenon apparently does not occur when going from the 15 ft slabs to the 13 ft slabs because of less warping and less joint opening, both due to shorter slab lengths.

Additional monitoring of these sections, and of newer nondoweled JPCP sections that employ the random joint spacing, is recommended in order to more completely understand these findings. Measurements on the relative magnitude of slab warping would be extremely useful as part of that monitoring process.

#### Results of Field Testing

Table 9 summarizes the results of the field testing for the I-10 sections. The sections representing the 1980's design had a slightly larger elastic modulus value than those sections constructed in 1968, although the modulus of rupture of the 1968 sections is higher. It should be noted that the modulus of rupture was determined from the testing of only one core, whereas the elastic modulus was backcalculated from deflection testing obtained from 10 slabs.

It is interesting to note that the effective  $k$ -value of the 1980's design averaged only 239 psi/in (for an LCB), about the same as the effective  $k$ -value of the 1968 design (236 psi/in, for an aggregate base). The average load transfer efficiencies (LTE) were higher for the older designs than for the newer designs. This may be explained by the older designs being in a state of compression due to incompressibles in the joints. It is noted that the older designs have very high corner deflections, more than twice that of the newer designs, and also have more apparent voids beneath slab corners. Thus, while the older designs appear to provide better load transfer than the newer designs at the joints, their high corner deflections and the apparent voids beneath slab corners are a cause of concern.

#### **Interstate 17**

The design for the sections on I-17, constructed over a period of four years (1961 to 1965), consists of a 9 in JPCP over a 3 or 4 in aggregate base, with transverse joints spaced at 15 ft intervals. This design is essentially the same as the 1968 design

used on I-10 with the exception of the uniform joint spacing and the fact that every fourth joint was formed with a metal insert. In the late 1970's and early 1980's, all of these sections on I-17 were diamond ground with the exception of 17-06.

Table 9. Summary of results of field testing for I-10 sections.

Pavement Property	1968 Design	1980's Design
PCC Elastic Modulus, psi	4,800,000	5,202,000
Effective <i>k</i> -value, psi/in	236	239
PCC Modulus of Rupture, psi	914	778
LTE, %	98	79
Loaded Corner Deflection, mils	23.0	10.5
% Joints with Voids	94	38
LTE Across PCC Shoulder, %	---	85

#### Results of Condition Survey

A summary of the performance indicators for the outer lanes of sections on I-17 is provided in table 10. There does not appear to be large differences in the performance of the various sections. The only exception to this is section 17-06, which had a low PSR (2.9) and exhibited significant joint faulting (0.09 in). However, this can be explained by the fact that it had not been diamond ground. The remaining sections had PSR values in the range of 3.6 to 4.1, Mays roughness measurements between 50 and 103 in/mi, and transverse joint faulting ranging from 0.01 to 0.06 in. It is believed that all of these sections would have developed significant faulting and roughness had they not been diamond ground.

One section (17-03) had a small amount of transverse slab cracking, and only two sections (17-03 and 17-11) displayed significant amounts of longitudinal cracking. However, a great deal of transverse joint spalling was observed, ranging from 5

Table 10. Distress indicators for primary survey lane of I-17 sections.

Section	Primary Survey Lane <sup>1</sup>	PSR	Mays Rough, in/mi	Avg. Fault, in	Trans. Crks/ mile <sup>2</sup>	Long. Crks, ft/mi <sup>2</sup>	Spalling, % Joints <sup>3</sup>	ESAL's, millions <sup>4</sup>
AZ 17-01	1	3.6	95	0.01	0.0	0.0	18	1.5/2.9
AZ 17-02	1	3.7	95	0.01	0.0	30.0	42	1.6/2.8
AZ 17-03	3	3.9	91	0.05	5.0	134	64	2.0/14.4
AZ 17-04	3	3.7	50	0.02	0.0	15	34	9.5/18.0
AZ 17-05	3	4.1	77	0.06	0.0	0.0	5	2.1/14.7
AZ 17-06	3	2.9	N/A	0.09	0.0	0.0	21	19.2/19.2
AZ 17-10	3	4.1	103	0.03	0.0	18	18	10.8/19.3
AZ 17-11	3	4.1	83	0.01	0.0	200	90	3.6/15.6

Notes: Every fourth joint was formed with a metal insert, which is believed to have contributed to the joint spalling.  
All sections except AZ 17-06 have been diamond ground.

<sup>1</sup>Lane 1 is the inside (median-side) lane, lane 2 is the center lane, and lane 3 is the outermost lane.

<sup>2</sup>Transverse and longitudinal cracking include all severity levels of cracking.

<sup>3</sup>Transverse joint spalling includes only medium- and high-severity spalls.

<sup>4</sup>In indicated traffic lane, one direction (first number is ESAL's since grinding, second number is total ESAL's since opening to traffic).

percent to 90 percent of the transverse joints. Partial-depth spall repairs had been placed at most of the joints. The joints were in various stages of resealing, with the sealant condition ranging from poor to excellent. The spalling was probably due to the use of the metal insert at every fourth joint and to infrequent joint resealing.

Another way of looking at the performance data is to group the sections by year of construction. This is done in figures 9 and 10. Figure 9 shows the average faulting and spalling for the three years of construction and shows that a significant level of spalling was present for each construction year. However, the faulting for the 1961 and 1965 construction years is much lower than that of the 1963 construction, due to the fact that these sections had been diamond ground.

Figure 10 displays the average PSR and Mays roughness for each section. It is observed that the average rideability of the 1961 and 1965 sections is approximately the same. This is not surprising considering that they have both been diamond ground, whereas the 1963 section (17-06) has not. Unfortunately, roughness measurements were not recorded for the 1963 section.

The performance of the inner and middle lanes on I-17 was excellent. There was minimal faulting and little transverse and longitudinal cracking. However, there was a good deal of transverse joint spalling in both of these lanes, comparable to the amount observed in the outer lanes. This seems to confirm that a combination of a lack of joint maintenance (which allowed the entry of incompressibles) and poor joint construction practices caused the spalling.

### Results of Field Testing

A comparison of the results of the field testing for the three construction years of the I-17 sections is shown in table 11. The deflection data indicated that there was exceptionally good load transfer across the transverse joints and that the corner deflections were small. However, it should be noted that the deflection data for these sections were obtained at temperatures in the upper 70's. The data also indicated that there were some voids at the transverse joints, particularly for the 1963 section.

The elastic modulus values and the modulus of rupture values for the sections were consistent with one another for each section and are indicative of sound concrete. The effective *k*-value of the different sections are fairly representative of aggregate bases, and are evidently providing good support.

### **State Route 360 (Superstition Freeway)**

A variety of concrete pavement designs have been constructed on S.R. 360 since 1972. These designs are indicated in table 12 and consist of several JPCP designs of different thicknesses and base types, a prestressed pavement design, and a

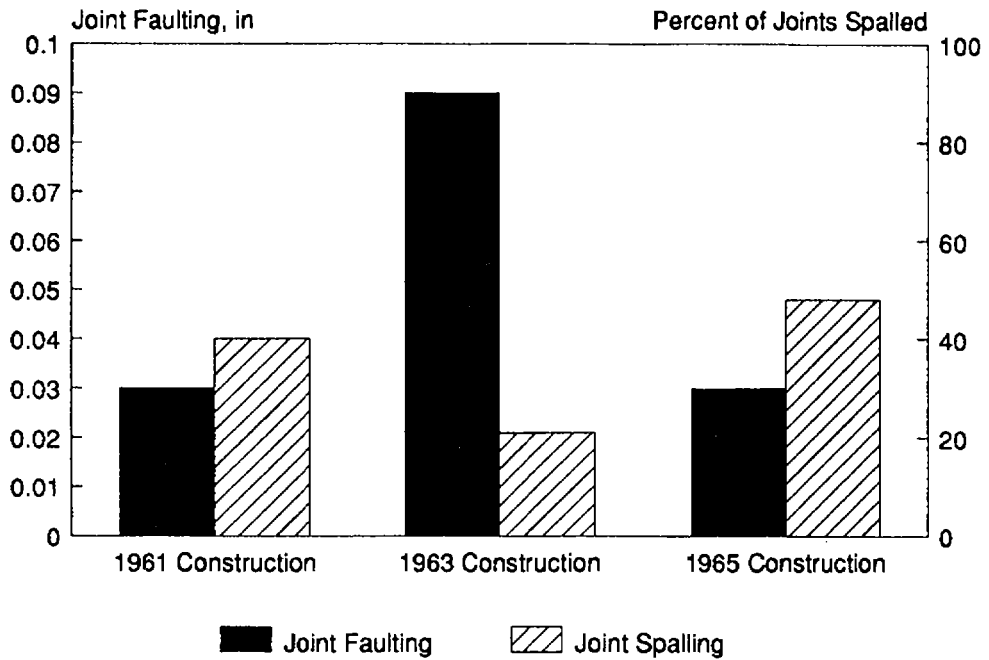


Figure 9. Transverse joint faulting and joint spalling on I-17.

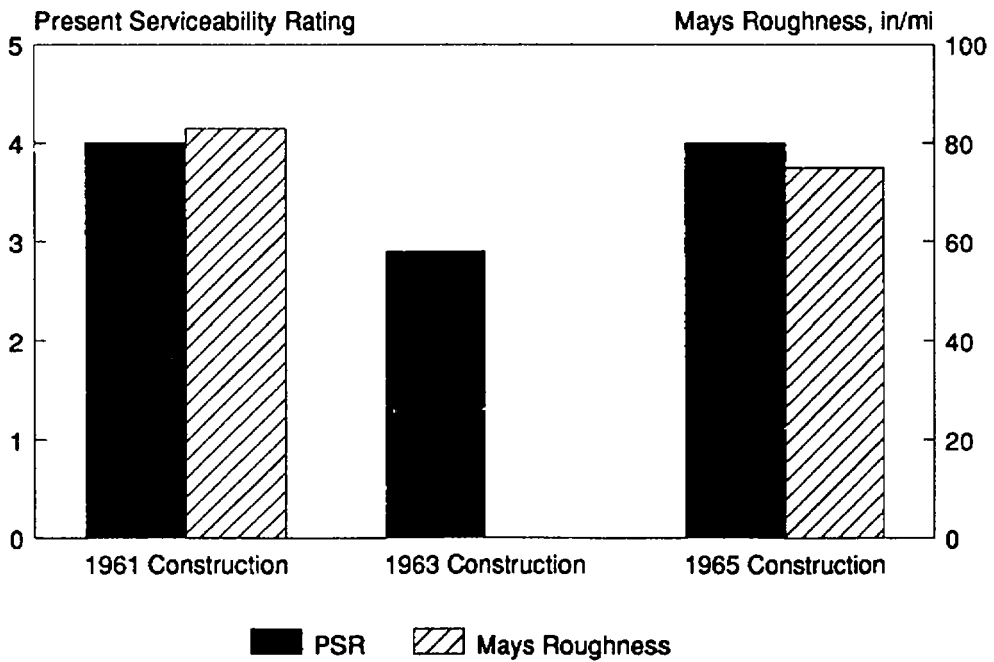


Figure 10. Pavement rideability and roughness measurements for I-17.

Table 11. Summary of results of field testing for I-17 sections.

Pavement Property	1961 Sections	1963 Section	1965 Section
PCC Elastic Modulus, psi	4,757,000	5,690,000	6,385,000
Effective <i>k</i> -value, psi/in	216	359	144
PCC Modulus of Rupture, psi	759	848	984
LTE, %	100	100	96
Loaded Corner Deflection, mils	12.3	13.0	11.1
% Joints with Voids	33	77	12
LTE Across PCC Shoulder, %	70	---	---

Table 12. Summary of pavement designs on S.R. 360.

Construction Year	Pavement Type	Base Type	Joint Spacing, ft	Corresponding Sections
1972	9 in JPCP	6 in CTB	13-15-17-15	AZ 1-1
1975	13 in JPCP	None	13-15-17-15	AZ 1-2, 360-09
1977	6 in Prestressed	4 in LCB	200-500 ft	360-05, -06, -10a, -10b
1979	13 in JPCP	None	13-15-17-15	AZ 1-4
1979	11 in JPCP	None	13-15-17-15	AZ 1-5, 360-04
1981	9 in JPCP	4 in LCB	13-15-17-15	AZ 1-6, AZ 1-7
1983	9 in JPCP	4 in LCB	13-15-17-15	360-03
1984	9 in CRCP	4 in AGG	N/A	360-07, 360-08
1985	9 in JPCP	4 in LCB	13-15-17-15	360-01, 360-02

CRCP design. Several sections of each design type were surveyed in order to obtain a more realistic assessment of their performance.

### Results of Condition Survey

The performance indicators for these various pavement sections are given in table 13. Generally speaking, the overall performance of these sections is very good. Little transverse and longitudinal cracking is evident, which is very typical of concrete pavements in Arizona.

With the exception of AZ 1-1, transverse joint faulting was not significant. AZ 1-1, which was constructed on a CTB, displayed 0.08 in of faulting, or approximately twice that of the average of the other sections. This faulting is consistent with similar concrete pavement designs constructed in California over CTB. The average level of faulting for the various designs is shown in figure 11.

AZ 1-1 was also one of the poorest performers in terms of roughness and rideability, with a PSR of 3.4 and a Mays roughness of 114 in/mi. Only one of the prestressed sections (360-06) was rougher, and that was due to the extremely poor condition of the gap slabs and to "built-in" construction roughness. The newest sections constructed on the Superstition (360-01, -02, and -03), along with one of the slab-on-grade sections (360-09), are the smoothest riding. A summary of the rideability of the various designs is shown in figure 12.

Spalling of the transverse joints was not really a problem on the Superstition Freeway sections. Only one section, AZ 1-1, exhibited a significant amount of spalling (22 percent of the joints). The other sections displayed little joint spalling.

All but one of the prestressed sections were fairly smooth riding, evidenced by serviceability ratings around 4.0. There were some undulations that were apparent in the pavement from the paving, but these apparently did not translate into a roughness problem. A few transverse cracks had developed at random locations throughout the sections, but for the most part these cracks were tight.

The CRCP sections, which served as the inner lane (lane 1) to the prestressed sections, were surprisingly rough for only being 4 years old at the time of survey. However, this roughness must have been due to construction, because the sections were free of medium- and high-severity cracking. Tight transverse cracks were present and occurred at approximately 3.4 ft intervals.

The performance of each of the inner and middle lanes closely paralleled that of its corresponding outer lane. The inner and middle lane of those outer lane sections that were rough (AZ 1-1) likewise were rough; those inner and middle lanes of those sections that were smooth (e.g., 360-03) were also smooth.

Table 13. Distress indicators for primary survey lane of S.R. 360 sections.

Section	Primary Survey Lane <sup>1</sup>	PSR	Mays Rough, in/mi	Avg. Fault, in	Trans. Crks/ mile <sup>2</sup>	Long. Crks, ft/mi <sup>2</sup>	Spalling, % Joints <sup>3</sup>	ESAL's, millions <sup>4</sup>
AZ 360-01	3	4.4	62	0.05	0.0	0.0	0	0.8
AZ 360-02	3	4.2	80	0.02	0.0	0.0	0	0.8
AZ 360-03	3	4.1	86	0.02	0.0	0.0	0	1.1
AZ 360-04	3	4.3	55	0.04	0.0	18	0	2.6
AZ 360-05	3	3.9	88	N/A	0.0	—	N/A	3.1
AZ 360-06	3	3.3	131	N/A	0.0	—	N/A	3.1
AZ 360-07	1	3.9	86	—	0.0	—	—	0.2
AZ 360-08	1	4.0	80	—	0.0	—	—	0.2
AZ 360-09	3	4.8	64	0.02	35	35	0	3.8
AZ 360-10a	3	4.0	—	N/A	0.0	—	N/A	3.1
AZ 360-10b	3	4.0	—	N/A	0.0	—	N/A	3.1
AZ 1-1	3	3.4	114	0.08	0.0	0.0	22	3.3
AZ 1-2	3	3.8	65	0.01	0.0	0.0	1	2.8
AZ 1-4	3	3.6	102	0.01	0.0	0.0	1	2.0
AZ 1-5	3	3.8	85	0.03	0.0	0.0	0	2.3
AZ 1-6	3	3.5	97	0.01	0.0	0.0	0	1.7
AZ 1-7	3	3.8	91	0.02	0.0	0.0	0	1.3

<sup>1</sup>Lane 1 is the inside (median-side) lane, lane 2 is the center lane, and lane 3 is the outermost lane.

<sup>2</sup>Transverse and longitudinal cracking include all severity levels of cracking (transverse cracking for CRCP includes medium- and high-severity levels only).

<sup>3</sup>Transverse joint spalling includes only medium- and high-severity spalls.

<sup>4</sup>In indicated traffic lane, one direction.

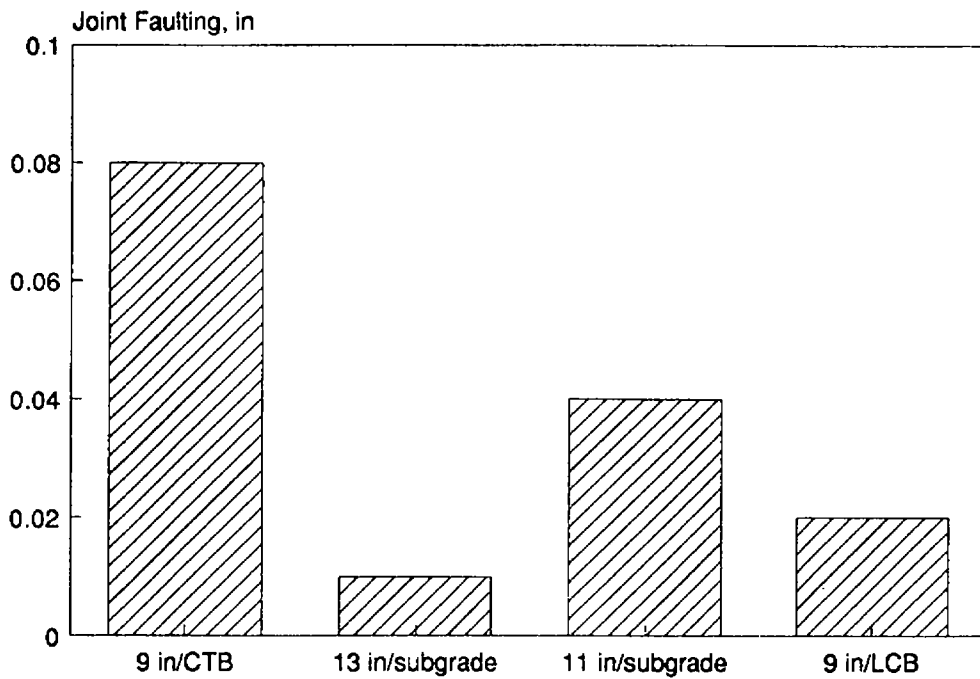


Figure 11. Transverse joint faulting on S.R. 360.

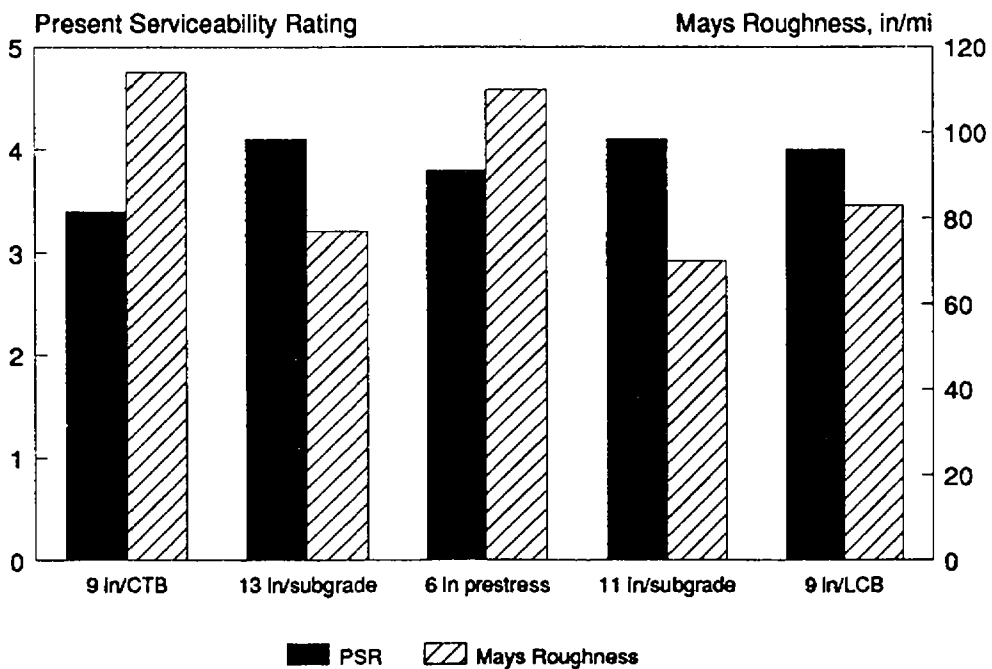


Figure 12. Pavement rideability and roughness measurements for S.R. 360.

### Results of Field Testing

A comparison of the results of the field testing for the various pavement designs is provided in table 14. The backcalculated elastic modulus values and the modulus of rupture values for the older sections are lower than those of the newer sections. It is also surprising that the effective  $k$ -values for the CTB and the aggregate base sections are as high as they are. In fact, the effective  $k$ -value for the section with the CTB was higher than for any of the sections constructed with an LCB. This may be due to the CTB being bonded to the slab, whereas the LCB may not be.

The deflection data showed that the highest loaded corner deflection and the worst load transfer efficiency were found on the 9 in JPCP slabs constructed on LCB. These sections also exhibited a significant amount of corners with voids. The 13 in slab-on-grade design displayed the best overall response to the deflection testing, showing low corner deflections, high load transfer efficiency, and no voids.

Table 14. Summary of results of field testing for S.R. 360 sections.

Pavement Property	9 in JPCP/ 6 in CTB	13 in slab on grade	11 in slab on grade	9 in JPCP/ 4 in LCB	6 in Pre- stressed	9 in CRCP
PCC Elastic Modulus, psi	3,140,000	3,313,000	3,440,000	4,866,000	5,590,000	4,740,000
Effective $k$ -value, psi/in	546	415	444	425	249	323
PCC Modulus of Rupture, psi	687	740	820	887	---	---
LTE, %	94	100	99	63	N/A	N/A
Loaded Corner Deflection, mils	8.6	5.0	12.0	12.6	N/A	N/A
% Joints with Voids	37	0	46	38	N/A	N/A
LTE Across PCC Shoulder, %	---	81	48	92	84	100

### 3. OVERALL PERFORMANCE SUMMARY OF DESIGN TYPES

This section presents an overall summary of the performance of the various concrete pavement design *types* that ADOT has employed in the Phoenix Urban Corridor. Each design is examined for its ability to perform in the urban

environment, keeping in mind the special requirements that urban pavements possess (for example, long-lasting designs, good rideability, low maintenance requirements, and uncomplicated rehabilitation requirements).

## **Design Summaries**

### 1960's Design

This design includes all of the sections constructed on I-17 and three sections on I-10. The design consists of a 9 in JPCP on a 3- or 4-in aggregate base. The transverse joints were not doweled and were either placed at 15 ft intervals (I-17 sections) or 13-15-17-15 ft intervals (I-10 sections).

These sections, the oldest concrete pavement in the Phoenix Urban Corridor, have performed very well. The sections are beginning to show deterioration, however, as they are exhibiting higher levels of transverse joint spalling. The joint spalling was the result of the metal joint insert employed by ADOT at every fourth joint in the 1960's concrete construction, and the lack of regular joint sealing.

The sections exhibit high roughness levels as compared to the other sections. This may be explained by the emergence of transverse joint faulting and by the fact that the sections were constructed somewhat rough due to these sections being the first concrete pavement construction in the Phoenix Urban Corridor. The roughness was presumably such a problem that it necessitated the diamond grinding that was performed on selected sections of I-17 in the 1980's. Also, the aggregate base course seemed to be somewhat susceptible to erosion as evidenced by the large number of slab corners exhibiting voids. This would also help to explain the emergence of joint faulting on these sections. In addition, all of the sections representing the 1960's design were constructed with asphalt concrete shoulders. This too would help to explain the development of some of the joint faulting as there would be no support provided by the shoulder to the mainline pavement. Finally, it was observed that there was more faulting on joints where traffic was moving from the 17-ft slab to the 15-ft slab, which may be because of a combination of thermal contraction and moisture warping.

### 1972 Design

The 1972 concrete pavement design was a 9-in JPCP built on a 6 in CTB. Transverse joints were placed at 13-15-17-15 ft intervals and not doweled. The 1972 design was represented by only one construction section (AZ 1-1 on S.R. 360).

This design, which essentially was the same used by the California Department of Transportation (CALTRANS) in the 1970's, did not perform that well in Arizona. The section displayed significant levels of faulting (0.08 in) and spalling (22 percent

of joints spalled), and was also one of the roughest sections evaluated (Mays Roughness 114 in/mi and PSR of 3.4). The faulting was not helped by the fact that the section had AC shoulders.

The use of a cement stabilized base course on this section was not successful in reducing faulting. It was further noted from the field testing that voids had developed beneath 37 percent of the slab corners.

#### Slab-on-Grade Design (1975, 1979)

Five slab-on-grade sections, in which the slab was thickened considerably and placed directly on the subgrade, were included in the study. Of these five, three are 13-in JPCP and two are 11-in JPCP. All of these sections have 13-15-17-15 ft joint spacing, contain no dowel bars, and are located on S.R. 360.

This design was extremely effective in reducing the amount of joint faulting occurring at the transverse joints. These sections also displayed virtually no joint spalling or slab cracking, and the roughness measurements and PSR evaluations indicated that the sections were smooth and provided good rideability. It is also interesting to note that the 13 in slabs displayed less than one-half the faulting that the 11 in slabs displayed (0.013 in vs. 0.035 in), although the faulting levels are both quite small. It should be further pointed out that these pavements on S.R. 360 have been subjected to far less traffic loadings than those on I-10 and I-17 (2.0 to 3.8 million cumulative 18-kip ESAL applications, at a current rate of approximately 0.3 to 0.6 million ESAL's per year).

Overall, the slab-on-grade design appears to be performing quite well in the mild Phoenix climate and under the relatively low truck traffic volumes. It is strongly believed that these two factors combined are the primary factors allowing for the slab-on-grade pavements to perform so well. In fact, heavy truck loadings and excessive moisture and/or severe freeze-thaw cycles are believed to have caused other slab-on-grade designs to perform poorly.<sup>(4)</sup>

#### 1980's Designs

The designs of the 1980's consisted first of a 9 in slab on a 4-in LCB without dowels (S.R. 360) and then a 10 in slab on a 5-in LCB with dowels (I-10). The latter is the design currently in use by ADOT.

The overall performance of these sections is considered to be very good. These sections exhibit good rideability and generally have little joint faulting or joint spalling. Those sections with dowel bars exhibited slightly less faulting and a higher load transfer efficiency than those without dowel bars. However, the overall roughness for both the doweled and nondoweled sections was about the same.

The results of the deflection data suggested that there were voids beneath 38 percent of the joints. This would appear to indicate that either some erosion of the lean concrete base is occurring or that slab curling was taking place. These voids were detected at both the nondoweled and doweled joints.

Overall, these pavement sections appear to be providing good performance at this time. However, it should be acknowledged that these designs are the newest in the Phoenix Urban Corridor and generally have sustained less traffic loadings than the other sections.

### Prestressed Design

Prestressed pavements are an intriguing concrete pavement design in which the concrete is placed in a constant state of compression. In this way, the slab should not experience large tensile stresses and the thickness can theoretically be reduced. The prestressed section built on S.R. 360 represents one of the few prestressed highway pavements in the nation. The prestressed pavement was constructed 6 in thick on a 4 in LCB and had gap slabs placed at 200 to 500 ft intervals.

The performance of the prestressed sections has been mixed. While the sections are fairly smooth riding, there have been major problems associated with the maintenance of the gap slabs. These gap slabs have deteriorated with age and traffic and have become frequent recipients of patching materials. Because of all of the patching that has been performed at these locations, the gap slabs are the primary cause of roughness of these sections.

Because of the maintenance requirements and a perceived lack of performance of the prestressed sections, they are slated for removal and will be replaced by a conventional pavement.

### CRCP Design

Two CRCP sections, located on S.R. 360, were included in the study. The design of these sections consists of a 9 in slab placed on a 4 in aggregate base. These sections were constructed as the innermost lane (lane 1) of the prestressed concrete sections on S.R. 360.

The CRCP sections are performing well, but do appear to be a little rough after only 4 years of service and 200,000 ESAL applications. It is believed that some of this roughness may be due to the contractor's inexperience with CRCP construction, as CRCP performance has been shown to be very sensitive to construction practices.

## Roughness Evaluation

As part of their monitoring program, ADOT has obtained roughness measurements over time for the concrete pavements located within the Phoenix Urban Corridor. Like the roughness data collected by the survey team in 1988, this time-sequence roughness data was also collected with a Mays Roughness Meter. However, it should be emphasized that the data is not entirely compatible with one another. This is because it was collected by two different pieces of equipment that used different calibration procedures. In addition, the ADOT data, in most cases, was not collected over the exact limits of each section that was included in the study. Furthermore, while the bulk of the roughness data was collected by the survey team in 1988, part of it was collected in 1987 under the parallel FHWA study using different calibration procedures. Because of these incompatibilities, there are bound to be some anomalies when comparing some of the data.

The ADOT time-sequence roughness data was evaluated to provide a broad overview of the roughness history of the various pavement sections. Figure 13 shows the roughness history of the pavement sections on I-10. This figure shows that the 1968 sections were at one time as smooth as the newer 1980's sections. However, beginning in the mid-1970's, the roughness of those sections increased tremendously, reaching a peak of nearly 300 in/mi in 1984. It is not known why the roughness decreases after 1984, although it is possible that differences in equipment, operation procedures, or calibration techniques may have slightly altered the roughness measurements over time.

The roughness history of the I-17 pavement sections from 1972 to the present is depicted in figure 14. Over the course of that 15-year period, the older sections (built in 1961 and 1963) were much rougher than the sections built in 1965. Roughness for all sections increased through the 1970's until each was diamond ground: the 1961 sections in 1979, the 1963 sections in 1984, and the 1965 sections in 1984. While the specific 1963 section included and evaluated in this study was not diamond ground, diamond grinding was apparently performed on other sections constructed in 1963.

Figure 15 traces the roughness of the pavement sections on S.R. 360. Several observations are apparent upon examination of this figure. The first observation is that the prestressed and CRCP section have higher roughness values than the other sections. The other primary observation is that slab-on-grade designs (11- and 13-in slabs) are among the smoothest of all of the pavements and appear to be able to maintain that pavement smoothness over time.

The time-sequence roughness data is averaged by design type and presented in figure 16. This figure indicates that the 9 in JPCP over aggregate base, the 6 in prestressed pavement, and the 9 in CRCP are the roughest of all of the pavement

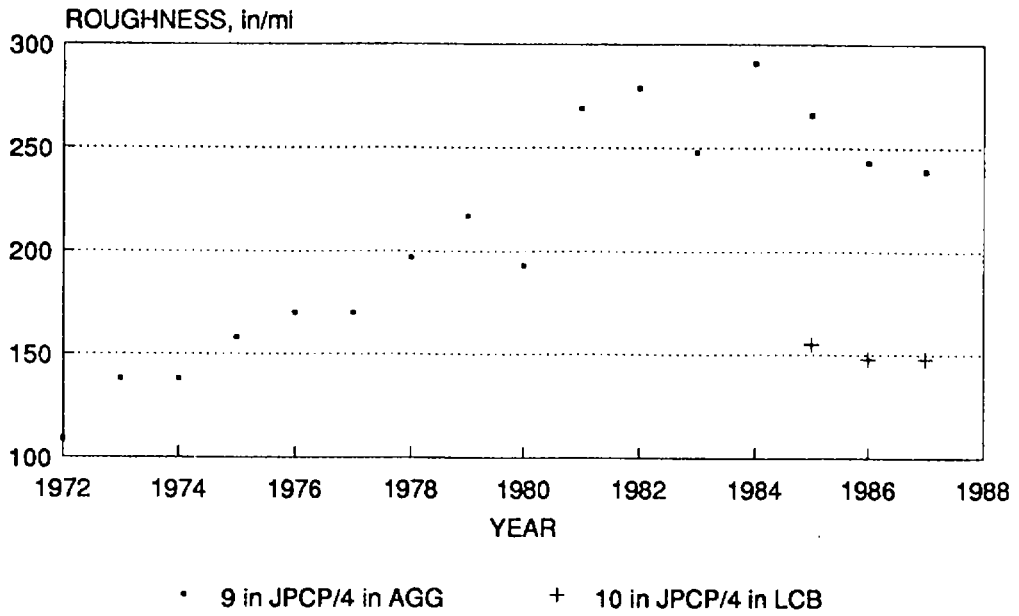


Figure 13. Roughness history for I-10 sections.

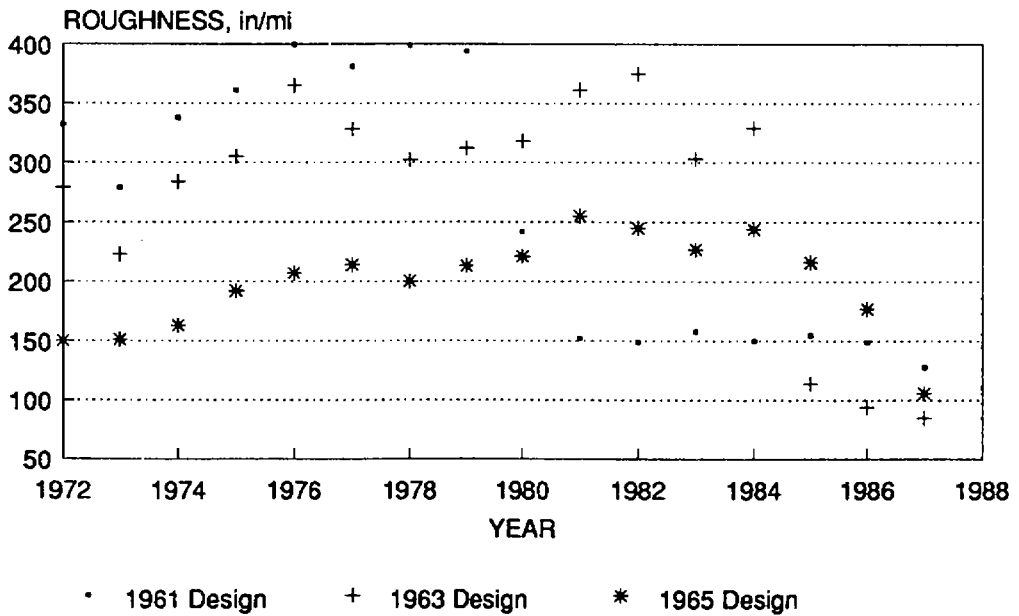


Figure 14. Roughness history for I-17 sections.

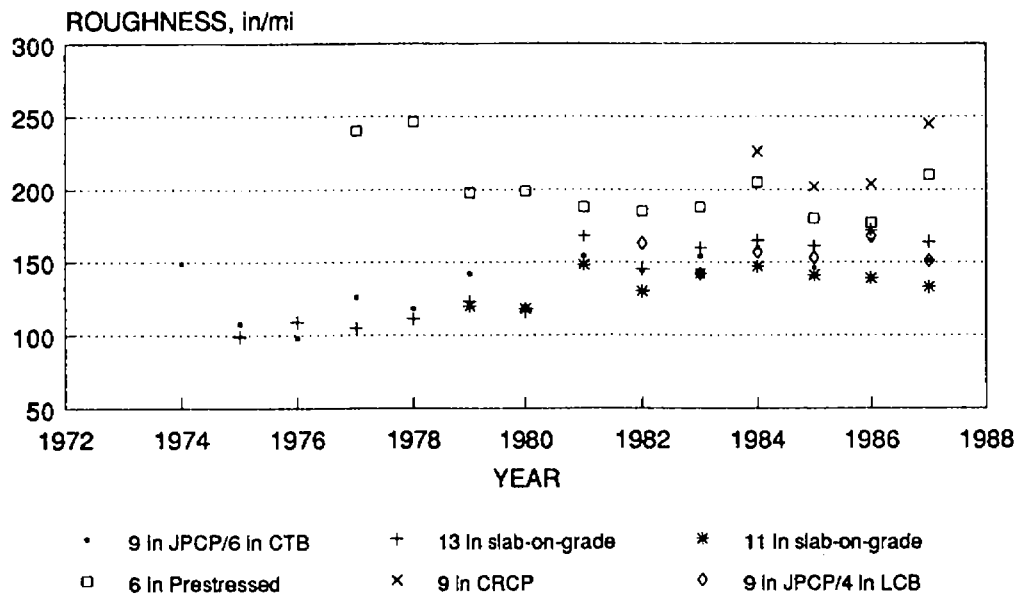


Figure 15. Roughness history for S.R. 360 sections.

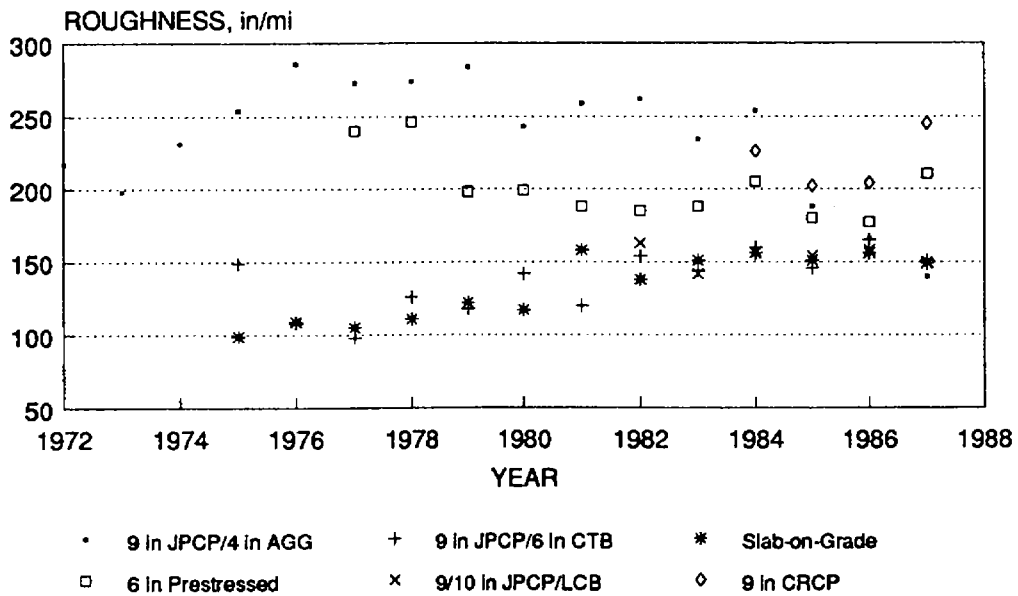


Figure 16. Roughness history by pavement design type.

sections. On the other hand, the smoothest pavement sections are the slab-on-grade designs and the newer 9/10 in JPCP over LCB. This figure should be interpreted very carefully, however, since traffic loadings for each section are not the same (i.e., the older sections have sustained more ESAL applications).

Strictly from a rideability viewpoint, the time-sequence roughness evaluation indicates that the slab-on-grade design and the 9/10 in JPCP over LCB are the best performers. This seems to reflect the findings of the section-by-section engineering evaluation. Both the slab-on-grade design and the 9/10 in JPCP over LCB design exhibit the least amount of roughness of all the designs, although the 9/10 in over LCB is not that old and has not been subjected to significant traffic loadings. The slab-on-grade design has consistently shown the least amount of roughness over the monitoring period. While many slab-on-grade designs across the country have not performed that well, it is believed that the mild climatic conditions have a favorable influence on their performance in Arizona. Only long-term performance monitoring will conclusively determine the effectiveness of each of these designs.

### Voids Evaluation

Voids are an indication of erosion beneath the slab that can lead to joint faulting and corner breaks. From the deflection testing performed on all sections, it appeared that a linear correlation existed between the magnitude of the average loaded corner deflection and the detection of voids beneath the joints. A linear regression analysis yielded the following relationship:

$$V = 5.2165 \cdot D_L - 25.5066$$

where:

V = Percent Corners with Voids  
D<sub>L</sub> = Loaded Corner Deflection, mils

n = 27  
r<sup>2</sup> = 0.76  
std. dev. = 33.478

This relationship is illustrated in figure 17. The figure shows that even loaded corner deflection above 10 mils can lead to a significant amount of slab corners with voids. It appears that if the corner deflection under a 9000 lb wheel load can be limited to less than 8 mils, then the percent corners developing voids can be kept to a reasonable level.

## 4. PRELIMINARY EVALUATION

It is interesting to note that all of the pavements evaluated in this study exhibited little, if any, structural deterioration. Indeed, most of the problems

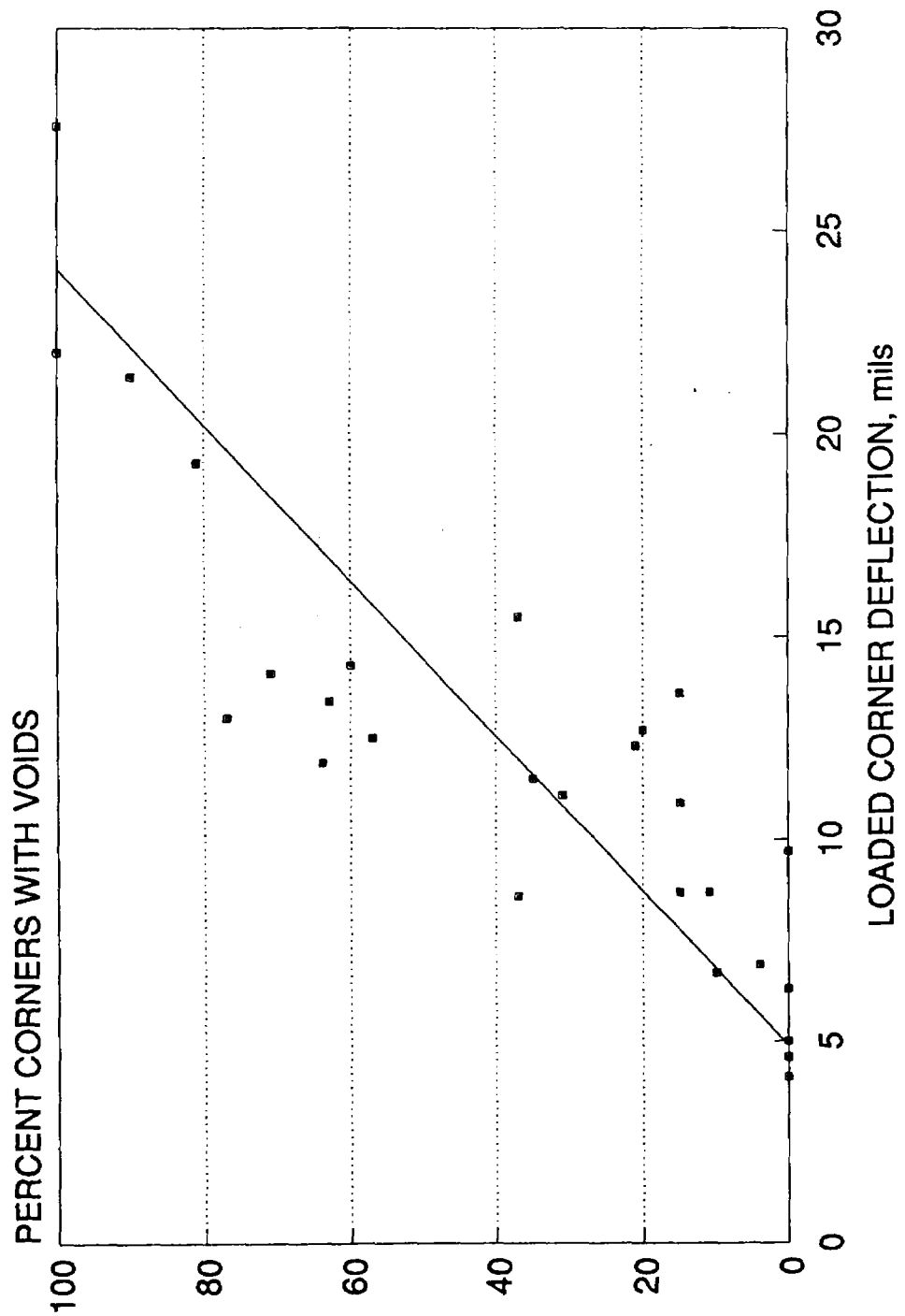


Figure 17. Percent slab corners with voids as a function of loaded corner deflection.

observed were related to nonstructural aspects of pavement design, such as joint spalling, joint faulting, and overall roughness. ADOT has taken several steps in recent years to correct these problems, including the use of dowel bars at transverse joints.

Based upon the results of the performance evaluation of the various concrete pavement designs in the Phoenix Urban Corridor, it appears that there are two designs that have performed better than the others. These designs are:

- 10 in JPCP over LCB (with dowels).
- Thickened JPCP placed directly on grade.

The JPCP over LCB exhibited a good rideability, had low faulting, and had fewer voids developing beneath the corners. The slab-on-grade design displayed an ability to maintain pavement smoothness over time. However, because of the tendency of some of the older nondoweled sections to exhibit high corner deflections and loss of support, the use of dowel bars is recommended in the thick slab-on-grade designs to help ensure the long-term performance of that design.

It is acknowledged that there were too few of sections of each design type to make a complete and statistically valid analysis. It is further acknowledged that some data was missing and some of the sections are not very old and have not yet sustained a good deal of traffic loading. Indeed, there is a wide difference in traffic loadings among the sections. However, from an overall examination of the data that was available from the limited number of sections, the 9/10 in JPCP over LCB and the thick slab-on-grade designs appear to be performing the best.

Comments on the performance of the other pavement design types are listed below:

- The 9 in JPCP on aggregate base design developed a considerable amount of faulting over the years that ultimately necessitated diamond grinding. This design also developed significant voids beneath slab corners.
- The 9 in JPCP on CTB design displayed fair performance, displaying significant levels of faulting and joint spalling. The same design in California has also exhibited similar performance.
- The prestressed pavement performed fairly well, although there was a good deal of trouble in maintaining the gap slabs. While there is definitely promise for this type of design, it is still in its infancy and will require more evolution.

- The 9 in CRCP is performing very well as the innermost lane (lane 1) to the prestressed pavement. However, ever since its construction, it has exhibited a good deal of roughness that was evidently built-in during construction. This type of design holds the promise of increased rideability and lower maintenance costs, both of which would make it a candidate design for the Phoenix Urban Corridor. It may be desirable for ADOT to construct a short section of CRCP in the truck lane to evaluate its potential as a feasible design.

It should be noted from the evaluation that all of the designs were structurally sound and displayed no signs of fatigue damage. The major problems that occurred in the pavements was joint faulting and joint spalling. The joint faulting problem can be linked to the lack of dowel bars (in the older concrete pavements) and perhaps to slab warping effects. The transverse joint spalling appeared to develop because of the lack of a good joint sealing program. Incompressibles lodge themselves in the joints and as the slabs expand, joint spalling and bridge pushing are often the result.

This preliminary assessment is based solely on a subjective evaluation of the data. Additional evaluations are conducted in chapters 4 and 5 in order to more thoroughly assess the applicability of the various pavement designs for use in the Phoenix Urban Corridor.

# CHAPTER 4 EVALUATION OF CONCRETE PAVEMENT DESIGN AND ANALYSIS MODELS

## 1. INTRODUCTION

There are a number of different design methods and analysis programs available for the design and evaluation of concrete pavements. These programs can be used for such things as the determination of the structural thickness of a concrete pavement, the assessment of a concrete pavement response to environmental and traffic loading, and the prediction of the future performance of inservice concrete pavements.

The Arizona Department of Transportation is interested in the applicability of some of the various design models and analysis procedures to their local conditions. This chapter discusses some of the various models of interest to ADOT and their potential applicability for use in Arizona.

Recently, a comprehensive review and evaluation of the various design and analysis models was conducted for the FHWA.<sup>(12,13)</sup> That evaluation consisted of a thorough description of some of the more prominent models, including a discussion of their capabilities and limitations, and a sensitivity analysis. Therefore, where appropriate, results of the FHWA study will be drawn upon in order to reduce duplication of effort.

## 2. ANALYSIS MODELS

Detailed case studies were performed under the previously-cited FHWA study to examine the capabilities of seven promising design and analysis models.<sup>(12)</sup> Four large experimental concrete pavement projects, one in each major climatic zone, were chosen to perform the analyses. The models used in the case studies were:

- Climatic Model—CMS<sup>(14,15)</sup>
- Drainage Characteristics Model—Liu-Lytton<sup>(16,17)</sup>
- Structural Analysis Model—ILLI-SLAB<sup>(18,19,20)</sup> and JSLAB<sup>(21,22)</sup>
- Design Method—JCP-1<sup>(23,24)</sup>
- Shoulder Design and Analysis Models—JCS-1<sup>(25)</sup> and BERM<sup>(26)</sup>

The case studies provided insight into the usefulness of these programs in the rigid pavement design process. The results of the analysis performed under the FHWA study as well as the applicability of the model for use under this study are summarized below.

## Climatic Model

The CMS (Climatic-Materials-Structural Model) was initially developed for the determination of the effect of climate and moisture on the structural properties on multilayered flexible pavement systems.<sup>(14,15)</sup> Because the model is based on fundamental principles of heat transfer, moisture movement, and material response to repeated loading, the theories are applicable for rigid pavements as well. Several of the input variables can be modified to accurately model rigid pavements.

This program fully models the effect of the environment on the pavement structure in terms of:

- Temperature changes in the slab.
- The effect of moisture (and temperature) on the paving layers in terms of stiffness of the layers.
- Frost penetration within the paving layers.

The thermal gradient capabilities of this program are used to determine the seasonal variation in thermal gradient. The thermal gradient, in turn, is used for the determination of stresses induced by temperature differences between the top and bottom of the slab. The CMS program is of interest to ADOT engineers and is more thoroughly discussed in section 3 of this chapter.

## Drainage Model

The Liu-Lytton drainage analysis model calculates the drainage capabilities of the pavement system, the average stiffness of the paving layers (both wet and dry), and the probabilities of wet and dry conditions.<sup>(16,17)</sup> The program accomplishes this with inputs on the drainability of the paving layers, the condition of the joints and cracks in terms of moisture infiltration, information on the design cross section, and climatic information about the area.

Several problems with the program were presented in reference 12. The major drawbacks of the program concerning its use in Arizona include:

- The program does not model impermeable base course layers.
- Default values for soil and base strength values under wet and dry conditions are unrealistic.
- The program will only allow a maximum of 99 consecutive dry days per year and Phoenix is very likely to have well over 99 consecutive dry days.

Because of these limitations, the program is not suitable for further analysis of Arizona's rigid pavement system.

## Structural Analysis Models

ILLI-SLAB is a finite element, structural analysis program for rigid pavements which was developed at the University of Illinois in 1977.<sup>(18,19,20)</sup> Since that time the program has gone through numerous technical changes, revisions, and refinements. Finite element analysis methods are used to model the pavement system and analyze the system's response to environmental and traffic loading.

Under the FHWA study, the ILLI-SLAB model was chosen as the preferred finite element, structural analysis model. Several technical problems were discovered regarding the use of the JSLAB finite element model.<sup>(12)</sup> That program was based on an early version of the ILLI-SLAB program, one in which the stiffness matrix was in error. The errors in the stiffness matrix result in an inaccurate calculation of stresses and deflections. Therefore, the most current version of the ILLI-SLAB program is used for additional analyses under this study.

## Design Method

A program that can be used to evaluate rigid pavement designs or to design a rigid pavement structure is JCP-1.<sup>(23,24)</sup> This program performs a detailed analysis of the fatigue characteristics associated with a particular design. The fatigue characteristics are evaluated in this program in terms of load, load placement, and the effect of thermal stresses. A separate analysis is also performed considering serviceability as a failure mode.

However, based upon the results of the performance evaluations in chapter 3, the pavement sections in Arizona have experienced little, if any, fatigue cracking. The cracking that did occur was more often longitudinal cracking and was believed to be more likely the result of inadequate or late sawing of the longitudinal joints. Thus, it is not believed that further investigation of the JCP-1 program is warranted.

## Shoulder Analysis and Design

The JCS-1 program can be used to design or to evaluate the design of a tied concrete shoulder.<sup>(25)</sup> Using the mainline pavement axle load distribution, a fatigue analysis is performed for the shoulder considering encroaching and parked traffic. The BERM program can be used to design or to evaluate the design of an asphalt concrete or tied concrete shoulders.<sup>(26)</sup> The materials properties of the shoulder layers are used to determine the shoulder's fatigue properties and the expected life, in terms of encroaching or parked equivalent axle loads, of the shoulder.

While these programs are extremely useful in the design of shoulders, they will not be used further in this study. Instead, where appropriate, the effects of shoulder type will be considered in the ILLI-SLAB program.

### 3. THE CMS PROGRAM

#### Introduction

The Climatic-Materials-Structural (CMS) program models the influence of climate on the behavior of pavement systems. Using climatic and materials information for a given pavement section, time-dependent temperature profiles, moisture profiles, and structural parameters of the pavement system are calculated. The program was originally developed for flexible pavements, although the basic theoretical principles also apply to rigid pavements. The input variables to be used when analyzing portland cement concrete were determined by the developer to enable the program to be used on rigid pavement systems; these are listed in table 15. The other required input variables are a function of the specific materials used for the base and subbase, subgrade conditions, and environmental factors.

The accurate modeling of the effects of moisture and temperature on paving layers is important in the design of a pavement system. The program was developed to be used as an integral step in the design process as shown in figure 18. Using site-specific climatic data and detailed information about the paving materials, the program generates materials properties and temperature and moisture profiles over time. These outputs are used as inputs to structural analysis models, fatigue analysis models, and predictive models to aid the engineer in the design of the pavement.

The FHWA recently developed a comprehensive program that integrates the CMS models, the Liu-Lytton models, and the CRREL frost heave models into a package for the evaluation of climatic effects on pavements. While not evaluated under this project, this program should prove useful in evaluating the effects of temperature and rainfall on concrete pavement performance.

#### Brief Technical Description

The CMS program contains three discrete models: a temperature model, a moisture model, and a material stiffness model. A detailed explanation of these models is presented in reference 14, but a brief summary is presented below:

1. The effect of temperature on the pavement system is modeled through the use of a one-dimensional, forward-finite difference heat transfer model. This heat transfer model was developed to evaluate the frost action and temperature distribution in multilayered pavement systems.
2. The moisture model, used to predict moisture movements through soils subject to isothermal conditions, is based on a finite-difference solution of 1- and 2-dimensional moisture movements. The model characterizes the transient moisture conditions in subgrade soil for a range of boundary conditions.

Table 15. CMS inputs for use with concrete pavements.

VARIABLE	CONCRETE INPUT
Thermal conductivity, btu/hr-ft-°F	
dry	0.54
10 % moisture	0.70
wet	1.0
Heat capacity, BTU/lb-°F	0.23 (0.20-0.25)
Air content of surface, %	4.0
Short-wave absorptivity	0.65
Emissivity factor	0.65
Material Code	1
Penetration value	60.0
Poisson's ratio	0.15
Ring and Ball value	170.0
Stiffness value, kg/cm <sup>2</sup>	PCC stiffness
Gravimetric Water Content (percent of weight of solids)	3.0

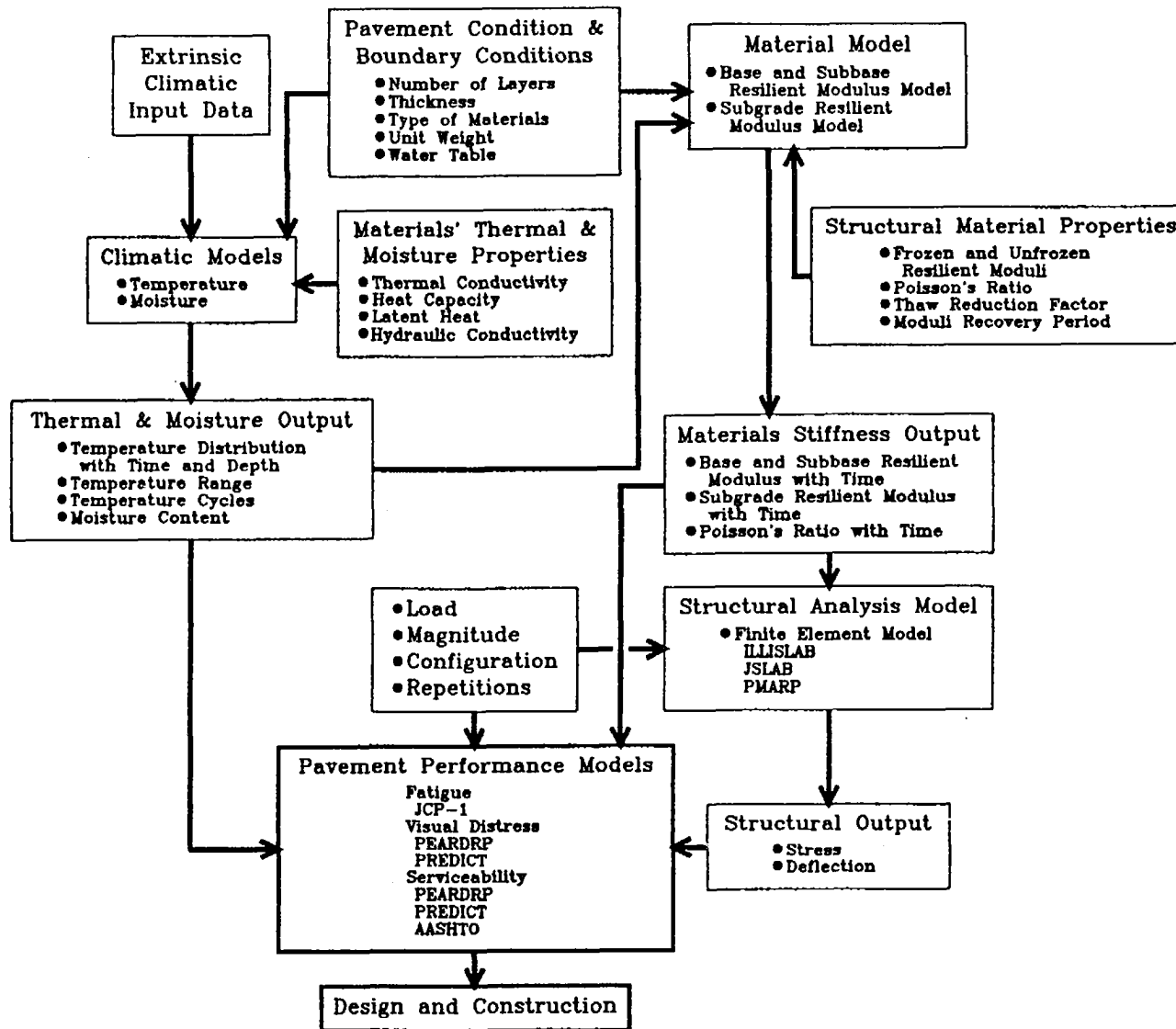


Figure 18. Use of CMS in the design process.

3. The properties of the granular materials are modeled though the use of the resilient modulus. The resilient modulus of the granular materials will change with varying moisture and temperature (frozen, unfrozen, or thaw-recovery) conditions. Based on work by many researchers, regression equations were developed to determine the material's properties as a function of temperature and moisture conditions.<sup>(27,28,29)</sup>

The accuracy of the CMS program output is highly dependent on the quality of the input data. It is extremely important that the boundary conditions, climatic conditions, and materials properties accurately represent the system to be analyzed. The theoretical validity of the individual models comprising the CMS model have been demonstrated, although the validity of the interaction of the models has not been proven.<sup>(14)</sup> This validation would require the instrumentation and long-term monitoring of pavement sections to compare the outputs from the CMS program to the actual field-measured values.

### Analysis of Results

The CMS program is used to calculate the thermal gradient that may develop in a rigid pavement under the climatic conditions of the Phoenix area. However, the moisture and material characterization models have limited applicability to this project and will not be considered in this analysis. Due to the voluminous program outputs and the proximity of the sections within the urban corridor, a representative section (AZ 2) was randomly chosen for analysis.

The CMS program was executed using site-specific climatic data to analyze the temperature differential through the portland cement concrete slab. The program was executed for the entire year of 1987 to examine the fluctuation in thermal gradient at 6 a.m. and 3 p.m.

The average thermal gradient is defined as shown below:

$$g = [\text{TEMP}_{\text{top}} - \text{TEMP}_{\text{bottom}}] / \text{THICK} \quad (1)$$

where:

- $g$  = average thermal gradient, °F/in
- $\text{TEMP}_{\text{top}}$  = temperature at the top of the slab, °F
- $\text{TEMP}_{\text{bottom}}$  = temperature at the bottom of the slab, °F
- $\text{THICK}$  = thickness of the slab, in

A positive gradient indicates the top of the slab is warmer than the bottom and normally occurs during the day. A negative gradient indicates that the bottom of the slab is warmer than the top. The negative gradient condition typically occurs during the cooler hours of the evening. The effect of the thermal gradient on the development of stresses in concrete pavements is discussed in section 4.

The temperature profile through the depth of the 10 in slab is shown in figure 19. This figure shows the temperatures of various portions of the slab at specified times on the day of July 15, 1987. The largest thermal gradient occurred at 4 p.m., while the smallest thermal gradient occurred at 2 a.m. It is of importance to note the magnitude of the thermal gradient that develops in the slab, even at such hours as 10 a.m. or 8 p.m.

Figures 20 and 21 show the thermal gradient at 6 a.m. varies throughout the year (1987) for AZ 2. The thermal gradient at 6 a.m. is negative for the majority of the year, as expected. The 6 a.m. gradient is highly variable throughout the year. There are several periods where the thermal gradient is positive during the morning hours. Typically, periods of positive morning thermal gradient may be attributed to relatively small daily temperature changes. For example, the average temperature change in February 1987 was 24.9 °F, whereas, during the period of positive thermal gradient, the average temperature drop was 18 °F. Under the FHWA study, similar trends were observed for sections located at Tracy, California.<sup>(12)</sup>

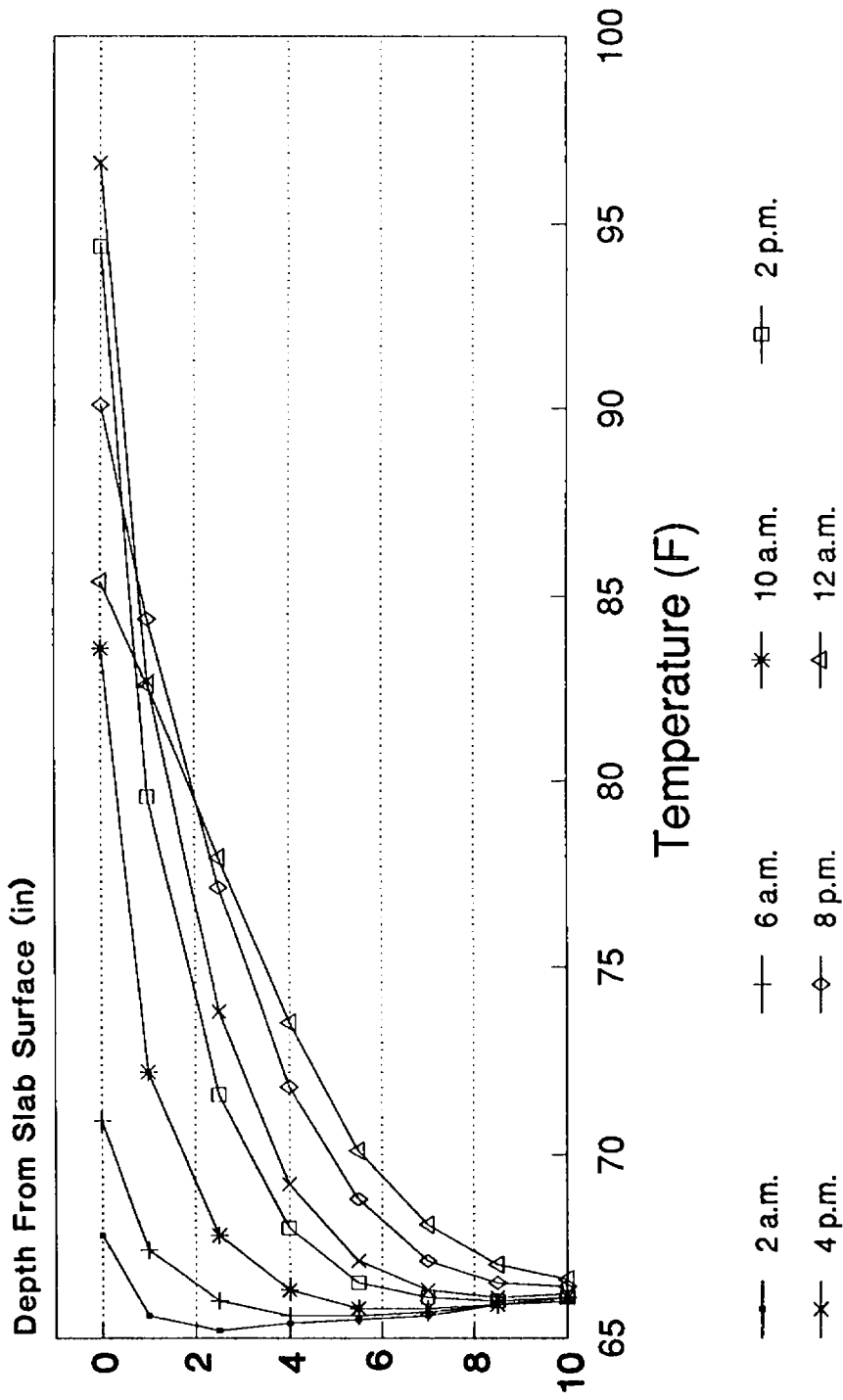
Periods where the thermal gradient is highly negative typically correspond to days when the maximum daytime temperature is much higher than the minimum nighttime temperature. This change causes the slab surface to heat up during the hot day and cool down quickly at night. On the other hand, the temperature at the bottom of the slab is not affected by the solar radiation and temperature nearly as much due to its greater depth.

The gradient at 3 p.m. for 1987 is shown in figures 22 and 23. The thermal gradient is positive throughout the whole year, as expected, during the hot hours of the day. The sun warms the surface of the pavement rapidly while the bottom of the slab is still cool. As a general trend, the 3 p.m. thermal gradient peaks during the summer months when the solar radiation, the temperatures, and the number of hours of sunshine are at their yearly maximums. During the cooler months of the year, the 3 p.m. gradient is much closer to zero. This may be due to less intense solar radiation, more frequent cloud cover, lower temperatures, and less severe temperature variation between day and night during the cooler months.

The relationship between the 6 a.m. and 3 p.m. thermal gradient is interesting. It appears that the days when the 6 a.m. gradient is higher (more positive), then the 3 p.m. gradient is higher also. The opposite is also true; on days when the 6 a.m. gradient is lower (more negative), the 3 p.m. gradient is lower. This phenomenon may be due to the fact that the cyclic air temperature fluctuations affect both the top and bottom of the slab. The top of the slab and the bottom of the slab respond to the changes in ambient temperature. As the air temperature increases, the temperature at the top and bottom of the slab also increase. However, they do so at different rates. The top of the slab is significantly affected by exposure to solar radiation.

# AZ 2

## Temperature vs. Depth



Temperature Change 33°F

Figure 19. Temperature profile for AZ 2 on July 15, 1987.

### AZ 2 Gradient vs Day

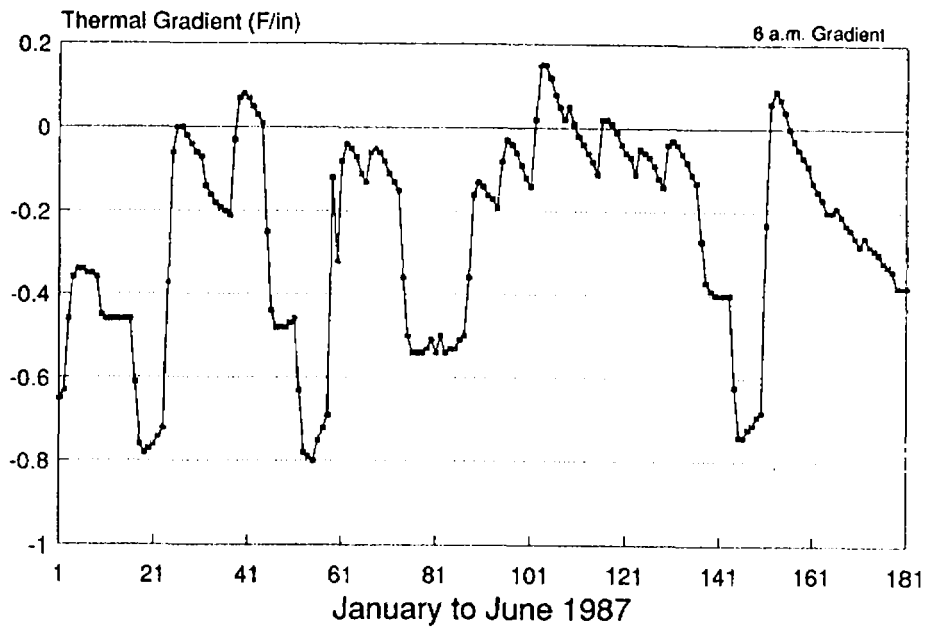


Figure 20. Variation in 6 a.m. thermal gradient for AZ 2, January to June 1987.

### AZ 2 Gradient vs Day

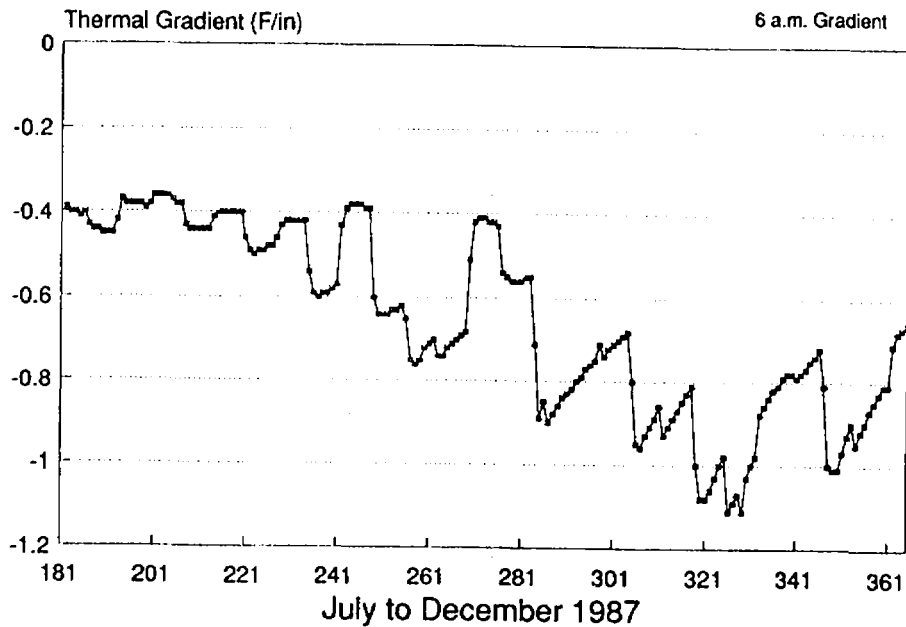


Figure 21. Variation in 6 a.m. thermal gradient for AZ 2, July to December 1987.

AZ 2  
Gradient vs Day

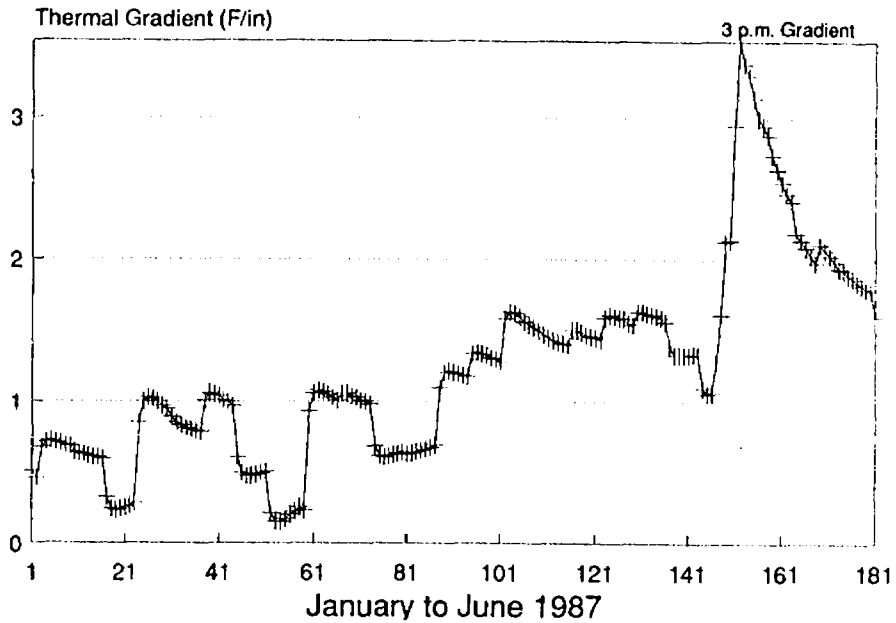


Figure 22. Variation in 3 p.m. thermal gradient for AZ 2, January to June 1987.

AZ 2  
Gradient vs Day

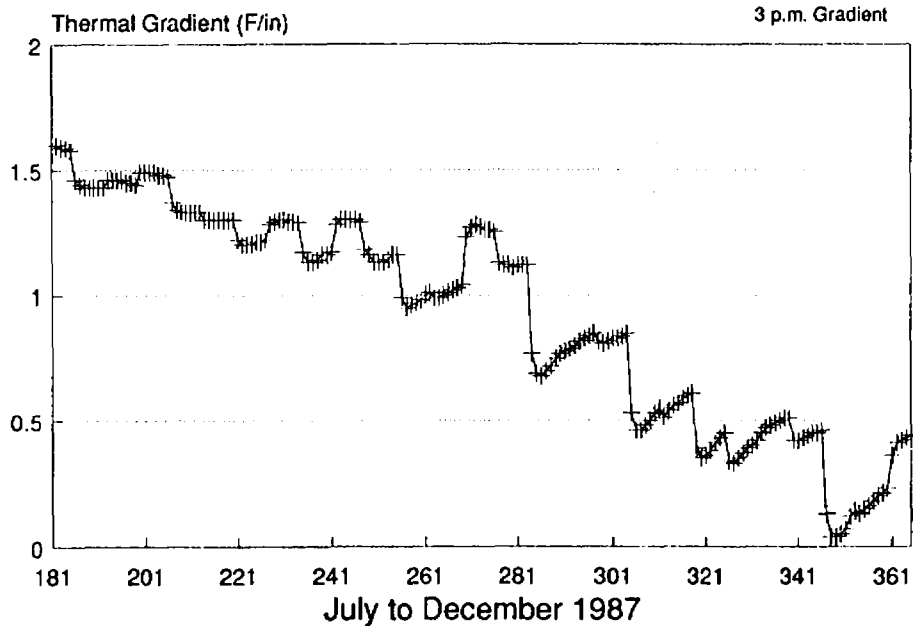


Figure 23. Variation in 3 p.m. thermal gradient for AZ 2, July to December 1987.

## Use of Thermal Gradient

The temperature gradient determined by CMS can be used as an input into the ILLI-SLAB program to examine the stresses that develop in a concrete slab due to temperature, loading, and the combination of temperature and load. The gradient was calculated during the month with the most severe daily temperature fluctuation because this would cause the largest change in gradient. In 1987, the month of June had an average maximum daily temperature of 104.6 °F and an average minimum daily temperature of 73.2 °F. The maximum daily temperature ranged from 99 °F to 112 °F. The minimum daily temperature ranged from 68 °F to 78 °F. The maximum gradient (occurring at 3 p.m.) during this time period ranged from 1.80 °F/in to 3.54 °F/in. The maximum gradient occurred early in the month when the bottom of the slab had not been warmed by the warm air temperatures. After the long period of extremely hot temperatures, the bottom of the slab warms considerably and the difference between the top and bottom of the slab lessens.

The daytime gradient produces a tensile stress at the bottom of the slab. Although the top of the slab tries to expand under the daytime gradient, the weight of the slab restrains its movement and produces a compressive stress at the top of the slab and a tensile stress at the bottom. The larger the thermal gradient the larger the induced stress, as illustrated in reference 23. A thermal gradient of 3.22 °F/in was selected for the use with the ILLI-SLAB program. This is the average of the ten highest daytime (3 p.m.) thermal gradients observed for the month of June 1987 which, as shown in figure 22, exhibits the maximum gradient throughout the year.

## 4. THE ILLI-SLAB PROGRAM

### Introduction

The ILLI-SLAB program is a finite element structural analysis program for the analysis of rigid pavements. Using design and material properties information, the stresses, deflections, and moments are calculated for the given slab configuration. The program is capable of modeling many design and analysis features, including, among others, various subgrade formulations, load transfer configurations, bonding conditions between layers, and axle load configurations. The program can examine any number of slabs in any arrangement and is also capable of calculating stress due to a temperature difference between the top and bottom of the slab.

### Brief Technical Description

The ILLI-SLAB finite element program is based on medium-thick plate theory, employs the four-noded, 12-degree of freedom plate bending (ACM or RPB 12) element.<sup>(18,19)</sup> While the complex mechanics of finite element theory will not be discussed here, additional information on the subject may be found in reference 30.

The ILLI-SLAB program was first developed in 1977 and has been under continuous revision, verification, and expansion at the University of Illinois. Through several research studies, the program's accuracy and ease of application has been improved. Revisions have also been made to facilitate meaningful interpretation of its results and to incorporate new foundation models. A short description of the basic assumptions regarding the concrete slab, base course, subgrade type, overlay, dowel bars, and aggregate interlock follows:

1. Small deformation theory of an elastic, homogeneous medium thick plate is employed for the concrete slab, stabilized base, and overlay. Such a plate is thick enough to carry a transverse load by flexure, yet it is not so thick that transverse shear forces become important.
2. The weight of the slab is neglected in the load stress calculations, but is considered in the calculation of temperature-induced stresses.
3. In the case of a bonded base or overlay, full strain compatibility exists at the interface. For the case of an unbonded base or overlay, shear stresses at the interface are neglected.
4. Dowel bars at joints are linearly elastic and are located at the neutral axis of the slab.
5. When aggregate interlock is specified for load transfer, load is transferred from one slab to another through shear. However, with dowel bars, some moment as well as shear is transferred across the joints. The *aggregate interlock factor* can range from 0.0 to more than  $1 * 10^8$  for associated deflection load transfer efficiencies of 0 percent to 100 percent. This relationship is nonlinear and quite complex.
6. Several foundation support models have been incorporated into the ILLI-SLAB program, including the traditional Winkler foundation, an elastic solid foundation, a spring model foundation, a "resilient" foundation model, and the Vlasov two-parameter foundation.
7. Loss of support beneath the slab may be modeled through the reduction of the support values at user specified areas.

### **Analysis of Results**

The ILLI-SLAB program was executed for the jointed concrete pavement (JCP) sections in this study to analyze the stress developing in the slab for three different loading conditions: the edge loading condition, with the load placed at the slab edge at the midpoint between the transverse joints; the corner loading condition, with the

load placed on the corner of the approach slab; and the thermal gradient loading condition, in which a stress is induced by a temperature difference between the top and bottom of the slab (no wheel loading considered).

In the corner loading analysis, and in the edge loading analysis when tied PCC shoulders existed, the deflection load transfer efficiency (LTE) was modeled through the use of the aggregate interlock factor and dowel and tiebar configuration. This value could be varied to match, within 5 percent, the deflection load transfer efficiencies calculated from the FWD testing.

The design information required to execute the program (slab thickness, joint spacing, PCC modulus of elasticity, static  $k$ -value on top of the base, and others) are readily available from the summary tables given in appendix A. A joint spacing of 15 ft was used for the edge and corner loading analyses, since this represented the average joint spacing. However, for the thermal gradient loading analysis, the 13 and 17 ft segments were also analyzed.

The prestressed and CRCP sections included in the study were not analyzed with ILLI-SLAB. To do so, the average crack spacing of these sections would have to be considered the "joint spacing" and the rebar would then be assumed to provide a certain amount of load transfer across the crack. However, under that approach, very short crack spacings would have to be employed and that violates the medium-thick plate theory upon which ILLI-SLAB is based. Furthermore, ILLI-SLAB does not consider any additional bending stiffness that the reinforcement may provide.

#### Edge Loading Condition

In the analysis of the edge loading condition, the slab was loaded at the midpoint between the joints with a 14.4 kip dual wheel load having tire pressures of 120 psi. A finite element mesh with this load configuration is shown in figure 24.

Those sections with tied PCC shoulders were modeled as a two-slab system (concrete shoulder slab and concrete mainline slab). In the ILLI-SLAB program, the deflection load transfer efficiency (LTE) across the longitudinal lane-shoulder joint was matched to within 5 percent of the LTE from the FWD testing. This was accomplished by adjusting the aggregate interlock factor in the program. Those sections with asphalt concrete shoulders were modeled as a one-slab system with no lateral support (free edge).

The results of the edge loading condition are shown in table 16. As expected, the point of maximum tensile stress, subgrade stress, and edge deflection was at the midpoint of the slab and at its outermost edge. The overall trends observed in the data are outlined below:

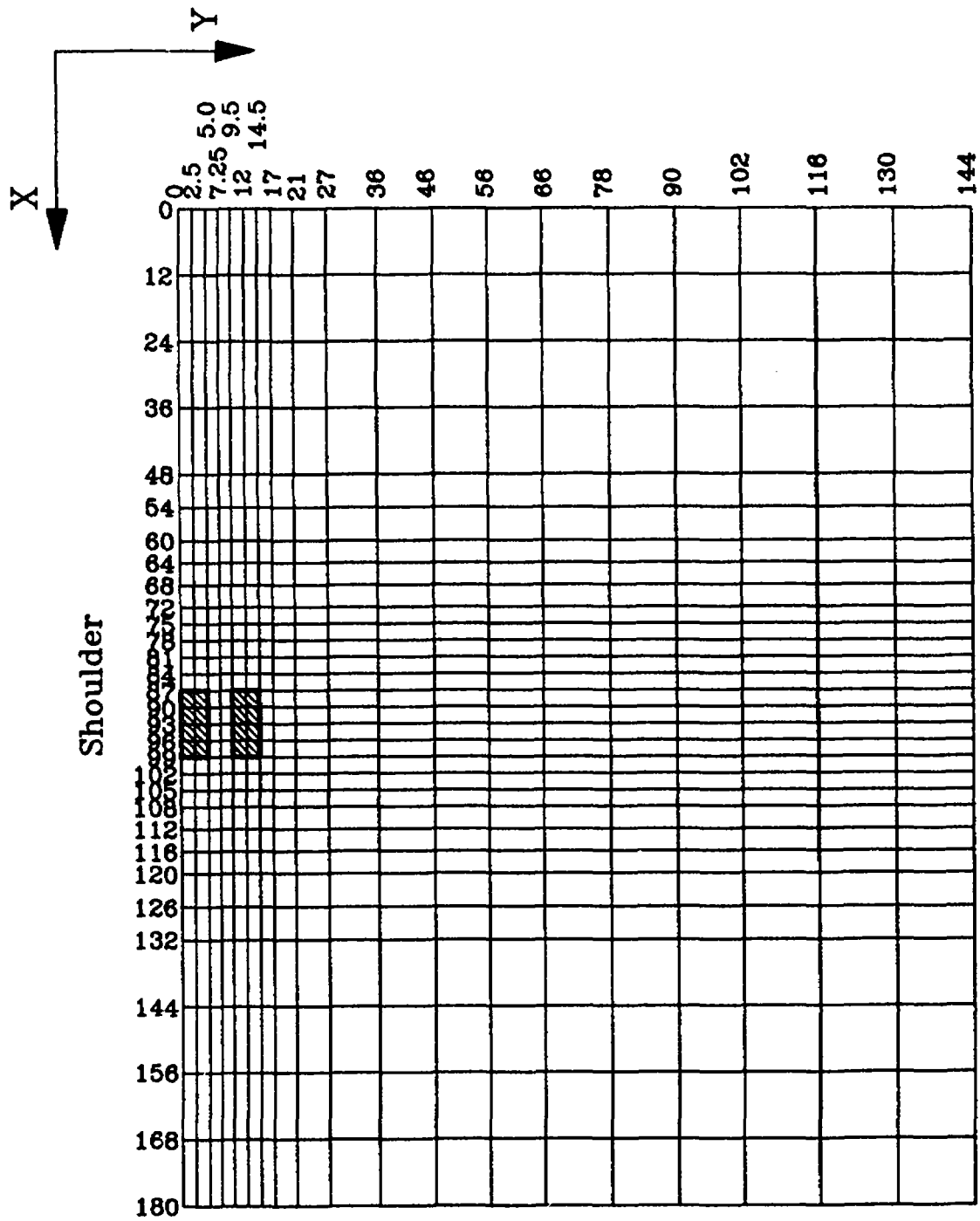


Figure 24. Example finite element mesh for edge loading condition.

Table 16. Summary of slab response to edge loading condition (14.4 kip dual wheel load with a tire pressure of 120 psi).

Section	Max. Edge Deflection, mils	Calculated Lane-Shoulder LTE, %	Max. Edge Stress, psi	Max. Subgrade Stress, psi
AZ 1-1				
15 ft slab	22.6	N/A	372	6.18
13 ft slab	23.2	N/A	372	6.34
17 ft slab	22.3	N/A	372	6.08
AZ 1-2	8.4	85	158	2.07
AZ 1-4	11.0	81	173	1.89
AZ 1-5	11.6	74	223	2.56
AZ 1-6	10.6	100	189	3.29
AZ 1-7	11.1	97	216	3.23
360-01	13.5	96	288	1.88
360-02	12.0	88	302	2.35
360-03	15.2	93	298	1.91
360-04	15.1	27	268	3.38
360-09	10.2	81	164	2.01
AZ 2	17.9	100	198	1.56
10-01	35.5	N/A	457	3.36
10-02	37.7	N/A	437	3.90
10-03	26.7	N/A	428	4.16
10-04	16.7	75	315	1.81
10-05	11.8	87	251	2.28
10-06	14.6	82	289	1.89
10-07	15.4	90	253	2.01
17-01	19.6	75	360	2.11
17-02	23.8	63	397	2.07
17-03	47.3	N/A	477	2.91
17-04	32.6	N/A	458	3.34
17-05	41.2	N/A	477	2.91
17-06	23.1	N/A	428	4.15
17-10	33.1	N/A	423	4.31
17-11	52.3	N/A	484	2.75

Notes: Except where noted, 15 ft joint spacing was assumed.  
Effect of thermal gradient not included.

1. The effect of joint spacing on the edge loading response is negligible for the given designs. The edge stresses and deflections were calculated for the 13 ft and 17 ft slab lengths of the random joint spacing pattern of AZ 1-1 and are given in table 16. For this section, it is observed that there is virtually no difference between the various slab responses.
2. Sections with tied PCC shoulders exhibited lower edge deflections, edge stresses, and subgrade stresses than sections with AC shoulders. This trend is shown in figure 25. An average edge stress of 444 psi was calculated for the 9-in thick sections with AC shoulders, whereas the average edge stress for the 9-in thick section with tied PCC shoulders was 293 psi (87 percent average deflection LTE).
3. Slab thickness has a large effect on the calculated stresses and deflections. As would be expected, the thicker the slab, the less the stresses and edge deflection. This trend is illustrated in figure 25, in which there is a trend to lower stresses as the slab thickness increases.
4. A parameter often used to estimate the fatigue damage of a slab is the ratio of the edge stress to the PCC modulus of rupture. It has been postulated that if this ratio is kept to a minimum level, then the cumulative fatigue damage on a pavement should not be excessive. If a pavement continually sees high stress ratios, then fatigue damage in the form of transverse cracking is expected to develop.

For illustration purposes only, this ratio was plotted as a function of slab thickness for each of the JPCP sections (see figure 26). It is interesting to note that many of the sections have ratios less than 0.5, and, as expected, the ratio decreases with increasing thickness. As most of the surveyed sections exhibited little, if any, slab cracking, it is possible that the fatigue damage has not accumulated to the point where cracking occurs or that the slabs are in a state of compression that reduces the actual edge stress. It should be pointed out that the stresses plotted in figure 26 do not include stresses due to a temperature gradient through the slab.

5. For sections with tied PCC shoulders, the higher the deflection LTE across the lane-shoulder joint, the lower the edge deflection, edge stresses, and subgrade stresses. This is illustrated in figure 27 for the maximum edge stress. As an example, AZ 1-5 and 360-04 are both of similar design, but AZ 1-5 exhibits 74 percent LTE across the lane-shoulder joint and 360-04 displays only 27 percent LTE. The edge stress, subgrade stress, and edge deflection for AZ 1-5 are 17 percent, 24 percent, and 23 percent less, respectively, than those of 360-04.

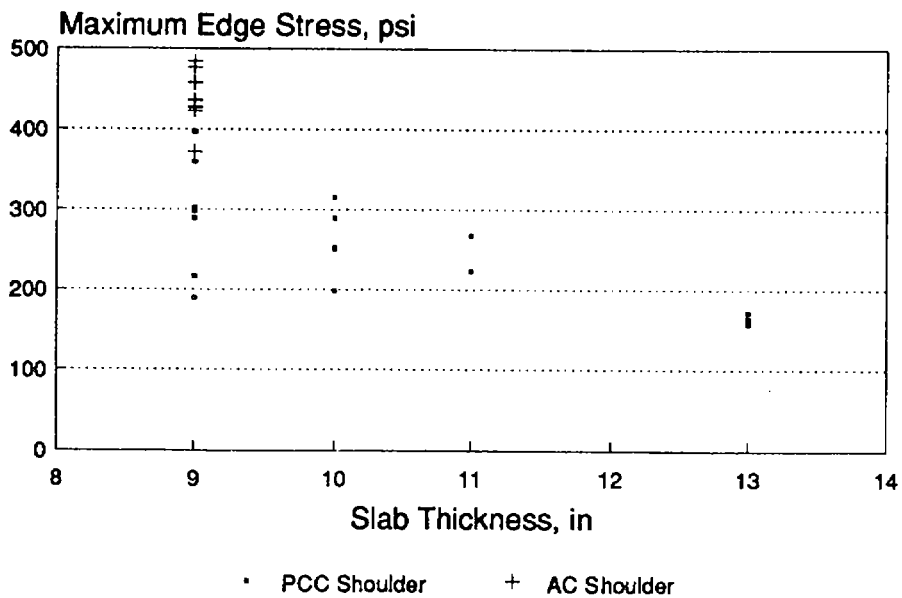


Figure 25. Variation in edge stress as a function of slab thickness and shoulder type.

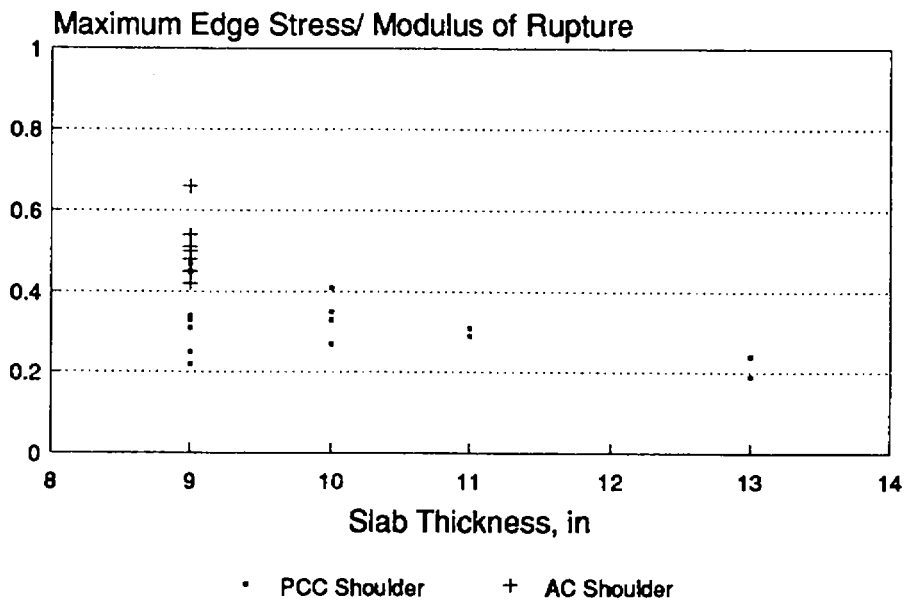
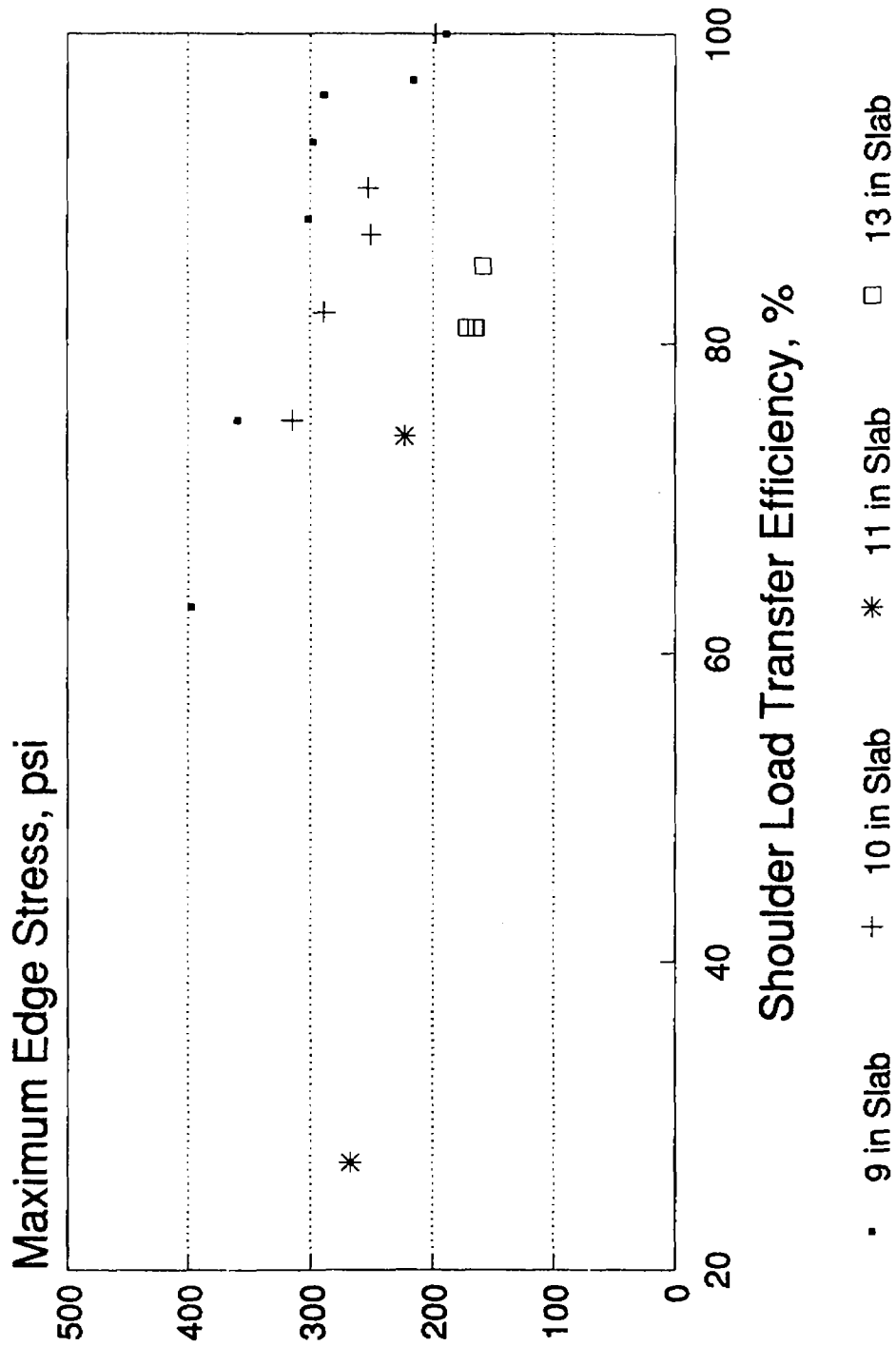


Figure 26. Variation in stress ratio as a function of slab thickness and shoulder type.



### Corner Loading Condition

For the corner loading condition, a 14.4-kip dual wheel with tire pressures of 120 psi was placed at the corner of the slab adjacent to the approach joint. The deflection load transfer across the transverse joints were matched to within 5 percent of that obtained from the FWD testing. A joint spacing of 15 ft was used in the analysis. The results of the corner loading analysis are shown in table 17. Observations from the data include:

1. Deflections are higher at the corner than at the edge for the same pavement sections. For example, the deflection at the free edge for AZ 1-1 is 22.6 mils, whereas the corner deflection (with 97 percent LTE) is 28.8 mils.
2. The corner stresses are lower than the edge stresses for the same pavement sections. For example, AZ 1-1 has an edge stress of 372 psi, whereas the corner stress is 167 psi. This is with 97 percent LTE and both the edge and the corner fully supported.
3. A reduction in stress and deflection is observed for sections with higher load transfer efficiency. Sections with deteriorated load transfer will experience higher deflections and much higher levels of stress than sections with satisfactory load transfer efficiency. If a section exhibits poor load transfer, as the load passes from the approach slab to the leave slab, the approach and leave slabs will experience higher stresses and deflections. This can lead to pumping and loss of support beneath the slab.

### Thermal Gradient Loading Condition

A temperature gradient through a slab causes stresses to develop. A positive thermal gradient, which indicates that the top of the slab is warmer than the bottom, results in the development of a tensile stress at the bottom of the slab, whereas a negative thermal gradient results in a compressive stress at the bottom of the slab. During the times when the gradient is positive, typically during the daytime, the total combined stress (combination of thermal stress and load-induced stress) at the bottom of the slab edge is much greater than when the gradient is negative.

The ILLI-SLAB program was executed to examine development of thermal stresses in the slab (load was not considered). The average maximum daytime gradient, determined from CMS, was used in the analysis since this is the gradient that produces the maximum tensile stress at the bottom of the slab. Generally a joint spacing of 15 ft was used, although for those sections with random joint spacing, the thermal gradient analysis was conducted for each slab length in the pattern.

Table 17. Summary of slab response to corner loading condition (14.4 kip dual wheel load with a tire pressure of 120 psi).

Section	Loaded Corner Deflection, mils	Unloaded Corner Deflection, mils	Deflection LTE, %	Max. Tensile Corner Stress, psi	Max. Corner Subgrade Stress, psi
AZ 1-1	28.8	27.9	97	167	7.86
AZ 1-2	10.4	9.8	96	62	2.55
AZ 1-4	12.8	12.3	96	65	2.20
AZ 1-5	14.7	14.2	96	92	3.23
AZ 1-6	13.6	13.3	97	92	4.23
AZ 1-7	14.3	13.7	96	93	4.16
360-01	21.5	5.3	25	91	4.07
360-02	21.1	8.6	41	83	4.12
360-03	23.2	12.1	52	93	2.99
360-04	25.9	25.2	98	113	3.21
360-09	12.6	12.1	96	66	2.56
AZ 2	21.9	16.5	75	198	1.91
10-01	41.7	41.0	99	186	3.94
10-02	45.5	44.9	99	181	4.71
10-03	32.7	32.0	98	178	5.10
10-04	24.1	11.7	49	413	2.61
10-05	15.5	13.6	88	156	2.66
10-06	16.7	14.8	89	162	2.15
10-07	17.5	17.0	97	138	2.28
17-01	23.4	22.9	98	142	2.52
17-02	28.8	28.2	98	158	2.50
17-03	52.3	51.6	99	191	3.27
17-04	38.3	37.6	98	186	3.92
17-05	46.1	45.5	99	191	3.25
17-06	28.4	27.7	98	178	5.09
17-10	40.7	40.0	98	178	5.29
17-11	52.3	48.7	93	186	3.27

Note: Effect of thermal gradient not included.

The results of the thermal stress analysis for the study sections are presented in table 18. Examination of the data in table 18 yields the following observations:

1. A positive thermal gradient (daytime gradient) results in tensile stresses at the bottom of the slab. The maximum thermal tensile stress occurs at the center of the slab, and maximum *edge* thermal tensile stress occurs at the edge of the slab exactly midway between the joints.
2. Sections with stiffer bases result in higher thermal stresses. This trend is illustrated in figure 28, which shows the maximum thermal edge stress for 15 ft slabs as a function of the effective *k*-value. Although there is some scatter of data, the general trend is that sections with lower *k*-values have lower maximum thermal edge stress. For the most part, those sections with the lowest stresses were constructed on an aggregate base with relatively low *k*-values. The reason for this is that stiffer base materials resist the movement of the curling slab, whereas very soft bases allow the slab to curl and conform more to the shape of the curling slab, thus resulting in less stress.
3. Figure 28 also shows that slab thickness influences the maximum thermal edge stress. As the slab thickness increases, the maximum thermal edge stress decreases. Thicker slabs exhibit less thermal stress than thinner slabs.
4. In figure 29, the maximum thermal edge stress was plotted against the radius of relative stiffness (*ℓ*-value), a parameter that represents the overall stiffness of a concrete pavement system. This was an attempt to account for some of the variation that was noted in figure 28. The *ℓ*-value is defined as follows:

$$\ell = \left[ (E \cdot h^3) / (12 \cdot k \cdot (1 - \mu^2)) \right]^{0.25} \quad (2)$$

where:

- E = PCC Elastic Modulus, psi
- h = Slab thickness, in
- k = Effective Modulus of Subgrade Reaction, psi/in
- μ = Poisson's Ratio (generally assumed to be 0.15)

Using the exact slab values for each section, the radius of relative stiffness was calculated and tabulated in table 18. The maximum thermal edge stress was then plotted against the radius of relative stiffness in figure 29. The trend from that figure is that higher *ℓ*-values result in lower stresses. And, upon examining equation 2, it is apparent

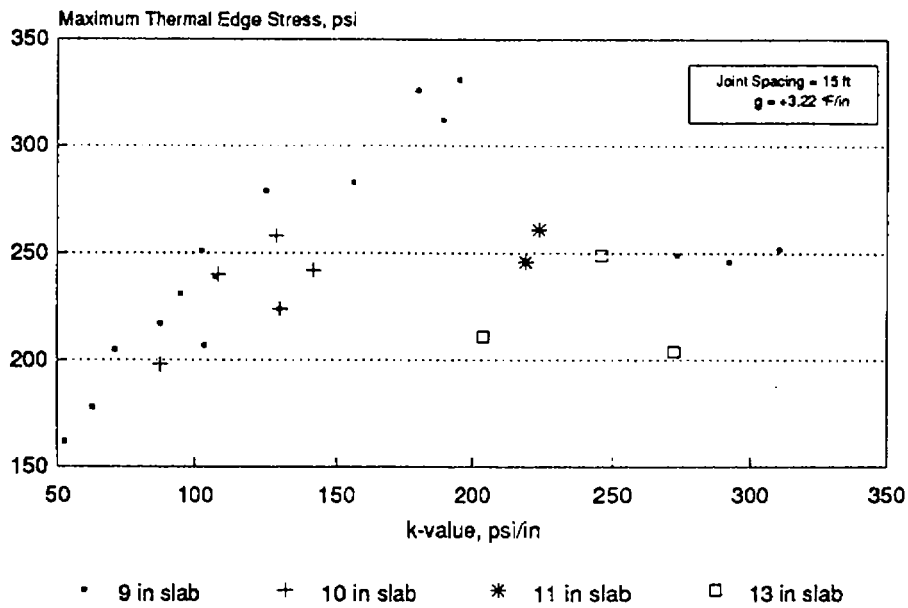


Figure 28. Variation in thermal edge stress as a function of k-value and slab thickness.

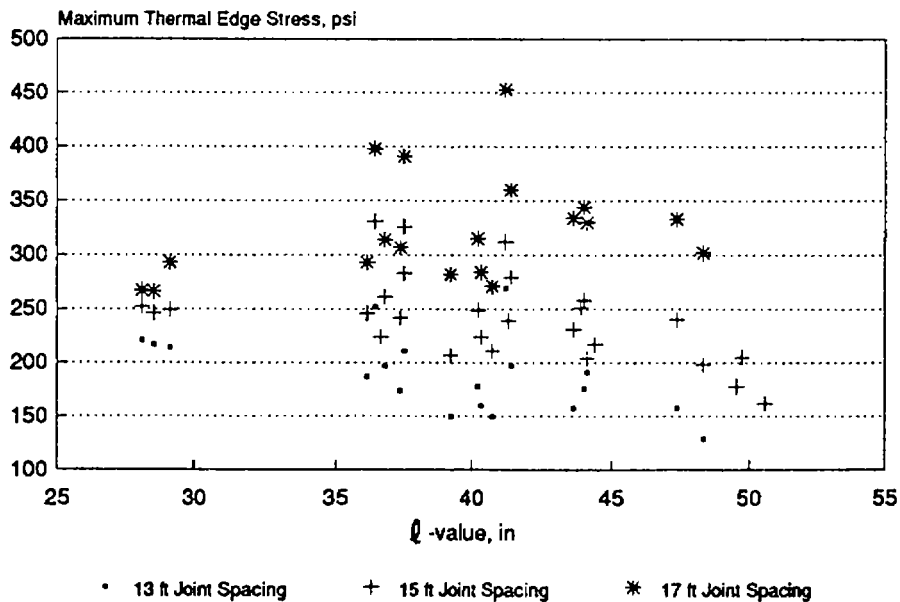


Figure 29. Variation in thermal edge stress as a function of l-value and joint spacing.

Table 18. Summary of maximum thermal stresses for each section due to daytime thermal gradient of 3.22 °F.

Section	t-value	13 ft Slabs		15 ft Slabs		17 ft Slabs	
		Max. Thermal Tensile Stress, psi	Max. Edge Thermal Tensile Stress, psi	Max. Thermal Tensile Stress, psi	Max. Edge Tensile Stress, psi	Max. Thermal Tensile Stress, psi	Max. Edge Tensile Stress, psi
AZ 1-1	29.08	242	214	277	249	324	293
AZ 1-2	40.23	198	178	267	249	333	315
AZ 1-4	44.15	212	191	217	204	350	330
AZ 1-5	36.09	209	187	267	246	314	293
AZ 1-6	28.05	250	221	281	252	298	267
AZ 1-7	28.48	245	217	273	246	295	266
360-01	41.65	299	269	334	312	482	453
360-02	36.37	281	252	359	331	426	398
360-03	41.44	218	197	299	279	379	360
360-04	36.72	219	197	282	261	336	314
360-09	40.77	167	150	227	211	285	271
AZ 2	48.31	143	129	210	198	314	302
10-01	43.67	175	158	246	231	350	334
10-02	39.19	167	150	222	207	298	282
10-03	37.44	236	211	306	283	414	391
10-04	47.34	175	158	255	240	346	333
10-05	37.30	193	174	260	242	325	307
10-06	44.04	195	176	275	258	360	344
10-07	40.34	178	160	240	224	300	284
17-01	41.35	N/A	N/A	256	239	N/A	N/A
17-02	44.42	N/A	N/A	232	217	N/A	N/A
17-03	49.54	N/A	N/A	189	178	N/A	N/A
17-04	43.93	N/A	N/A	268	251	N/A	N/A
17-05	49.73	N/A	N/A	216	205	N/A	N/A
17-06	37.44	N/A	N/A	353	326	N/A	N/A
17-10	36.57	N/A	N/A	243	224	N/A	N/A
17-11	50.58	N/A	N/A	171	162	N/A	N/A

that the larger elastic modulus values or slab thicknesses will increase the  $\ell$ -value and thereby reduce stress. Furthermore, increasing the  $k$ -value will decrease the  $\ell$ -value and thereby increase the stress, as is shown in figure 28.

5. Shorter jointed pavements exhibit less thermal stress than longer jointed pavements. This is apparent from examining table 18 for those sections that had random joint spacing. This is also illustrated in figure 29, which shows that longer joint spacing produce larger maximum thermal edge stresses.
6. Figures 30 and 31 are graphs of maximum thermal edge stress as a function of the ratio of the slab length (in inches) to the radius of relative stiffness. This parameter was postulated by Ioannides and Salsilli-Murua as critical to the development of transverse slab cracking.<sup>(3)</sup> It is apparent from figures 30 (stabilized base) and 31 (aggregate base/no base) that as  $L/\ell$  increases, there is a general trend in increasing stresses. A recent FHWA study, which evaluated this parameter with field data from 95 pavement sections, suggests the following maximum values for the  $L/\ell$  parameter to control transverse cracking:<sup>(4)</sup>

$$\begin{array}{ll} L/\ell \leq 5.5 & \text{for aggregate bases} \\ L/\ell \leq 4.5 & \text{for stabilized bases} \end{array}$$

Figures 30 and 31 indicate that, at the above critical  $L/\ell$  value, the maximum thermal edge stresses are in the neighborhood of 300 psi.

### Conclusions and Recommendations

The ILLI-SLAB program is a comprehensive finite element program that was specifically developed to analyze rigid pavement structures. The inputs required for execution of the program are readily obtainable. However, the user must carefully observe the recommendations on the development of the finite element mesh as this can have a large impact on the accuracy of the program's outputs.

This program is directly applicable to the design of rigid pavements. The accurate calculation of the stresses that develop in rigid pavements under loading (due to temperature or traffic) is critical for the determination of the life of a given pavement cross section. Several design procedures have been developed that rely on the calculation of stresses induced by given axle loads and configurations. Relationships have been developed that relate the number of repeated loadings at a given stress level (relative to the strength of the material) to the life of a concrete pavement.

**MAXIMUM THERMAL EDGE STRESS vs.  $L/\ell$   
STABILIZED BASE**

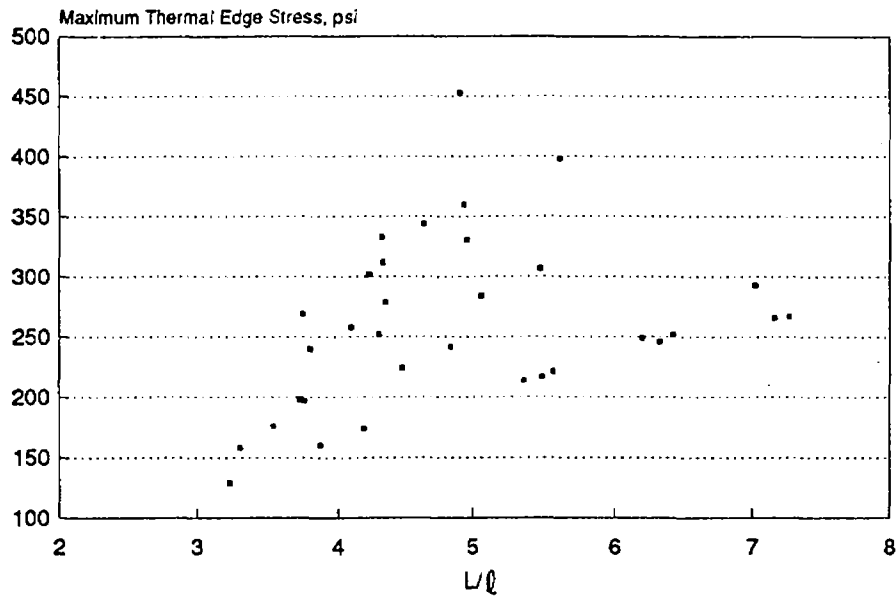


Figure 30. Thermal edge stress vs.  $L/\ell$  (stabilized bases).

**MAXIMUM THERMAL EDGE STRESS vs.  $L/\ell$   
AGG BASE/NO BASE**

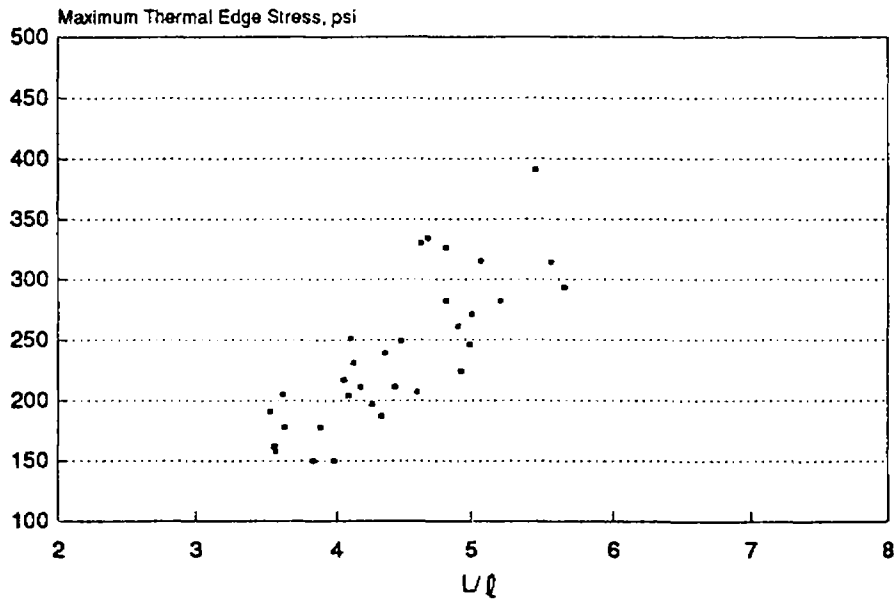


Figure 31. Thermal edge stress vs.  $L/\ell$  (aggregate base/no base).

## 5. ANALYSIS OF PAVEMENT PREDICTION MODELS

The models presented up to now have been analytical models used to calculate pavement responses to traffic or environmental loading. Another variety of models are prediction models that attempt to predict the inservice performance of a pavement at different time intervals based upon a set of inputs. Under a recent FHWA research project, the accuracy of several prediction models was tested.<sup>(12)</sup> That evaluation included seventeen sections from the dry-nonfreeze region, consisting of sections from Arizona and California.

The models were analyzed through a combination of the use of statistical procedures and a graphical examination of the results. A data set was created using the SAS™ statistical software package.<sup>(11)</sup> The paired-difference method, using a student *t*-distribution, was used to determine if the performance indicator (visible distress, faulting, roughness, and PSR) as predicted by the prediction models is statistically the same population (data set) as the *actual, field-measured* performance indicator. The paired difference test measures the mean difference of the measured and predicted performance indicator values, and then tests the null hypothesis, that is which assumes that the mean difference between the predicted and actual measurements is 0.0. In order to perform the paired difference test, a one-sample *t*-statistic is calculated for each data set ( $t_{\text{calc}}$  which is equal to the mean difference divided by the standard error of the mean) and then compared to a tabulated *t*-statistic ( $t_{\text{table}}$ ) for a specified confidence interval (90 percent was used in this case). If  $t_{\text{calc}} > t_{\text{table}}$ , then it can be inferred with 90-percent confidence that the sample of predicted performance indicators (from the models) is not statistically from the same population as the sample of measured performance indicators.

To reduce duplication of effort, portions of the following discussion is taken from reference 12 as it pertains to sections in the dry-nonfreeze region. The models evaluated included the AASHTO rigid pavement design model,<sup>(32)</sup> the PEARDARP models,<sup>(33,34,35)</sup> the NCHRP 1-19 (COPES) models,<sup>(36)</sup> and the PFAULT models.<sup>(37)</sup> An evaluation was also conducted on the new prediction models developed from the FHWA study.<sup>(12)</sup> A brief discussion of the various models and their ability to predict the performance of those sections in Arizona follows.

### AASHTO Design Model

The 1986 AASHTO Design Guide represents a revision of the original AASHTO design procedure.<sup>(32)</sup> The basic design equation was developed from the results of the AASHO Road Test, conducted in Northern Illinois in the late 1950's. The Road Test included both jointed plain concrete pavements (JPCP) and jointed reinforced concrete pavements (JRCP). The JPCP sections were doweled and had 15-ft joint spacing. These pavements were subjected to a fixed number of axle loads and types over a 2-year period. The modified equation is presented below:

$$\log_{10}(\text{ESAL}) = z_R^* s_o + 7.35 \log_{10}(\text{THICK} + 1) - 0.06 + \frac{\log_{10} [(\Delta\text{PSI}/(4.5-1.5))]}{[1 + (1.624 \cdot 10^7 / (\text{THICK} + 1)^{8.46})]}$$

$$+ (4.22 - 0.32 \cdot p_t) \cdot \log_{10} \left[ \frac{[M_R \cdot C_d^* (\text{THICK}^{0.75} - 1.132)]}{\{215.63 \cdot J^* [\text{THICK}^{0.75} - (18.42 / (E_{pcc} / k)^{0.25})]\}} \right] \quad (3)$$

where:

- ESAL = Cumulative 18-kip equivalent axle loads expected during the design period
- $z_R^*$  = Standard normal deviate based on level of reliability
- $s_o$  = Overall standard deviation
- D = THICK = slab thickness, in
- $p_i$  = Initial serviceability directly after construction
- $p_t$  = Terminal serviceability at the end of the design period
- $\Delta\text{PSI}$  = Change in serviceability over the design period  
=  $p_i - p_t$
- $M_R$  = Mean modulus of rupture, psi
- $C_d^*$  = Drainage coefficient
- J = J-factor
- $E_{pcc}$  = Concrete slab modulus of elasticity, psi
- k = Effective modulus of subgrade reaction, pci

\* indicates new variables added in 1986 revision

The AASHTO design equation is used differently for this analysis than it would typically be used in design. In design, the engineer determines the design thickness based on the forecasted traffic over the design life. The design life is based on a specific change in serviceability ( $\Delta\text{PSI}$ ). In this analysis, the thickness of a specific section is known and the cumulative ESAL's are calculated. The  $\Delta\text{PSI}$  is calculated as the difference between the initial serviceability (assumed to be 4.5) and the serviceability at the time of survey ( $\text{PSR}_{\text{survey}}$ ). Therefore, the design equation will predict the amount of ESAL's that the pavement *should have* sustained (if the equation predicts accurately) to reach a  $\Delta\text{PSI}$  of  $4.5 - \text{PSR}_{\text{survey}}$ .

The summary of the statistical analyses for the various models, including the AASHTO design model, is presented in table 19. This table is for sections in the dry-

Table 19. Summary of the statistical analysis of the selected prediction models using sections from the dry-nonfreeze climatic region (adapted from reference 12).

Model	Number of Observations	$t_{calc}$	$t_{table}^*$	$t_{calc} > t_{table}$	Adequately Predict Performance?
<b>AASHTO</b>					
PSR	17	2.915	1.746	YES	NO
<b>PEARLARP</b>					
PSI	17	6.509	1.746	YES	NO
ROUGHNESS	17	9.233	1.746	YES	NO
SPALLING	17	3.413	1.746	YES	NO
FAULTING	17	4.606	1.746	YES	NO
CRACKING	17	6.958	1.746	YES	NO
<b>COPEs</b>					
PUMPING	17	1.951	1.746	YES	NO
FAULTING	17	4.280	1.746	YES	NO
JT DETERIORATION	17	2.219	1.746	YES	NO
CRACKING	17	1.899	1.746	YES	NO
PSR	17	5.833	1.746	YES	NO
<b>PFAULT</b>					
FAULTING	17	3.569	1.746	YES	NO
<b>NEW FHWA MODELS</b>					
PSR	27	1.379	1.708	NO	YES
SPALLING	27	2.832	1.708	YES	NO
FAULTING (nondoweled)	22	6.341	1.721	YES	NO
CRACKING	27	3.882	1.708	YES	NO

\*  $t_{table}$  based on 90 percent confidence level.

nonfreeze climatic region only, and it is observed that  $t_{calc}$  is greater than  $t_{table}$  for the AASHTO model. This indicates that the AASHTO model does not adequately predict the ESAL's actually sustained by those pavement sections.

Figure 32 shows the predicted ESAL's versus the actual ESAL's for the sections in the dry-nonfreeze climatic zones. It is clear that the model generally overpredicts traffic. An examination of these results highlights the fact that one of the key terms in the AASHTO model is serviceability loss. This change in serviceability can occur prematurely due to materials problems, design problems, construction problems, and climatic conditions. These factors are typically not considered in design. In addition, while an average initial PSI of 4.5 was assumed, many of these projects may have had a much lower initial PSI.

### PEARDARP Prediction Models

As part of a comprehensive analysis on pumping of rigid pavements that was conducted for the FHWA, prediction models were developed for pumping, faulting, cracking, spalling, roughness, and serviceability.<sup>(33)</sup> The models were developed from various sources of data and the exact data base used is a function of the particular model in question. The models for each distress type are presented in the following sections.

#### PSI Model

$$PSI = 5.41 - 1.80 \log (SV + 1) - 0.09 (C + P)^{0.5} \quad (4)$$

where:

- PSI = Present Serviceability Index
- SV = slope variance (radians<sup>2</sup> X 10<sup>6</sup>)
- = SVR + SVF
- C = linear cracks, lin ft/1000 ft<sup>2</sup>
- P = patched area, sq ft/1000 ft<sup>2</sup>
- SVR = 0.000145 R<sup>2.255</sup>
- SVF = (0.00159/I) \* F<sup>1.729</sup>
- F = average faulting, in
- R = roughness, in/mi

Table 19 provides the summary of the statistical analysis of the PEARDARP predictive models, including the model for PSI. This table shows that the PEARDARP PSI model does not adequately predict the actual PSI for the pavement sections included from the dry-nonfreeze region. Figure 33 shows the comparison between the predicted PSI and actual PSR for the dry-nonfreeze region, and the model consistently overpredicts the results.

### AASHTO Design Equation Dry-Nonfreeze Region

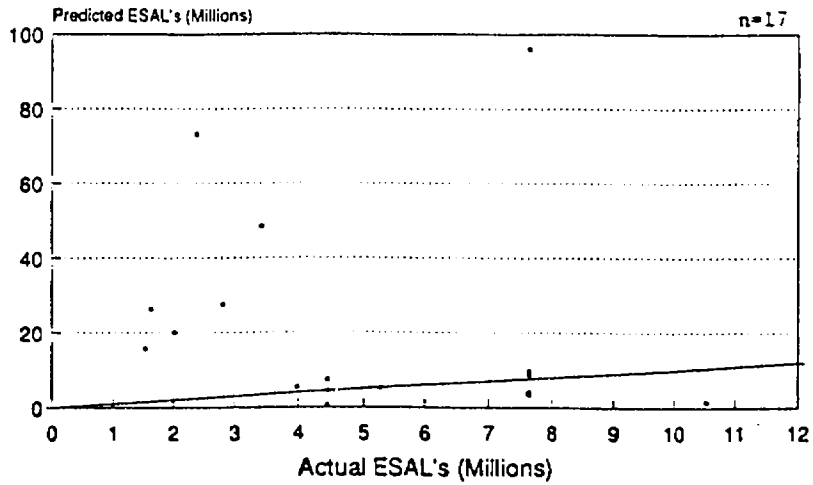


Figure 32. AASHTO predicted ESALs vs. actual ESALs for 17 sections in dry-nonfreeze region.

### PEARLARP PSI Model Dry-Nonfreeze Region

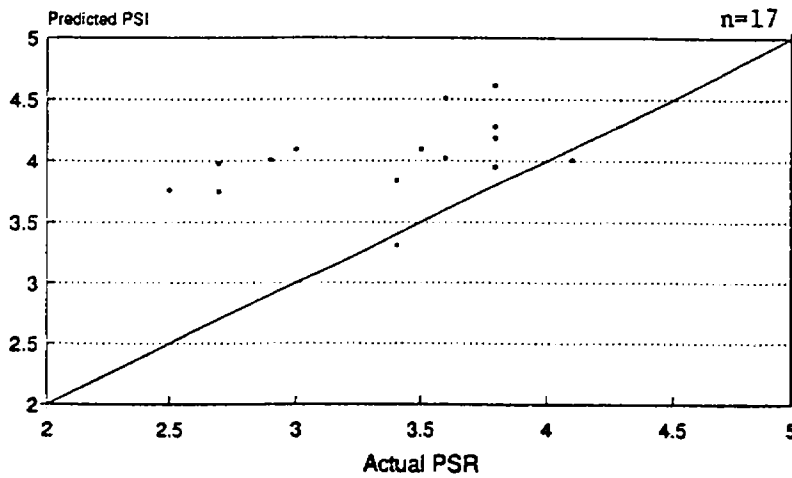


Figure 33. PEARLARP predicted PSI vs. actual PSI for 17 sections in dry-nonfreeze region.

### Roughness Model

$$R = 360 - 216 \left[ 1.5 - (1 + e^{-\beta/\rho X})^{-1} + (1 + e^{\Sigma ESAL - \beta/\rho X})^{-1} \right] \quad (5)$$

where:

R = roughness, in/mi

$\beta = -50.088 - 3.775*D + 30.644*D^{0.5}$

$\rho = -6.697 + 0.139*D^2$

$X = 10^{1.774Y}$

$$Y = \log \left[ \left( M_R / 690 \right) \frac{4 * \log(8.789 D^{0.75} / F) + 0.359}{4 * \log(Z^{0.25} (0.54 D^{0.75} / F)) + 0.359} \right]$$

$F = (30.56 + D^2)^{0.5} - 0.675D$

Z = E/k

D = slab thickness, in

E = modulus of the slab, psi

k = effective modulus of subgrade reaction, pci

$M_R$  = mean 28-day modulus of rupture, psi

$\Sigma ESAL$  = cumulative 18-kip equivalent single axle loads, millions

The statistical analysis of the PEARDARP roughness model is also summarized in table 19. The results indicate that the roughness model is not able to satisfactorily predict the measured pavement roughness for the pavement sections from the dry-nonfreeze region. Figure 34 shows the data for the sections from the dry-nonfreeze climatic zone, and the model always overpredicted.

### Spalling Model

$$F_s = 1 - e^{-\alpha(J-\beta)} \quad (6)$$

where:

$F_s$  = fraction of joints spalled

$\alpha = 0.0000162 A^{3.0806}$

J = transverse joint spacing, ft

A = pavement age, years

The results of the statistical analysis for the joint spalling model are shown in table 19 for the sections in the dry-nonfreeze climatic region. Again, the results of the statistical analysis indicate that the model is not able to satisfactorily predict the

### PEARDARP Roughness Model Dry-Nonfreeze Region

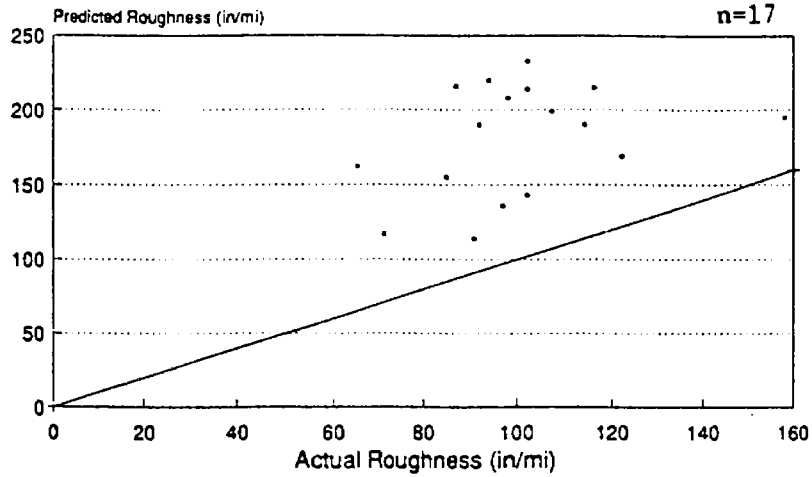


Figure 34. PEARDARP predicted roughness vs. actual roughness for 17 sections in dry-nonfreeze region.

### PEARDARP Spalling Model Dry-Nonfreeze Region

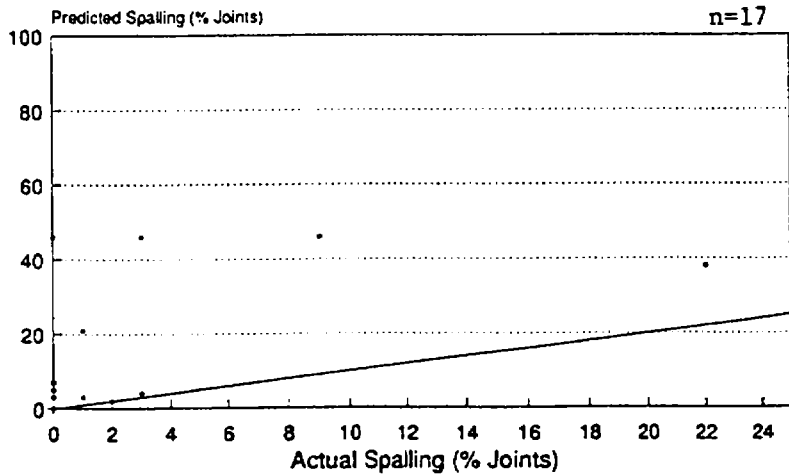


Figure 35. PEARDARP predicted spalling vs. actual spalling for 17 sections in dry-nonfreeze region.

spalling for these sections. This is illustrated in figure 35 in which it is shown that the model tended to overpredict transverse joint spalling for the dry-nonfreeze climatic region.

### Pumping Models

$$\text{NPI} = F * e^{-2.884 + 1.652 \log(\Sigma\text{ESAL} * \text{DE} / 10,000)} \quad (7)$$

$$P = 36.67 * \text{NPI} \quad (8)$$

$$\text{PU} = P + (1 * \text{nP}) \quad (9)$$

where:

- NPI = normalized pumping index, in<sup>3</sup>
- DE = deformation energy per application, in-lb
- log(DE) = 3.5754 - 0.3323\*D
- P = volume of pumped material, ft<sup>3</sup>/mi
- PU = volume of underseal material required, ft<sup>3</sup>/mi
- nP = number of pumping joints per mile
- nP = P/vvoid
- vvoid = average void volume per joint, ft<sup>3</sup>
- D = slab thickness, in
- ΣESAL = cumulative 18-kip equivalent single axle loads, millions
- F =  $f_{\text{JPCP}}$ , if nonreinforced PCC
- F =  $f_{\text{JRCP}}$ , if reinforced PCC
- $f_{\text{JPCP}} = f_{\text{sbl}} * f_{\text{d}} * f_{\text{lt}} * f_{\text{prec}} * f_{\text{sg}}$
- $f_{\text{sbl}}$  = subbase adjustment factor
- = 1.0, for granular material
- = 0.65 + 0.18log(ΣESAL), for stabilized material
- $f_{\text{d}}$  = drainage adjustment factor
- = 1.0, for poor drainage
- = 0.91 + 0.12log(ΣESAL) - 0.03\*D, for fair drainage
- = 0.68 + 0.15log(ΣESAL) - 0.04\*D, for good drainage
- = 0.01, for excellent drainage
- $f_{\text{lt}}$  = load transfer adequacy adjustment factor
- = 1.0, with dowels
- = 1.17 + 0.68log(ΣESAL) - 0.078\*D, without dowels
- $f_{\text{prec}}$  = rainfall adjustment factor
- = 0.89 + 0.26log(ΣESAL) - 0.07\*D, for dry climates
- = 0.96 - 0.06log(ΣESAL) + 0.02\*D, for wet climates
- $f_{\text{sg}}$  = subgrade adjustment factor
- = 1.0, for coarse subgrades
- = 0.57 + 0.21log(ΣESAL), for fine subgrades
- $f_{\text{JRCP}} = f_{\text{sb2}} * f_{\text{e}}$

- $f_{sb2}$  = subbase adjustment factor  
 = 1.0, for nonstabilized subbase  
 =  $0.91 - 0.02 \cdot D$ , for stabilized subbase  
 $f_e$  = adjustment for climate  
 =  $0.011 + 0.003 \log(\Sigma ESAL) - 0.001 \cdot D$ , for a dry, warm climate  
 =  $1.44 - 0.03 \log(\Sigma ESAL) - 0.06 \cdot D$ , for a wet, warm climate  
 =  $1.04 - 0.32 \log(\Sigma ESAL) - 0.08 \cdot D$ , for a dry, cold climate  
 =  $0.54 - 0.85 \log(\Sigma ESAL) + 0.19 \cdot D$ , for a wet, cold climate

The PEARDARP pumping model could not be directly compared to field pumping measurements. This is because the PEARDARP pumping model calculates the volume of pumped material, the number of joints pumping, and the volume of undersealing necessary to fill the voids. In the field surveys of the projects in this study, only the presence and severity of pumping was noted.

### Faulting Models

$$F_{n-avg} = (1.29 + (K_1 * (T * A^2)) * f_{SD}) / 32.0 \quad (10)$$

$$F_{d-avg} = f_d * F_{n-avg} \quad (11)$$

where:

- $F_{n-avg}$  = average faulting for nondoweled pavements, in  
 $F_{d-avg}$  = average faulting for doweled pavements, in  
 $K_1$  =  $[48.95 * S^{0.610} (J - 13.5)^b] / D^{3.9}$   
 $T$  =  $(\Sigma Vol * p_t) / n$   
 $f_d$  =  $(1 + A)^{-0.5}$   
 $A$  = age, years = n  
 $f_{SD}$  = subdrainage factor  
 = 0.1, if subdrainage is excellent  
 = 0.6, if subdrainage is good  
 = 1.0, if subdrainage is fair  
 = 1.4, if subdrainage is poor  
 $S$  = subgrade drainage  
 = 1, if subgrade drainage is good  
 = 2, if subgrade drainage is poor  
 $J$  = slab length, ft  
 $b$  = 0.241 for granular subbase  
 = 0.037 for stabilized subbase  
 $D$  = slab thickness, in  
 $\Sigma Vol$  = cumulative traffic volume in one direction, millions  
 $p_t$  = proportion of trucks in the design lane

The results of the statistical analysis of the PEARDARP faulting model are given in table 19 for the dry-nonfreeze sections. The analysis indicates that the model does not adequately predict joint faulting for these sections. This is portrayed graphically in figure 36, which indicates that the model is underpredicting joint faulting.

### Cracking Model

$$CR = (DA/4000) * 2 * 5280/63.35 \quad (12)$$

where:

$$DA = e^{(a_1 \tan(a_1 + a_2 \log(\Sigma ESAL) + a_3 D + a_4 k_R) * 6)}$$

$$a_1 = 39.006$$

$$a_2 = 3.941$$

$$a_3 = -4.387$$

$$a_4 = -0.0036$$

for *stabilized* materials,

$$\log(k_c) = 0.7405 \log(D) + 0.7256 \log(k) + 0.5559, \text{ and}$$

$$k_R = k_c$$

for *nonstabilized* materials,

$$\log(k_c) = 0.3483 \log(D) + 0.8163 \log(k) + 0.8163, \text{ and}$$

$$k_R = 1.7 * k_c$$

and where:

- DA = damage area per joint, in<sup>2</sup>
- CR = length of crack, lin ft/1000 ft<sup>2</sup>
- (ΣESAL) = cumulative equivalent 18-kip single axle loads, millions
- D = slab thickness, in
- k = modulus of subgrade reaction, pci
- k<sub>c</sub> = composite modulus of slab support (on top of the base), pci

Table 19 provides the summary of the statistical analysis of the PEARDARP cracking model. These results indicate that the model does not adequately predict slab cracking for the pavement sections in the dry-nonfreeze region. Figure 37 provides a graphical representation of that table, and shows that the majority of the *predicted* cracking fell into a very narrow band of between 320 and 420 lin ft/1000 ft<sup>2</sup> when there was actual cracking measured, and between 0 and 320 lin ft/1000 ft<sup>2</sup> when there was no actual cracking measured.

PEARDARP Faulting Models  
Dry-Nonfreeze Region

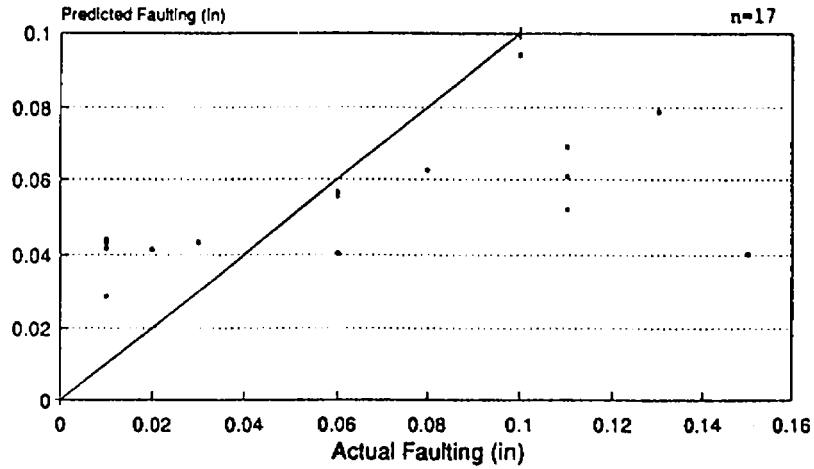


Figure 36. PEARDARP predicted faulting vs actual faulting for 17 sections in dry-nonfreeze region.

PEARDARP Cracking Model  
Dry-Nonfreeze Region

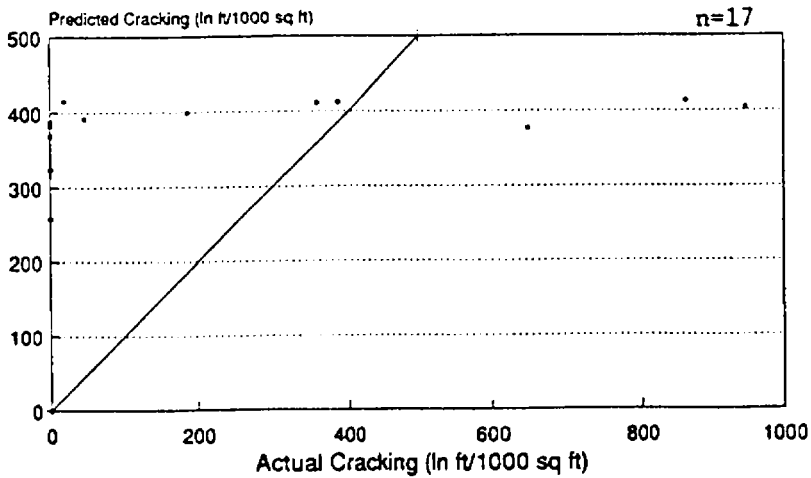


Figure 37. PEARDARP predicted cracking vs. actual cracking for 17 sections in dry-nonfreeze region.

## COPES Prediction Models

Under NCHRP Project 1-19, termed the COPES study, design and performance data was collected from rigid pavement sections in seven States.<sup>(36)</sup> Nationwide regression models were developed for joint faulting, joint deterioration (spalling), slab cracking, pumping, and Present Serviceability Rating (PSR) for both JPCP and JRCP. The models are presented below for JPCP only since this is the concrete pavement type in Arizona. In order to avoid duplication, only previously undefined variables are defined for each equation.

### IPCP Pumping Model

$$\begin{aligned} \text{PUMP} = \text{ESAL}^{0.443} [-1.479 + 0.255*(1-\text{SOILCRS}) + 0.0605*\text{SUMPREC}^{0.5} \\ + 52.65/(\text{THICK})^{1.747} + 0.0002269*\text{FI}^{1.205} ] \end{aligned} \quad (13)$$

where:

PUMP	=	pumping
	=	0, no pumping
	=	1, low severity pumping
	=	2, medium severity pumping
	=	3, high severity pumping
ESAL	=	accumulated 18-kip equivalent single axle loads, millions
SOILCRS	=	0, fine-grained subgrade soil
	=	1, coarse-grained subgrade soil
SUMPREC	=	Average annual precipitation, cm
THICK	=	Slab thickness, in
FI	=	freezing index

R <sup>2</sup>	=	0.68
SEE	=	0.42
n	=	289

The latter statistical information indicates that the model accounts for 68 percent of the variability in the prediction of pumping. The standard error of the estimate (SEE) indicates that the model predicts pumping within  $\pm 0.42$  for the specified confidence level. Finally, there were 289 observations used in the development of the model.

Unlike the PEARDARP pumping model, the COPES pumping model predicts the severity of pumping expected to occur within a pavement section, instead of the volume of pumping. This allows for a direct comparison of the actual pumping observed on the pavement sections included in this study. It should be noted that the actual pumping and the predicted pumping from the COPES pumping model are

both based on visible signs of pumping. Therefore, sections that are experiencing pumping but do not display any visible evidence could not be appraised in the field surveys or in the development of the model.

The results of the statistical analysis for the COPES pumping model are displayed in table 19. The results indicate that the model is not able to adequately predict pumping for the sections included in dry-nonfreeze region. Figure 38 shows predicted values both above and below the line of equality for these sections.

IPCP Joint Faulting Model

$$\begin{aligned}
 \text{FAULT} = & \text{ESAL}^{0.144} [-0.2980 + 0.2671*\text{THICK}^{-0.3184} - 0.0285*\text{BASETYP} + \\
 & 0.00406*(\text{FI} + 1)^{0.3598} - 0.0462*\text{EDGESUP} + 0.2384*(\text{PUMP} + 1)^{0.0109} - \\
 & 0.0340*\text{DOW}^{2.0587}] \qquad \qquad \qquad (14)
 \end{aligned}$$

where:

- FAULT = mean transverse joint faulting, in
- BASETYP = 0, if granular base  
= 1, if stabilized base
- EDGESUP = 0, if AC shoulder  
= 1, if tied PCC shoulder
- PUMP = 0, if no pumping  
= 1, if low severity pumping  
= 2, if medium severity pumping  
= 3, if high severity pumping
- DOW = diameter of dowel bar, in

R <sup>2</sup>	=	0.79
SEE	=	0.02
n	=	259

Analysis of JPCP Faulting Model

The results of the statistical analysis performed on the COPES faulting models are provided in table 19. For the consideration of the sections from the dry-nonfreeze climatic region, the model is unable to adequately predict the actual faulting. The overall graph of predicted versus actual results for the dry-nonfreeze region is shown in figure 39. The largest faulting predicted by the model is 0.07 in, although the actual faulting was as high as 0.15 in. The model appeared to do reasonably well on the sections from Arizona, but had problems with the California sections. This is an interesting phenomenon since the original COPES data base did not include any sections from Arizona while containing many sections from California.

## COPES Pumping Model Dry-Nonfreeze Region

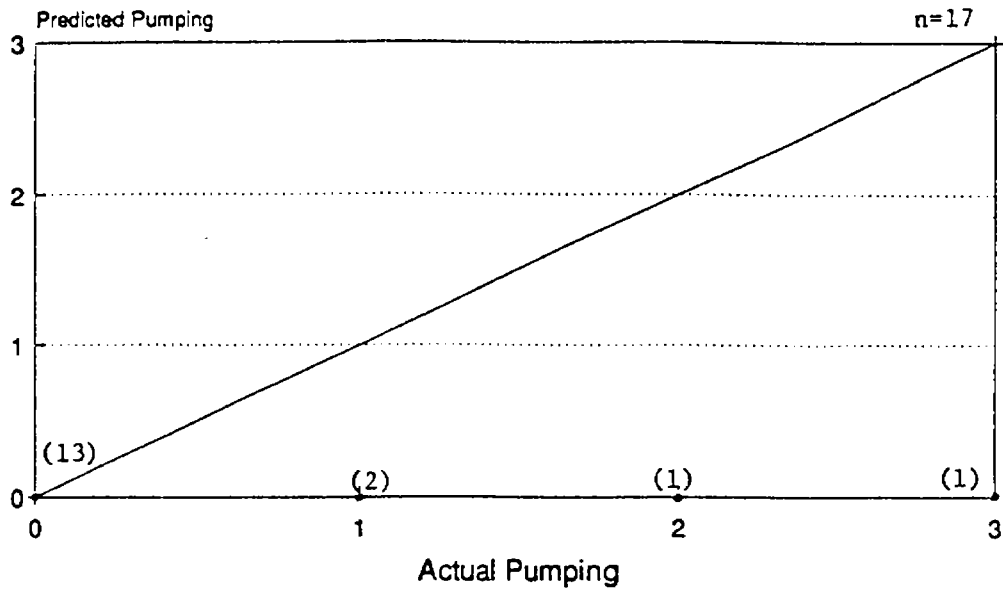


Figure 38. COPES predicted pumping vs. actual pumping for 17 sections in dry-nonfreeze region.

## COPES Faulting Model Dry-Nonfreeze Region

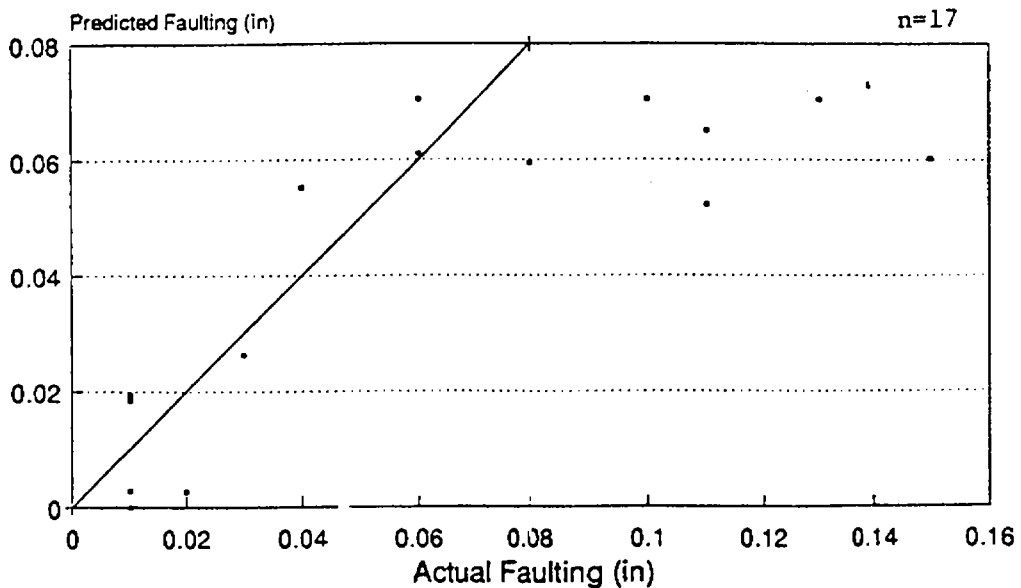


Figure 39. COPES predicted faulting vs. actual faulting for 17 sections in dry-nonfreeze region.

### IPCP Joint Deterioration Model

$$\text{DETJT} = \text{AGE}^{1.695} (0.9754 * \text{DCRACK}) + \text{AGE}^{2.841} (0.01247 * \text{UNITUBE}) + \text{AGE}^{3.038} (0.001346 * \text{INCOMP}) \quad (15)$$

where:

DETJT = number of deteriorated (medium and high severity) joints/mile  
AGE = time since construction  
UNITUBE = 0, if no unitube inserts used  
          = 1, if unitube inserts used  
INCOMP = 0, if no incompressibles are visible in the joints  
          = 1, if incompressibles are visible in the joints

$$\begin{aligned} R^2 &= 0.59 \\ \text{SEE} &= 16 \text{ joints/mi} \\ n &= 252 \end{aligned}$$

The summary of the statistical analysis for joint deterioration is shown in table 19. It is observed that the model is unable to adequately predict joint deterioration for the sections included in the study. The overall graph of predicted versus actual results for the dry-nonfreeze region is shown in figure 40. It appears from the figure that the model predicts fairly well, although the statistical analysis indicates that the model does not adequately predict joint deterioration. With the exception of the oldest section in Arizona, it is interesting that the range of predicted values falls nicely in line with the range of actual values.

### IPCP Slab Cracking Model

$$\text{CRACKS} = \text{ESAL}^{2.755} [3092.4(1 - \text{SOILCRS}) * \text{RATIO}^{10.0}] + \text{ESAL}^{0.5} * (1.233 * \text{TRANGE}^{2.0} * \text{RATIO}^{2.868}) + \text{ESAL}^{2.416} (0.2296 * \text{FT}^{1.53} * \text{RATIO}^{7.31}) \quad (16)$$

where:

CRACKS = total length of cracking of all severities (ft/lane mi)  
RATIO = Westergaard edge stress/mean 28-day modulus of rupture  
TRANGE = difference between average maximum temperature in July and average minimum temperature in January

$$\begin{aligned} R^2 &= 0.69 \\ \text{SEE} &= 176 \text{ ft/mi} \\ n &= 303 \end{aligned}$$

## COPES Joint Deterioration Model Dry-Nonfreeze Region

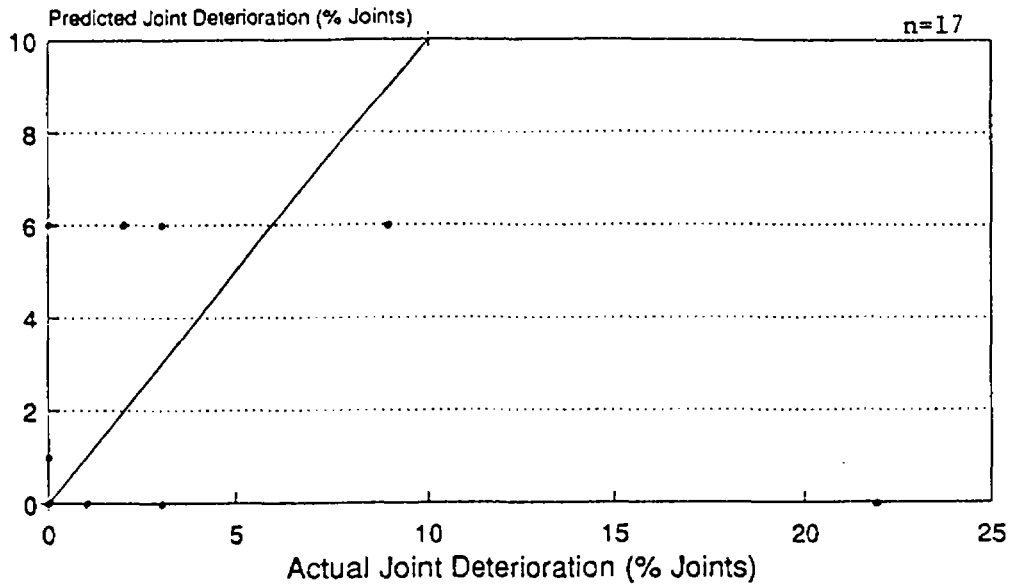


Figure 40. COPES predicted joint deterioration vs. actual joint deterioration for 17 sections in dry-nonfreeze region.

## COPES Cracking Model Dry-Nonfreeze Region

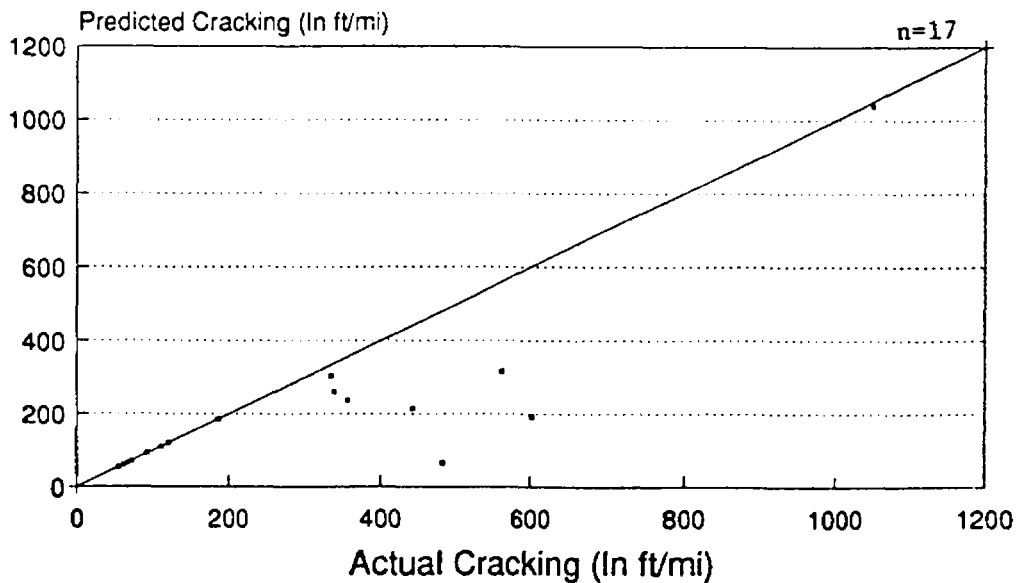


Figure 41. COPES predicted cracking vs. actual cracking for 17 sections in dry-nonfreeze region.

The COPES cracking models predict total linear feet of cracking, including both transverse and longitudinal. This required the conversion and addition of the transverse and longitudinal cracking obtained in this study since it was grouped separately. The fact that the COPES cracking models do not distinguish between transverse and longitudinal cracking is a shortcoming of the model, since different mechanisms are responsible for the development of each type of cracking. The COPES cracking model for JPCP includes cracking of all severity levels.

Table 19 provides the summary of the statistical analysis for the COPES cracking models. These results show that the models were unable to adequately predict cracking for the sections from the dry-nonfreeze region. The overall graph of predicted versus actual results for the dry-nonfreeze region is shown in figure 41. In this region, the models are observed to underpredict the actual cracking. It is interesting to note from the figure that, for small amounts of cracking (say, less than 300 ft/mile), the model predicts the cracking with extraordinary accuracy. However, above the 300 ft/mile level, the accuracy of the model decreases.

JPCP Present Serviceability Rating (PSR) Model

$$PSR = 4.5 - 1.486*ESAL^{0.1467} + 0.4963*ESAL^{0.265}RATIO^{-0.5} - 0.01082*ESAL^{0.644}(SUMPREC^{0.91} / AVGMT^{1.07})*AGE^{0.525} \quad (17)$$

where:

- PSR = present serviceability rating
- SUMPREC = average annual precipitation, cm
- AVGMT = average monthly temperature, °C

$$R^2 = 0.69$$

$$SEE = 0.25$$

$$n = 316$$

The COPES models for PSR are based on a panel rating of serviceability of the pavement sections included in that study's data base. It is a measure of the effects of distress and other factors, such as joint spacing, on pavement rideability. These results are directly comparable to the PSR values obtained from the actual field surveys in this project.

Table 19 provides the summary of the statistical analysis for the COPES PSR models. It is observed that the models are unable to adequately predict PSR for the sections included in the dry-nonfreeze region. The overall graph of predicted versus actual results for the dry-nonfreeze region is shown in figure 42. It is observed that, in this region, the model typically overpredicts the actual PSR values. The model overestimated PSR values for the thick slab designs and mild climates of Arizona and

## COPES PSR Models Dry-Nonfreeze Region

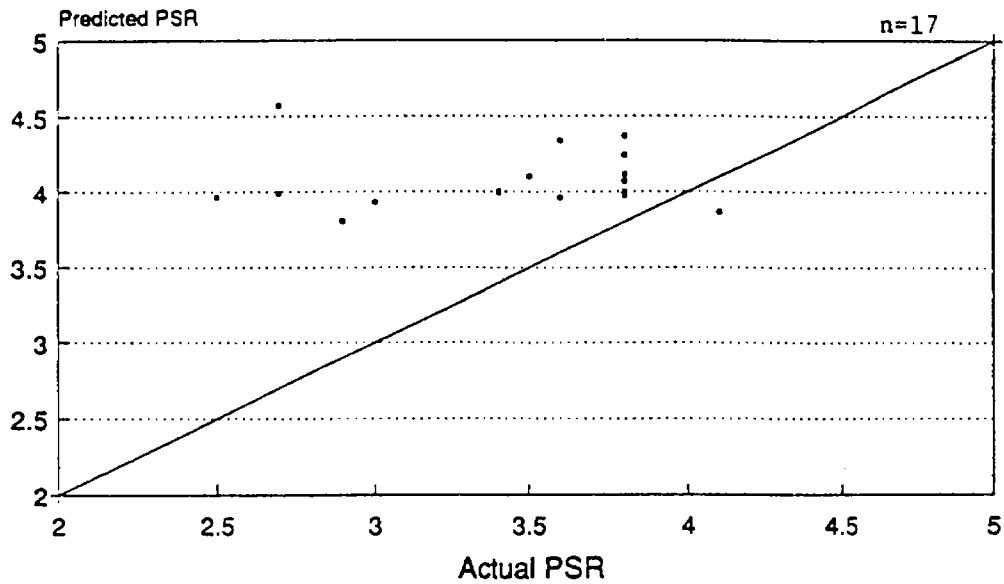


Figure 42. COPES predicted PSR vs. actual PSR for 17 sections in dry-nonfreeze region.

## PFAULT Faulting Models Dry-Nonfreeze Region

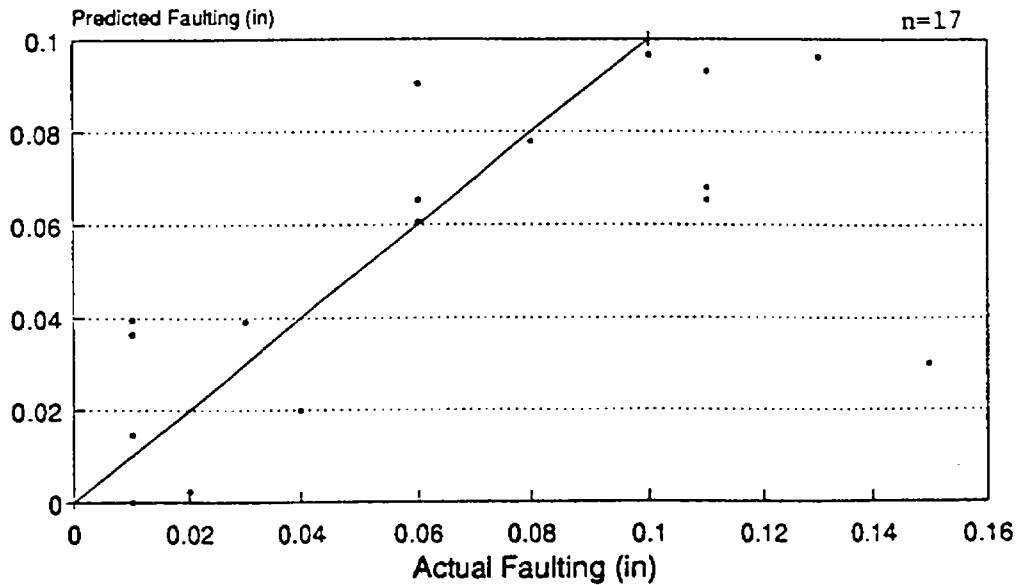


Figure 43. PFAULT predicted faulting vs. actual faulting for 17 sections in dry-nonfreeze region.

California. This may be due to the model assuming that a thicker slab results in a smoother-riding pavement, when in actuality there are often problems associated with the construction of thick slabs that could translate into roughness.

### PFAULT Faulting Prediction Models

In an effort to improve the faulting models developed under the COPES project, the COPES data base was expanded to include additional data and a new faulting model, PFAULT, developed.<sup>(37)</sup> Whereas the original models developed from the COPES data were divided into JPCP and JRCP pavements, the PFAULT models are divided by doweled and nondoweled pavements.

#### Doweled Jointed Concrete Pavements

$$\text{PFAULT} = \text{ESAL}^{0.5377} [2.2073 + 0.002171 \cdot \text{BSTRESS}^{0.4918} + 0.0003292 \cdot \text{JTSPACE}^{1.0793} - 2.1397 \cdot \text{KVALUE}^{0.01305}] \quad (18)$$

$$\begin{aligned} R^2 &= 0.53 \\ \text{SEE} &= 0.05 \text{ in} \\ n &= 280 \end{aligned}$$

#### Nondoweled Jointed Concrete Pavements

$$\begin{aligned} \text{PFAULT} = \text{ESAL}^{0.3157} [0.4531 + 0.3367 \cdot \text{OPENING}^{0.3322} - 0.5376 \cdot \\ (100 \text{ DEFL})^{-0.008437} + 0.0009092 \cdot \text{FI}^{0.5998} + 0.004654 \cdot \text{ERODF} - \\ 0.03608 \cdot \text{EDGESUP} - 0.01087 \cdot \text{SOILCRS} - 0.009467 \cdot \text{DRAIN}] \quad (19) \end{aligned}$$

$$\begin{aligned} R^2 &= 0.55 \\ \text{SEE} &= 0.03 \text{ in} \\ n &= 186 \end{aligned}$$

where:

- PFAULT = mean faulting of transverse joints, in
- ESAL = accumulated equivalent 18-kip single axle loads in traffic lane, millions
- BSTRESS = dowel/concrete bearing stress, psi, calculated using Friberg's procedure with an effective length of  $\ell$  instead of  $1.8\ell$  (where  $\ell$  is the radius of relative stiffness)
- JSPACE = transverse joint spacing, ft
- KVALUE = effective k-value on top of the base layer, psi/in
- OPENING = calculated joint opening for input temperature range, in

	=	CON JSPACE*12 [a TRANGE + e]
CON	=	adjustment factor due to subbase/slab frictional restraint (0.65 for stabilized base and 0.80 for granular base)
a	=	thermal coefficient of contraction of PCC, per °C
TRANGE	=	temperature range, °C (maximum mean daily air temperature in July minus minimum mean daily air temperature in January)
e	=	drying shrinkage coefficient of PCC ( $0.5\text{--}2.5 \times 10^{-4}$ strain)
DEFL	=	unprotected corner deflection from Westergaard's equation, in
FI	=	Freezing Index, degree days below freezing
ERODF	=	erodibility factor for base materials
	=	0.5, if lean concrete base
	=	1.0, if cement-treated base with granular subbase
	=	1.5, if cement-treated base without granular subbase
	=	2.0, if asphalt-treated base
	=	2.5, if granular base
EDGESUP	=	0, if no tied concrete shoulder exists
	=	1, if tied concrete shoulder exists
SOILCRS	=	AASHTO subgrade soil classification
	=	0, if A-4 to A-7
	=	1, if A-1 to A-3
DRAIN	=	0, if no longitudinal edge subdrains exist
	=	1, if longitudinal edge subdrains exist

Table 19 provides the summary of the statistical analysis for the PFAULT faulting model. The data shows that the model was unable to adequately predict faulting for the dry-nonfreeze data set. The overall graph of predicted versus actual results for the dry-nonfreeze region is shown in figure 43. On the whole, the model appeared to underpredict faulting in this region, although there is a wide amount of scatter.

### **New FHWA Prediction Models**

New prediction models were developed under a recent FHWA research study.<sup>(12)</sup> These models were developed using the inservice performance data from nearly 500 concrete pavement sections, including 145 sections from the dry-nonfreeze climatic region (California and Arizona). New models were developed for PSR, joint spalling, joint faulting, and transverse cracking (JPCP only).

These new models were evaluated using the field performance data from Arizona. Since several sections from the dry-nonfreeze climatic region were used in the model development, it was believed that the new models would be more representative of Arizona conditions.

### IPCP PSR Model

$$\text{PSR} = 4.356 - 0.0182 \text{TFAULT} - 0.00313 \text{SPALL} - 0.00162 \text{TCRKS} \\ - 0.00317 \text{FDR} \quad (20)$$

Where:

- PSR = Mean panel rating of pavement (0 to 5 AASHTO Scale)  
TFAULT = Cumulative transverse joint faulting, in/mi  
SPALL = Number of deteriorated (medium- and high-severity) transverse joints per mile  
TCRKS = Number of transverse cracks (all severities) per mile  
FDR = Number of full-depth repairs per mile

Statistics:

$$\begin{aligned} R^2 &= 0.58 \\ \text{SEE} &= 0.31 \text{ (units of PSR)} \\ n &= 282 \end{aligned}$$

The summary of the statistical analysis for the PSR model is provided in table 19. The results indicate that the PSR model accurately predicts PSR for the Arizona IPCP sections. Predictions of PSR calculated using this model and the PSR are shown in table 20. The results are displayed graphically in figure 44.

### IPCP Joint Spalling Model

$$\text{JTSPALL} = \text{AGE}^{2.178} * [ 0.0221 + 0.5494 \text{DCRACK} \\ - 0.0135 \text{LIQSEAL} - 0.0419 \text{PREFSEAL} + 0.0000362 \text{FI} ] \quad (21)$$

Where:

- JTSPALL = Number of medium-high joint spalls/mile  
AGE = Age since original construction, years  
DCRACK = 0, if no D-cracking exists  
= 1, if D-cracking exists  
LIQSEAL = 0, if no liquid sealant exists in joint  
= 1, if liquid sealant exists in joint  
PREFSEAL = 0, if no preformed compression seal exists  
= 1, if preformed compression seal exists  
FI = Freezing Index, degree days below freezing

Table 20. Predicted and actual PSR values for new FHWA PSR prediction model.

OBS	ID	PREDICTED PSR	MEASURED PSR	RESIDUAL
1	AZ1-1	3.6	3.4	0.2
2	AZ1-2	4.2	3.8	0.4
3	AZ1-4	4.3	3.6	0.7
4	AZ1-5	4.2	3.8	0.4
5	AZ1-6	4.3	3.5	0.8
6	AZ1-7	4.2	3.8	0.4
7	AZ-2	4.3	3.6	0.7
8	360-1	4.2	4.4	-0.2
9	360-2	4.2	4.2	0.0
10	360-3	4.2	4.1	0.1
11	360-4	4.1	4.3	-0.2
12	360-9	4.2	4.8	-0.6
13	10-01	3.6	3.2	0.4
14	10-02	3.6	3.2	0.4
15	10-03	3.7	3.8	-0.1
16	10-04	4.2	4.1	0.1
17	10-05	4.2	4.2	0.0
18	10-06	4.2	4.2	0.0
19	10-07	4.2	4.1	0.1
20	17-01	4.1	3.9	0.2
21	17-02	3.8	3.9	-0.1
22	17-03	3.3	3.9	-0.6
23	17-04	3.9	3.7	0.2
24	17-05	3.9	4.1	-0.2
25	17-06	3.6	2.9	0.7
26	17-10	4.0	4.1	-0.1
27	17-11	3.3	4.1	-0.8

Analysis Variable : Residual

N Obs	Mean	Std Error	T	Prob> T
27	0.1074074	0.0778862	1.3790294	0.1796

## FHWA PSR MODEL JPCP

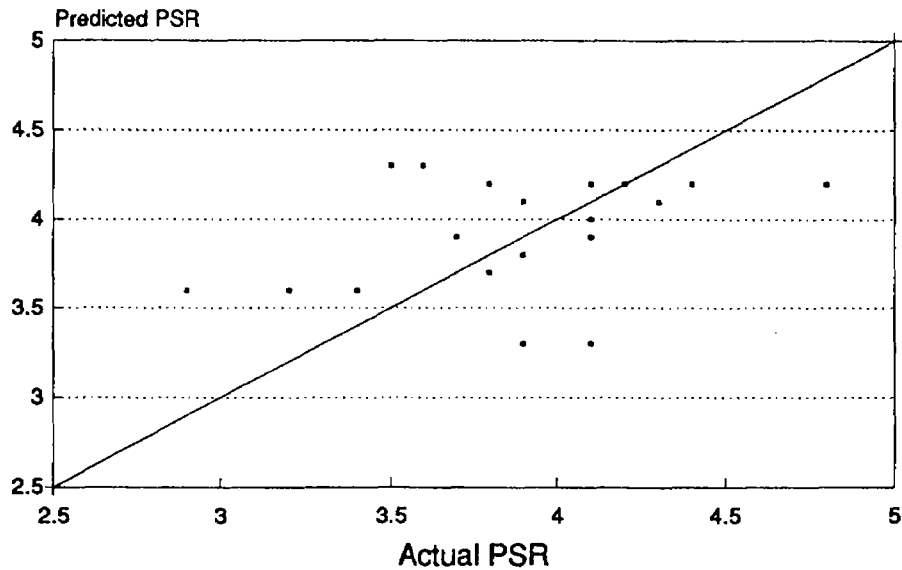


Figure 44. Predicted PSR using new FHWA model vs. actual PSR for ADOT study sections.

## FHWA SPALLING MODEL JPCP

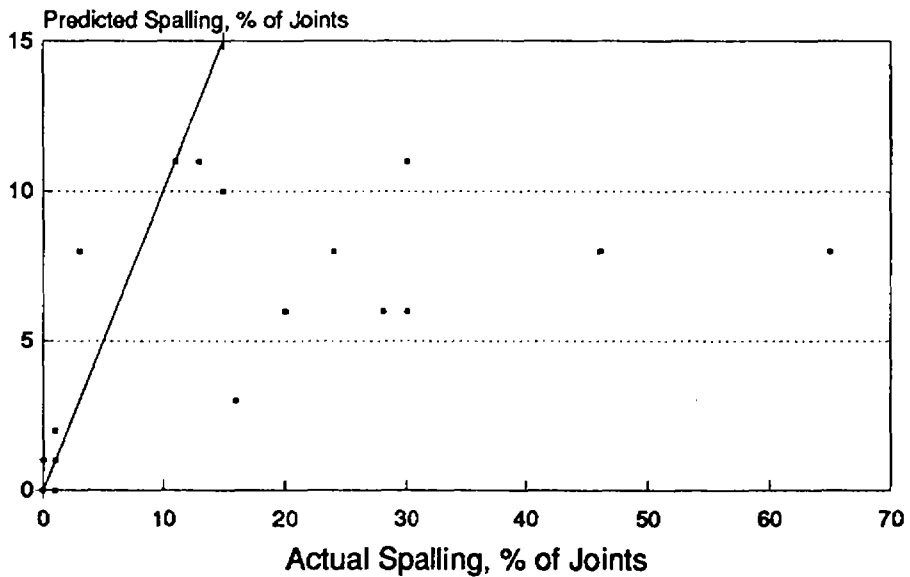


Figure 45. Predicted spalling using new FHWA model vs. actual spalling for ADOT study sections.

Statistics:

$$\begin{aligned} R^2 &= 0.59 \\ \text{SEE} &= 15 \text{ joints/mi} \\ n &= 262 \end{aligned}$$

The results of the statistical analysis show that the model is unable to accurately predict the joint spalling for Arizona conditions (see table 19). The predicted spalling calculated using this model for the JPCP pavement sections and the measured spalling are presented in table 21, and the results are graphically displayed in figure 45.

An inspection of the data clearly shows that the model underestimates the number of spalled joints for the JPCP sections. This may be due to the fact that much of the spalling occurring on the Arizona pavements was related to construction problems, which the model can not expect to accurately predict.

#### Joint Faulting Model for Doweled Concrete Pavements

$$\begin{aligned} \text{FAULT} = & \text{ESAL}^{0.5280} * [ 0.1204 + 0.04048 * ( \text{BSTRESS1} / 1000 )^{0.3388} + \\ & 0.007353 * ( \text{AVJSPACE} / 10 )^{0.6725} ] - 0.1492 \\ & * ( \text{KSTAT} / 100 )^{0.05911} - 0.01868 * \text{DRAIN} - 0.00879 \\ & * \text{EDGESUP} - 0.00959 * \text{STYPE} ] \end{aligned} \quad (22)$$

Where:

- FAULT = Mean transverse joint faulting, in;  
 ESAL = Cumulative equivalent 18-kip single-axle loads in lane, millions;  
 BSTRESS = Maximum concrete bearing stress using closed-form equation, psi;  
 =  $f_d * P * T * [ K_d * ( 2 + \text{BETA} * \text{OPENING} ) / ( 4 * E_s * I * \text{BETA}^3 ) ]$   
 BETA =  $[ K_d * \text{DOWEL} / ( 4 * E_s * I ) ]^{0.25}$   
 $f_d$  = Distribution factor;  
 =  $2 * 12 / ( \ell + 12 )$   
 $\ell$  = Radius of relative stiffness, in;  
 =  $[ E_c * \text{THICK}^3 / ( 12 * ( 1 - \mu^2 ) * \text{KSTAT} ) ]^{0.25}$   
 $E_c$  = Concrete modulus of elasticity, psi;  
 =  $14.4 * 150^{1.5} * \text{MR}_{28}^{0.77}$   
 $I$  = Moment of inertia of dowel bar cross section, in<sup>4</sup>;

Table 21. Predicted and actual percent joint spalling for new FHWA spalling prediction model.

OBS	ID	PREDICTED SPALLING	MEASURED SPALLING	RESIDUAL
1	AZ1-1	3	16	-13
2	AZ1-2	2	1	1
3	AZ1-4	1	1	0
4	AZ1-5	1	0	1
5	AZ1-6	0	1	-1
6	AZ1-7	0	0	0
7	AZ-2	0	0	0
8	360-1	0	0	0
9	360-2	0	0	0
10	360-3	0	0	0
11	360-4	0	1	-1
12	360-9	0	0	0
13	10-01	6	30	-24
14	10-02	6	20	-14
15	10-03	6	28	-22
16	10-04	0	1	-1
17	10-05	0	1	-1
18	10-06	0	0	0
19	10-07	0	1	-1
20	17-01	11	13	-2
21	17-02	11	30	-19
22	17-03	8	46	-38
23	17-04	8	24	-16
24	17-05	8	3	5
25	17-06	10	15	-5
26	17-10	11	11	0
27	17-11	8	65	-57

Analysis Variable : Residual

N Obs	Mean	Std Error	T	Prob> T
27	-7.7037037	2.7199876	-2.8322569	0.0088

	$= 0.25 * 3.1416 * ( DOWEL / 2 )^4$
THICK	= Slab thickness, in;
MR <sub>28</sub>	= Concrete modulus of rupture at 28 days, psi;
μ	= Poisson's Ratio, set to 0.15;
P	= Applied wheel load, set to 9000 lb;
T	= Percent transferred load, set to 0.45;
K <sub>d</sub>	= Modulus of dowel support, set to 1,500,000 pci;
BETA	= Relative stiffness of the dowel-concrete system;
DOWEL	= Dowel diameter, in;
E <sub>s</sub>	= Modulus of elasticity of the dowel bar, set to 29,000,000 psi;
KSTAT	= Effective modulus of subgrade reaction, on the top of base, psi/in;
OPENING	= Average transverse joint opening, in $= CON * AVJSPACE * 12 * ( ALPHA * TRANGE / 2 + e )$
AVJSPACE	= Average transverse joint spacing, ft;
CON	= Adjustment factor due to base/slab frictional restraint, = 0.65 if stabilized base, = 0.80 if aggregate base or lean concrete base with bond breaker
ALPHA	= Thermal coefficient of contraction of PCC, set to 0.000006 /°F;
TRANGE	= Annual temperature range, °F;
e	= Drying shrinkage coefficient of PCC, set to 0.00015 strain;
DRAIN	= Index for drainage condition, = 0, if no edge subdrain exists, = 1, if edge subdrain exists;
EDGESUP	= Index for edge support, = 0, if no edge support exists, = 1, if edge support exists;
STYPE	= Index for AASHTO subgrade soil classification, = 0, if A-4 to A-7, = 1, if A-1 to A-3;

Statistics:

R <sup>2</sup>	=	0.67
SEE	=	0.0571 in
n	=	559

Only five of the pavement sections included in the study were doweled. Because of the limited number of sections and the resulting difficulty in making an accurate assessment of the model, no attempt was made to evaluate the doweled concrete pavement model.

Joint Faulting Model for Nondoweled Concrete Pavements

$$\begin{aligned}
 \text{FAULT} = & \text{ESAL}^{0.2500} * [ 0.000038 + 0.01830 * ( 100 * \text{OPENING} )^{0.5585} \\
 & + 0.000619 * ( 100 * \text{DEFLAMI} )^{1.7229} + 0.0400 * ( \text{FI} / 1000 )^{1.9840} \\
 & + 0.00565 * \text{BTERM} - 0.00770 * \text{EDGESUP} - 0.00263 * \text{STYPE} \\
 & - 0.00891 * \text{DRAIN} ] \qquad \qquad \qquad (23)
 \end{aligned}$$

Where:

- FAULT = Mean faulting across the transverse joints, in;
- ESAL = Cumulative 18-kip equivalent single-axle loads in traffic lane, millions;
- OPENING = Average transverse joint opening, in;  
= CON \* AVJSPACE \* 12 \* ( ALPHA \* TRANGE / 2 + e )
- CON = Adjustment factor due to base/slab frictional restraint,  
= 0.65 if stabilized base,  
= 0.80 if aggregate base;
- AVJSPACE = Average transverse joint spacing, ft;
- ALPHA = Thermal coefficient of contraction of PCC, set to 0.000006 /°F;
- TRANGE = Annual temperature range, °F; (Minimum average January temperature - Maximum average July temperature)
- e = Drying shrinkage coefficient of PCC, set to 0.00015 strain;
- DEFLAMI = Ioannides' corner deflection, in;<sup>(38)</sup>  
= P \* ( 1.2 - 0.88 \* 1.4142 \* a / ℓ ) / (KSTAT \* ℓ<sup>2</sup>)
- ℓ = Radius of relative stiffness, in;  
= [ E<sub>c</sub> \* THICK<sup>3</sup> / ( 12 \* ( 1 - μ<sup>2</sup> ) \* KSTAT ) ]<sup>0.25</sup>
- E<sub>c</sub> = Concrete modulus of elasticity, psi;  
= 14.4 \* 150<sup>1.5</sup> \* MR<sub>28</sub><sup>0.77</sup>
- P = Applied wheel load, set to 9000 lb;
- a = Radius of the applied load, set to 5.64 in, assuming  
tire pressure = 90 psi;
- KSTAT = Modulus of subgrade reaction, on the top of base, psi/in;
- THICK = Slab thickness, in;
- μ = Poisson's Ratio, set to 0.15;
- MR<sub>28</sub> = Concrete modulus of rupture at 28 days, psi;
- BTERM = Base type factor;  
= 10 \* [ ESAL<sup>0.2076</sup> \* ( 0.04546 + 0.05115 \* GB + 0.007279 \* CTB  
+ 0.003183 \* ATB - 0.003714 \* OGB - 0.006441 \* LCB ) ]
- GB = Dummy variable for dense-graded aggregate base,  
= 1 if aggregate base,

- = 0 otherwise;
- CTB = Dummy variable for dense-graded, cement-treated base,  
= 1 if cement-treated base,  
= 0 otherwise;
- ATB = Dummy variable for dense-graded, asphalt-treated base,  
= 1 if asphalt-treated base,  
= 0 otherwise;
- OGB = Dummy variable for open-graded aggregate base  
or open-graded asphalt-treated base,  
= 1 if open-graded base,  
= 0 otherwise; and
- LCB = Dummy variable for lean concrete base,  
= 1 if lean concrete base,  
= 0 otherwise.
- FI = Freezing index, Degree-Days;
- DRAIN = Index for drainage condition,  
= 0, if no edge subdrain exists,  
= 1, if edge subdrain exists;
- EDGESUP = Index for edge support,  
= 0, if no edge support exists,  
= 1, if edge support exists;
- STYPE = Index for AASHTO subgrade soil classification,  
= 0, if A-4 to A-7,  
= 1, if A-1 to A-3;

Statistics:

$$\begin{array}{rcl}
 R^2 & = & 0.81 \\
 SEE & = & 0.028 \text{ in} \\
 n & = & 398
 \end{array}$$

The results of the statistical evaluation is provided in table 19. It is observed that the nondoweled faulting model was unable to accurately predict the faulting for the Arizona sections. The predicted and actual faulting values are tabulated in table 22, and the results displayed graphically in figure 46. In most cases the model overpredicts the actual joint faulting. However, it is noted that the magnitude of the difference between the actual and predicted faulting values are not that great.

#### IPCP Transverse Cracking Model

$$P = \frac{1}{0.01 + 0.03 * [ 20^{-\log (n/N)} ]} \quad (24)$$

where:

Table 22. Predicted and actual joint faulting for new FHWA faulting prediction model.

OBS	ID	PREDICTED FAULTING	MEASURED FAULTING	RESIDUAL
1	AZ1-1	0.07	0.08	-0.01
2	AZ1-2	0.06	0.01	0.05
3	AZ1-4	0.06	0.01	0.05
4	AZ1-5	0.06	0.03	0.03
5	AZ1-6	0.05	0.03	0.02
6	AZ1-7	0.04	0.02	0.02
7	360-1	0.04	0.05	-0.01
8	360-2	0.04	0.02	0.02
9	360-3	0.05	0.02	0.03
10	360-4	0.06	0.04	0.02
11	360-9	0.07	0.02	0.05
12	10-01	0.08	0.03	0.05
13	10-02	0.08	0.06	0.02
14	10-03	0.13	0.03	0.10
15	17-01	0.06	0.01	0.05
16	17-02	0.07	0.01	0.06
17	17-03	0.08	0.05	0.03
18	17-04	0.11	0.02	0.09
19	17-05	0.08	0.06	0.02
20	17-06	0.13	0.09	0.04
21	17-10	0.12	0.03	0.09
22	17-11	0.10	0.01	0.09

Analysis Variable : Residual

N Obs	Mean	Std Error	T	Prob> T
22	0.0413636	0.0065232	6.3410034	0.0001

## FHWA FAULTING MODEL NONDOWELED PAVEMENTS

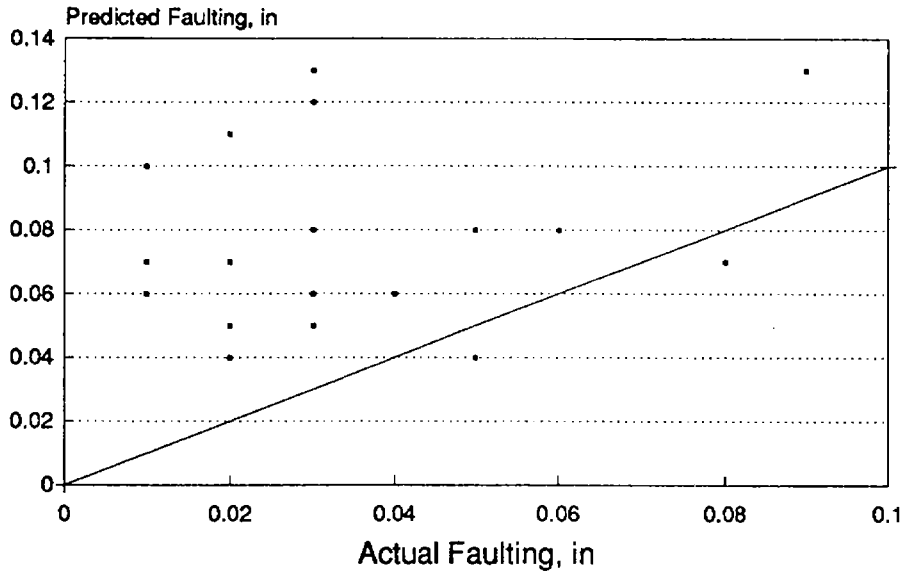


Figure 46. Predicted faulting using new FHWA model vs. actual faulting for ADOT study sections.

## FHWA TRANSVERSE CRACKING MODEL JPCP

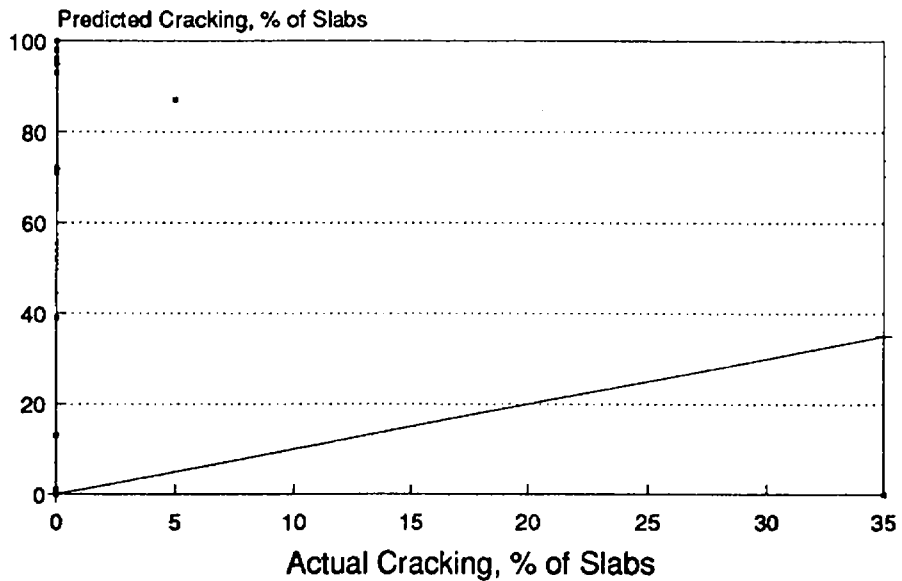


Figure 47. Predicted cracking using new FHWA model vs. actual cracking for ADOT study sections.

- P = Percent of Slabs Cracked  
 n = Number of 18-kip ESAL applications at *slab edge* (generally assumed to be between 3 and 7 percent of the lane ESAL applications)  
 N = Allowable 18-kip ESAL applications, where

$$\text{Log}_{10} N = 2.13 * [ 1 / \text{SR} ]^{1.2}$$

SR = Stress Ratio, ratio of computed edge stress (due to 9000 lb wheel load and thermal curling) to 28-day modulus of rupture

This model was used to predict slab cracking for the JPCP sections. The results of the statistical analysis are shown in table 19 and indicate that the model is unable to accurately predict the development of transverse cracking for the pavement sections in Arizona. Table 23 provides the actual and predicted values of transverse cracking and figure 47 illustrates those results graphically.

It is observed from figure 47 that, in all but one case, the model overestimates the percent of slabs cracked. That is, the model predicts more fatigue cracking than is actually occurring on the pavements. The absence of fatigue cracking was noted in the field surveys and can perhaps be explained by the slabs being in a state of compression (due to the warm temperatures) that reduces the actual stresses that the slabs experience.

## 6. MODEL DEVELOPMENT EFFORTS

The results from the preceding evaluation indicate that none of the models, except the new FHWA model for PSR, are capable of predicting the performance of pavements in the Phoenix Urban Corridor. The need for models more representative of Arizona conditions has been demonstrated.

Of particular interest to ADOT were models for faulting and PSR/roughness. A cracking model was not considered a high priority since there is little, if any, structural cracking in Arizona. Joint spalling often is influenced by construction practices and was therefore not strongly considered for further investigation. The new FHWA PSR model has been shown to provide reasonable estimates of PSR for Arizona conditions (at the 90 percent confidence level) and can therefore be used by ADOT to estimate PSR. Thus, efforts concentrated on new model development for faulting and roughness.

In order to develop models for Arizona conditions, representative data from the Phoenix Urban Corridor was needed. On the surface, the data from this study would appear to be sufficient to use in the development of new models. However, as will be discussed, this was not possible due to a number of constraints, including:

Table 23. Predicted and actual percent slab cracking for new FHWA slab cracking prediction model.

OBS	ID	PREDICTED CRACKING	MEASURED CRACKING	RESIDUAL
1	AZ1-1	100	0	100
2	AZ1-2	0	0	0
3	AZ1-4	0	0	0
4	AZ1-5	0	0	0
5	AZ1-6	0	0	0
6	AZ1-7	0	0	0
7	AZ-2	0	0	0
8	360-1	0	0	0
9	360-2	0	0	0
10	360-3	0	0	0
11	360-4	0	0	0
12	360-9	0	35	-35
13	10-01	93	0	93
14	10-02	95	0	95
15	10-03	98	0	98
16	10-04	1	0	1
17	10-05	0	0	0
18	10-06	0	0	0
19	10-7	0	0	0
20	17-01	13	0	13
21	17-02	39	0	39
22	17-03	87	5	82
23	17-04	71	0	71
24	17-05	72	0	72
25	17-06	100	0	100
26	17-10	100	0	100
27	17-11	96	0	96

Analysis Variable : Residual

N Obs	Mean	Std Error	T	Prob> T
27	34.2592593	8.8247568	3.8821760	0.0006

- Limited number of sections.
- Limited factorial design of sections.
- Limited number of replicates.
- Large number of confounding factors (thickness, base type, dowels, shoulder type, etc.)
- Performance data representing only one point in time.

The attempts at the development of models for faulting and roughness are discussed in the next sections.

### **Faulting Model Development**

For the development of a model using regression analysis, information must be available for several levels of each of the factors. There were 27 pavement sections in all, with thicknesses ranging from 9 to 13 in, divided into two levels (less than or equal to 9 in and greater than 9 in), on three base types (none, aggregate, stabilized). However, the sections were not selected as part of a designed experiment, but were instead chosen because of their availability and suitability for the general study.

Thus, although a considerable amount of data was collected on these 27 sections, only the data on transverse joint faulting, cumulative equivalent single axle loads (ESAL), and edge support condition are of any significance to faulting. On two of the pavement sections, the faulting measurements were taken in the inner lane of the three-lane roadway instead of the outer most-traveled lane. On seven other sections, the faulting and corresponding cumulative ESAL measurements were for joints which had been ground previously to remedy excessive faulting. In addition, five pavement sections with thicknesses between 10 and 13 in and stabilized bases were doweled.

In the end, a total of 13 sections remained for the development of a faulting model. While knowing that this number of sections was insufficient for use in developing a faulting model, the limited data was nevertheless used in such an attempt. Initially, the development of a new faulting model based on the data collected from the pavements was considered. However, due to the previously-noted limitations of the data, it was not possible to develop a new faulting model with its own form. Instead, the form of the new FHWA faulting model was assumed, and nonlinear regression analysis was used to determine new regression coefficients for that model that would be more representative of Arizona conditions. This effort using the 13 sections was not successful, as all five SAS nonlinear regression procedures did not converge to a solution. The data set was simply not adequate for this task.

An attempt was made to supplement the available data with data from other pavements which had experienced similar traffic and environmental conditions.

Thirteen pavements sections from southern California, with similar traffic, environmental, and pavement foundation materials, were included for such use.

For this larger data set, four of the five SAS nonlinear regression procedures did not converge to a solution. The procedure that did converge (Marquardt method) yielded regression coefficients that were not significantly different from zero. In fact, for every regression coefficient, the 95 percent confidence interval straddled zero. A plot of the residuals against the predicted faulting also showed serious departures from the model assumptions, with the error term increasing with the predicted faulting. This failure to provide any improvement to the model can be attributed to the similarity of the California sections to those in Arizona. Clearly, the unbalanced nature of the data obtained from the combined 26 sections are not adequate for the development of a model for predicting joint faulting on JPCP.

### **Roughness Model Development**

Efforts to develop roughness prediction models were even more hampered than those efforts to develop a faulting prediction model. Roughness in a pavement is caused by distress, such as faulting, cracking, spalling, settlements, heaves, and patching. The development of a representative roughness model for the Phoenix Urban Corridor must be based on the occurrence of those distresses.

However, an attempt to relate roughness to design features ended in the same results as the faulting model development. It is not possible to develop a roughness model directly from a set of design parameters since roughness is related directly to the pavement distress. That is, the independent variables must be the pavement distress parameters listed above, not the various design features of a pavement.

Historical roughness data was available from ADOT for many of the pavement sections (or within a reasonable proximity to each of the sections) from 1974 to 1987. Unfortunately, corresponding distress data was not available to allow for the development of a roughness model. Thus, distress data corresponding to roughness data was available for only one point in time, and much of that data had been tainted (e.g., due to grinding).

The historical roughness data did allow for the development of regression equations for each individual section (or group of sections of similar design). That is, a linear regression equations developed for a particular section or group of sections that could be used to predict future roughness as a function of ESAL applications. The regression equations could not, however, be extended to predict the future roughness of any other section.

Using this approach, regression equations were developed for some of the sections that related Mays Meter roughness (in inches/mile) to the number of applied

ESAL applications. Such efforts were not always successful, however, due to the large amount of variation in some of the roughness data (resulting in low  $R^2$  values), the difficulty in separating pre-grinding and post-grinding roughness, few roughness data points for some of the newer sections, or to other questionable aspects of the data (e.g., roughness data that *decreases* with time). Therefore, roughness regression equations were developed for only the following cases:

1. **AZ 360-04**

$$R = 138.22 * ESAL^{0.04}$$

$$R^2 = 0.40$$

This relationship is shown in figure 48. The  $R^2$  of the equation indicates that the relationship is marginal at best.

2. **AZ 360-09**

$$R = 133.26 * ESAL^{0.09}$$

$$R^2 = 0.72$$

The  $R^2$  of this regression equation indicates a good correlation between roughness and ESAL applications. This relationship is also shown in figure 48.

3. **AZ 10-03**

$$R = 106.57 * ESAL^{0.31}$$

$$R^2 = 0.83$$

An extremely good relation was obtained for this section, as indicated by the high  $R^2$  value. This relation is depicted in figure 49.

4. **AZ 17-03, AZ 17-04, AZ 17-05, AZ 17-06, AZ 17-10, AZ 17-11**

Attempts at regression models (before grinding) for these sections was marginally successful and are reported below. Subsequent attempts at post-grinding roughness were not successful.

**AZ 17-03**

$$R = 225.43 * ESAL^{0.17}$$

$$R^2 = 0.38$$

AZ360: JPCP with no base

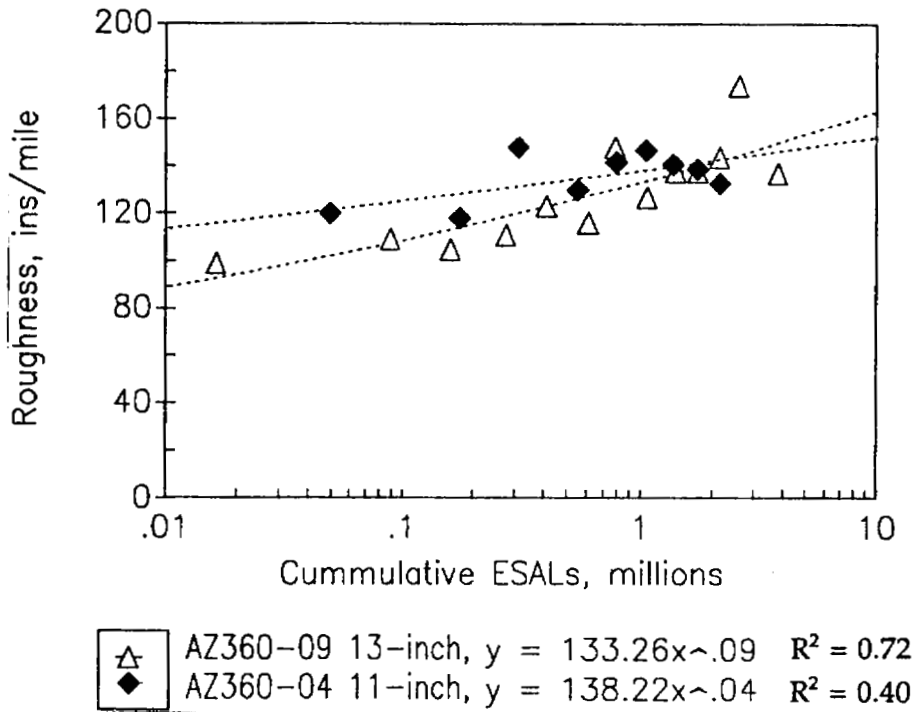


Figure 48. Roughness regression equations for 360-04 and 360-09.

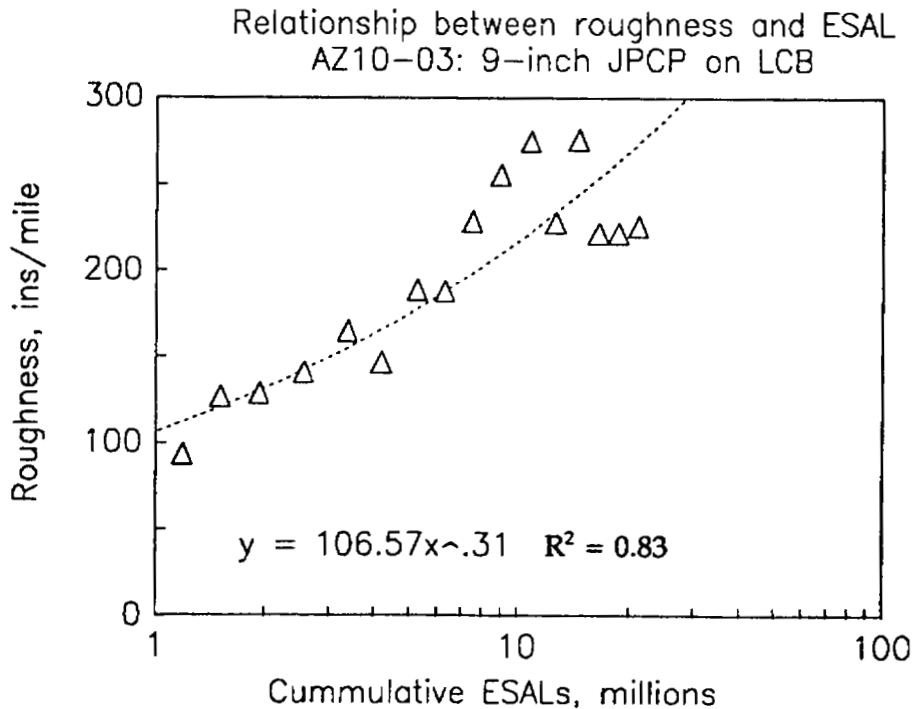


Figure 49. Roughness regression equation for 10-03.

**AZ 17-04**

$$R = 279.37 + 11.08 \cdot \text{ESAL}$$

$$R^2 = 0.28$$

**AZ 17-05**

$$R = 222.92 + 5.36 \cdot \text{ESAL}$$

$$R^2 = 0.34$$

**AZ 17-06**

$$R = 140.63 + 18.86 \cdot \text{ESAL}$$

$$R^2 = 0.74$$

**AZ 17-10**

$$R = 114.48 + 10.72 \cdot \text{ESAL}$$

$$R^2 = 0.61$$

**AZ 17-11**

$$R = 119.31 + 10.11 \cdot \text{ESAL}$$

$$R^2 = 0.63$$

As observed from the  $R^2$  values for the various relationships, the results range from poor to good. These relationships are illustrated in figure 50.

One factor that made the development of roughness regression equations difficult was the fact that diamond grinding had been performed on most of the I-17 sections. It should be noted that, while the effect of grinding usually had a positive effect on reducing the roughness, this often contributed to the scatter of the roughness data, thereby lowering the  $R^2$  of any regression equation. This is illustrated in figure 51 for 17-10, which shows how roughness was reduced by grinding, but the scatter in the data made it difficult to obtain a reasonable regression equation.

AZ117-03,04,05,06,10&11  
 9-inch JPCPs, AGG. BASE, BEFORE GRINDING

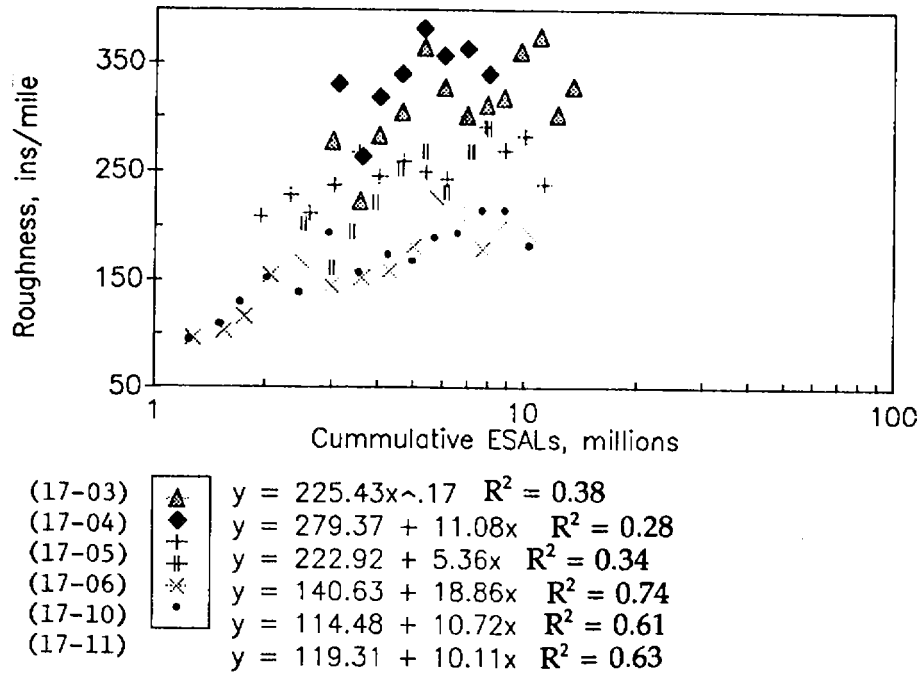


Figure 50. Roughness regression equations for selected sections on I-17.

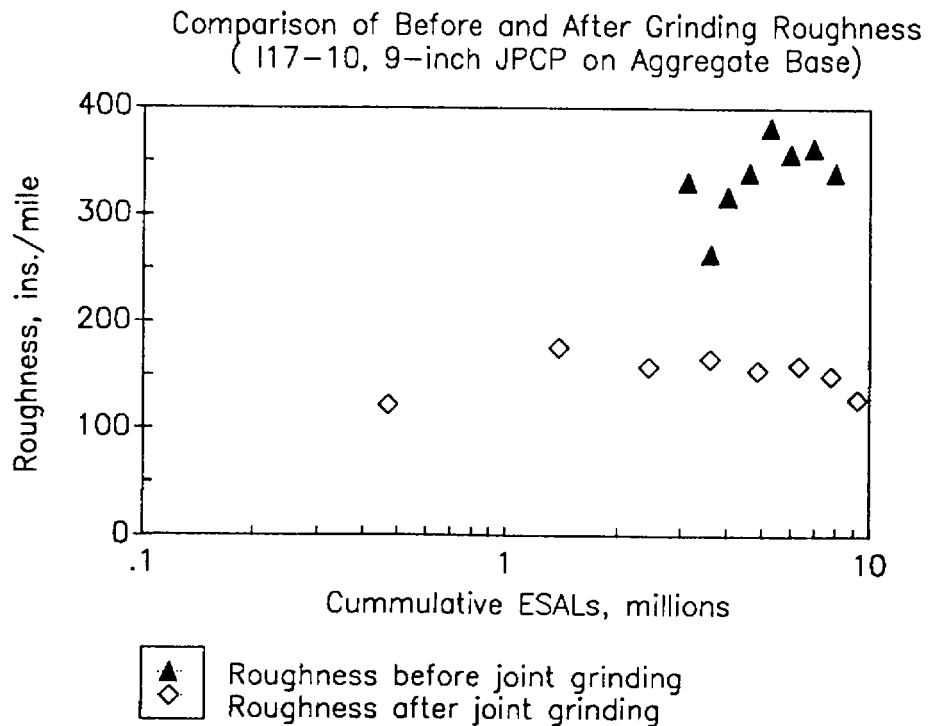


Figure 51. Effect of diamond grinding on 17-10 pavement roughness.

It must be reiterated that attempts were made to develop regression equations for every section in the study, but this often resulted in equations with extremely low  $R^2$  values. The low  $R^2$  values represent a large amount of scatter in the historical roughness data. Possible explanations for this could be that the data was not always obtained over exactly the same section or that the Mays Meter was not properly calibrated before and after each measurement.

Another possible explanation for the inability to consistently correlate pavement roughness to ESAL applications could be that the ESAL applications are not the only cause of roughness. That is, there are other factors in addition to traffic loading that are contributing to the roughness in the pavements. While the general trends in figures 48 through 51 indicate that roughness is increasing with ESAL's, it is believed that some of the measured roughness is due to the environmentally-induced geometry of the slab. For instance, the dry climate creates warping of the slabs, such that they could be warped upward at the joints, which could lead to roughness. In addition, thermal gradients through the slab could induce upward curling at the slab which, again, could lead to roughness. Large variations in pavement roughness could be recorded depending upon the time of day (or year) in which the measurements were obtained. It is recommended that additional investigations be conducted into the causes of roughness to determine the role that thermal curling and moisture warping may play in its development. This would have to include roughness measurements throughout the season and, in order to obtain repeatable measurements of the pavement profile, should be conducted using a profilometer.

## 7. SUMMARY

This chapter has presented a summary of various design, analysis, and predictive models for concrete pavements. The applicability of the models to Arizona conditions was examined, and efforts at developing models for Arizona conditions were described.

The two analytical models evaluated were the CMS model and the ILLI-SLAB program. The CMS model uses site-specific climatic data to determine the material's response to daily, seasonal, and yearly changes in the environmental conditions. The ILLI-SLAB program can be used in the structural analysis of a specific pavement cross section and was shown to have broad application to rigid pavement analysis by examining the stresses induced in a slab due to a temperature differential between the top and bottom of the slab, traffic loading, and the combination of these factors.

The outputs of the CMS model provides the design engineer the ability to determine the effects of the environment on the pavement. The CMS model may be used in conjunction with ILLI-SLAB to determine the stresses and deflections resulting from the environment and the combination of load and environment. These stresses and deflections can, with the use of a fatigue equation or transfer function, be

translated into the number of repetitions that a pavement slab before failing in fatigue. This is the basis of a mechanistic-empirical design procedure.

This chapter also examined several concrete pavement prediction models, including AASHTO, PEARDARP, COPEs, PFAULT, and the recently-developed FHWA models. With one exception, none of the models were able to accurately predict the distress (faulting, cracking, joint deterioration, pumping), serviceability or roughness measured on the pavements included in the study (at the 90 percent confidence level). Perhaps one of the primary reasons for their inability to predict performance is that all of the models are empirical to some extent and cannot accurately predict performance outside of the inference space from which they were developed.

The one prediction model that was shown to be acceptable for Arizona conditions was the new FHWA PSR model. That model uses pavement distress to provide an indication of the overall riding quality of a pavement (on a scale of 0 to 5). Such a model can be useful in determining how the traveling public may view the serviceability of a roadway that is exhibiting certain levels of distress, and therefore could be used in programming rehabilitation or maintenance activities.

Attempts at the development of new models for faulting and roughness were not successful. The limited nature of the data base, the confounding of various design factors, and the absence of time-sequence data made this task exceedingly difficult to obtain a reasonable model for Arizona conditions. Much more performance data distributed over time (i.e., time-sequence data for each section) and space (i.e., more sections added) are needed to allow for the development of acceptable faulting and roughness models.

Two-variable linear regressions, relating the ESAL applications sustained by a specific pavement section to the roughness, were performed using the historical roughness data. These regressions were successful for a selected number of sections and provide a means of estimating future roughness for the specific pavement section. However, these relations are only for those pavements for which they were developed and *can not* be applied to other pavements.

While the value of the analysis programs (i.e., CMS and ILLI-SLAB) evaluated in this chapter were clear, the benefits of the design and prediction models were not so evident. However, the use of reliable prediction models can contribute to the improvement of rigid pavement designs. The development of such models will require additional sections and additional (time-sequence) performance data. Nevertheless, it must be realized that the prediction models are only tools to assist in pavement design and analysis; they are intended to supplement, not replace, engineering judgment and knowledge.

# CHAPTER 5 DESIGN STRATEGIES FOR PCC PAVEMENTS IN THE PHOENIX URBAN CORRIDOR

## 1. INTRODUCTION

Over the past 30 years, many different portland cement concrete pavements have been designed and constructed in the Phoenix Urban Corridor. Originally, the designs were variations of short-jointed, nonreinforced concrete pavements constructed on a granular base. Over the years, however, that design strategy was modified and new ones were tried.<sup>a</sup>

The first modifications to the original design, made in the late 1960's, were from the short-jointed slab on an aggregate base with perpendicular transverse joints, to a similar design with random (13-15-17-15 ft), skewed transverse joints. This design was further modified by the substitution of a stabilized base for the aggregate base, and became the standard design for the 1980's. A design using cement-treated bases was followed by one with a lean concrete base. The addition of dowel bars to the design in 1984 (to control roughness problems due to faulted and curled/warped joints) completed the evolution of the JPCP design to its current standard.

While the doweled JPCP on a stabilized base became the "standard" design, during an experimental phase in the 1970's other designs were also being tried. These included thickened slabs (11 to 13 in) constructed directly on the subgrade, and thin, prestressed concrete slabs constructed over a stabilized base. Finally, in 1984, when an inner lane was added to S.R. 360, that portion of the project that was adjacent to the prestressed sections was constructed of continuously reinforced concrete pavement. This has since become a design that has been constructed in the Phoenix Urban Corridor in sections that were not evaluated as part of this project. A summary of the major design strategies employed by ADOT over the past 30 years is shown in table 24.

One of the purposes of this research was to develop a set of design strategies for future use on to-be-constructed portland cement concrete pavements. The basis for such a development was to be a life cycle cost analysis, which would be developed from the observation of the performance of these inservice pavements, and the projection of their future performance based on observable and predicted trends. In conjunction with an analysis of the costs of each of the different designs, it would

---

<sup>a</sup> For the purposes of this report, a *design strategy* applies to the selection of a pavement type, such as JPCP on a stabilized base or CRCP, and a *design procedure* is the set of steps to be followed within that design strategy.

Table 24. Summary of project sections by design strategy.

DESIGN 1 JPCP on Granular Base		DESIGN 2 JPCP on Stabilized Base		DESIGN 3 JPCP Slab on Grade		DESIGN 4 Prestressed Slab		DESIGN 5 CRCP	
Section	Year Built	Section	Year Built	Section	Year Built	Section	Year Built	Section	Year Built
17-01	1961	AZ 1-1	1972	AZ 1-2	1975	360-05	1977	360-07	1984
17-02	1961	AZ 1-6	1981	360-09	1975	360-06	1977	360-08	1984
17-10	1961	AZ 1-7	1981	360-04	1979	360-10a	1977		
17-06	1963	360-03	1983	AZ 1-4	1979	360-10b	1977		
17-03	1965	10-06*	1984	AZ 1-5	1979				
17-04	1965	10-07*	1984						
17-05	1965	360-01	1985						
17-11	1965	360-02	1985						
10-01	1968	AZ 2*	1985						
10-02	1968	10-05*	1985						
10-03	1968	10-04*	1986						

\* Section contains dowel bars

be possible to identify those design strategies that would be able to provide the best performance for the least cost. With such a variety of designs (as shown in table 24), it ought to be possible to discern significant differences in performance that would justify the support of one design strategy or group of design strategies over the others. However, as will be shown, in practice it is not that simple.

As the data analysis progressed, it became apparent that there would be insufficient data of a nature to be useful in the development of such design strategies. One proposed solution would be to extend the data base by the inclusion of similar sections in different locations. This was considered and ruled out because it was felt that the design parameters within the urban corridor varied so little that the inclusion of outside sections would unfavorably skew the data.

In chapter 4, the attempts made to implement such an approach are discussed. The interested reader should pay particular attention to section 5, which covers the analysis of pavement performance prediction models and their applicability to the pavements in the Phoenix Urban Corridor.

The approach finally taken is an empirical one. It is based on observations of the performance of the inservice concrete pavements in the Phoenix Urban Corridor, as well as the application of pavement design and performance information gleaned from around the country. Every effort was made to ensure that the resulting recommendations were appropriate for the specific conditions and needs of ADOT and the pavements in the Phoenix Urban Corridor.

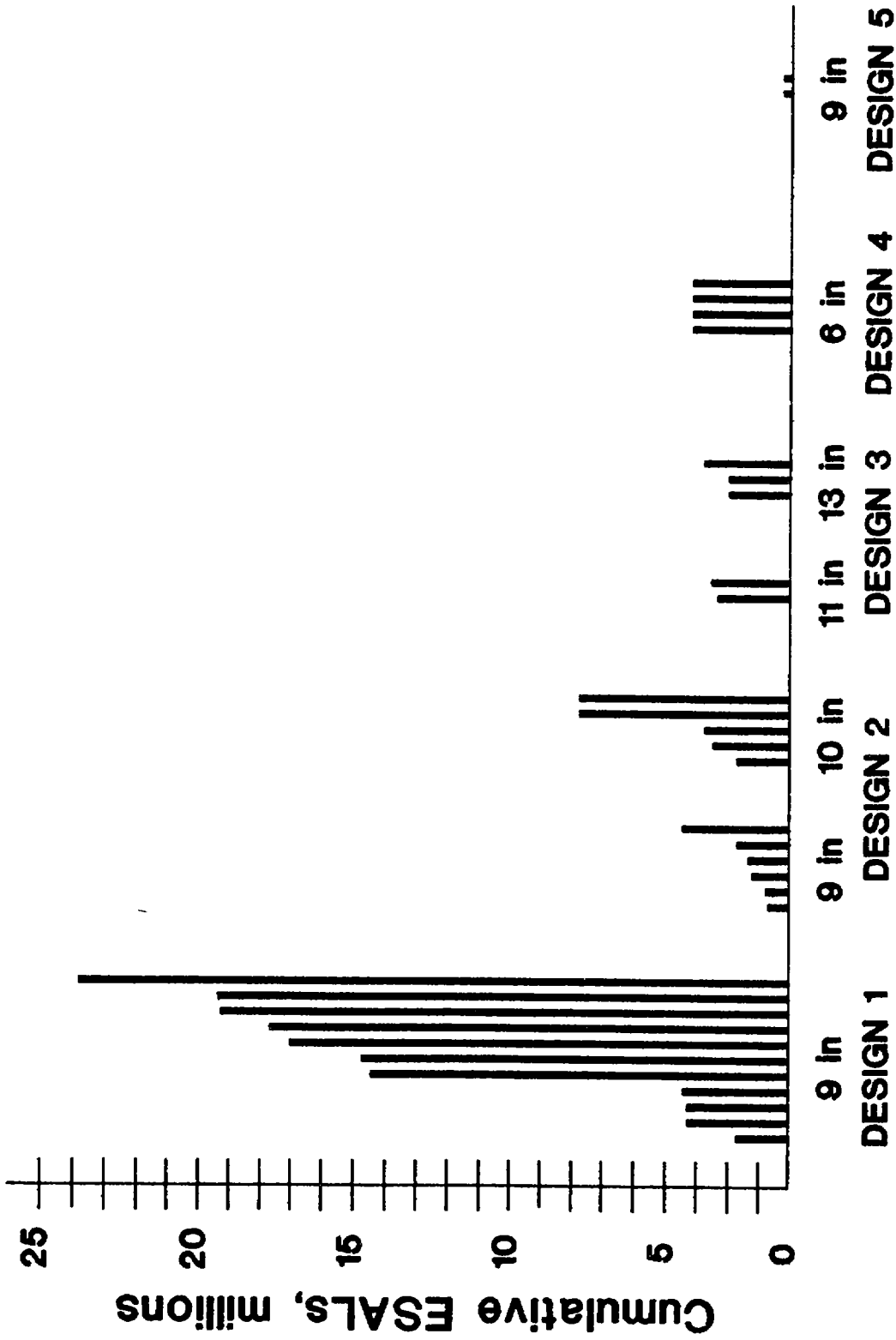
## 2. PERFORMANCE OF SELECTED DESIGN STRATEGIES

The performance of the different pavement designs was discussed in chapter 3 of this report. It was shown there that two designs stood out from the others in terms of their performance, the JPCP on LCB (with dowels), and the thick JPCP placed directly on grade. It was also noted that there were insufficient data from each design strategy available to draw complete and statistically valid conclusions. And because there were far too few failures, it would be very difficult to draw conclusions about long-term performance or life cycle costs.

An examination of figure 52 illustrates this situation. This graph shows the accumulated ESAL's carried by the lane evaluated in each pavement section of the study, by pavement design. In the first pavement design group, JPCP on a granular base, there are 11 different sections and a range in accumulated ESAL's from 2.8 to 23.8 million. The second grouping, JPCP on a stabilized base, also has 11 sections, but a range in accumulated ESAL's from 0.7 to 6.8 million. The number of sections included decreases from there, as does the range of ESAL's carried by all of the sections within a given design. The "worst" case is that of the CRCP, of which two sections had been included and both had carried 0.2 million ESAL's. While the performance had varied among the sections within each strategy and between different design strategies, it is obvious that there is insufficient data from which to draw meaningful conclusions.

The first observation to make about the performance of the project sections is that most of them had not carried significant volumes of traffic, and those that had were still carrying traffic. Given that sections 17-07 and 17-09 are not included in this summary, it can be said that none of the sections had failed in the sense of having been overlaid. In fact, it was noted in chapter 3 that, while none of the sections were exhibiting any structural distress or deficiency, several were approaching a critical serviceability level at which some sort of rehabilitation would be required.

Most portland cement concrete pavement design procedures emphasize the determination of the slab thickness or some other structural parameter (such as strength, reinforcement, etc.) and treat other aspects of design as secondary features (AASHTO or PCA, for example). Within the context of the performance of ADOT's concrete pavements in the Phoenix Urban Corridor, this would not be a valid approach. A comparison of slab thickness to accumulated ESAL's by pavement



## Distribution of Slab Thickness by Design Group

Figure 52. Accumulated ESAL's by design group and slab thickness.

section shows that thickness alone tells little about performance. Examining figure 52 again, it can be seen that several of the designs within design group 1 (JPCP on a granular base) had carried more traffic than any section within the entire study. While these pavements were exhibiting some deterioration, it was not related to structural inadequacy. The typical indicators of poor structural load-carrying capability—corner breaks, fatigue cracking, pumping—were, for the most part, absent. While there was faulting present, its range was from 0.01 to 0.09 in. Some of the sections had been diamond ground to remove faulting, but these values and projected pre-grinding values are well within acceptable levels nationwide.

Thus, in the designs consisting of 9 in to 13 in JPCP, 9 in CRCP, and even in the 6-in prestressed slabs, there was little discernible difference in structural performance. Selection of a design procedure whose ultimate output is the calculation of a required slab thickness appears to be an inappropriate exercise, as additional thickness will not necessarily improve performance.

This is not to say that all of these different designs performed similarly. In fact, there was a very wide range in the values of some of the performance parameters, most notably transverse joint spalling, but also to a lesser extent longitudinal cracking. There was also variation in transverse joint faulting and roughness and PSR. However, only the variation in PSR was found to be at all predictable. Many of the performance problems with the current designs (and therefore the variation in observed performance) are related to design or construction practices no longer followed, such as the use of steel inserts to form transverse joints, the formation of longitudinal joints with plastic inserts, and unrestricted hot weather paving. Some of the problems observed appeared to be related to poor construction practices or unfamiliarity with concrete pavement construction. These included high initial roughness that required extensive pre-acceptance grinding and the slab undulations caused by frequent stopping and starting of the paving train (allegedly due to the inability of the batch plants to keep the paver full of concrete). Again, these factors argue strongly against the development of a set of design strategies based on statistical evaluations or performance prediction equations.

### 3. RECOMMENDED DESIGN STRATEGIES

As previously mentioned, two design strategies emerged as superior to the others. These are the doweled JPCP on a stabilized (lean concrete) base, and the thick JPCP placed directly on the subgrade. In addition, the CRCP design appears to show promise for good performance and should be further studied for possible use in the Phoenix Urban Corridor. It must be emphasized here that due to the inability to apply a rational methodology to differentiate between the performance or expected lives of these designs, the cross-sections should be considered as equivalent designs. Additional performance information would be needed to recommend one alternative over the others.

Recommended cross-sections for each of these design strategies are shown in figures 53, 54, and 55. It is recommended that slab thickness be determined by a rational method acceptable to ADOT. However, given the observed performance of concrete pavements in this environment, there does not appear to be any reason to construct concrete slabs greater than 10 or 11 in when a base is used.

In the following section, additional guidance is provided to extend these design strategies to design procedures. For each pavement type, attention to the considerations presented in table 25 should help to ensure good performance.

Table 25. Additional design and construction considerations for the JPCP and CRCP design strategies.

JPCP	CRCP
Transverse Joint Spacing	Subdrainage
Subdrainage	Paving Restrictions
Transverse Joint Design	Construction Considerations
Construction Considerations	Number of Tied Lanes
Number of Tied Lanes	Longitudinal Reinforcement
Longitudinal Joint Design	Longitudinal Joint Design
Shoulder Design	Shoulder Design
Load Transfer	

#### 4. ADDITIONAL DESIGN/CONSTRUCTION CONSIDERATIONS

The cross-sections developed as part of the design strategies presented in section 3 above illustrate typical concepts related to those designs and relative locations and placements of key elements of the design strategies. Actual slab thickness should be handled using a methodology acceptable to ADOT. There are several other design features that need to be considered as part of a complete pavement design and not as independent variables. These are discussed below.

##### Transverse Joint Spacing

ADOT has used two different types of transverse joint spacing on JPCP. The 15-ft joint spacing, oriented perpendicular to the longitudinal joint, was characteristic of the pavement designs of the 1960's. That has since been changed to a random joint spacing of 13-15-17-15 ft (still averaging 15 ft), with the joints set at a skewed angle to the longitudinal joint. The concept of random joint spacing was introduced in California in the late 1950's, in response to a resonant vibration that developed in

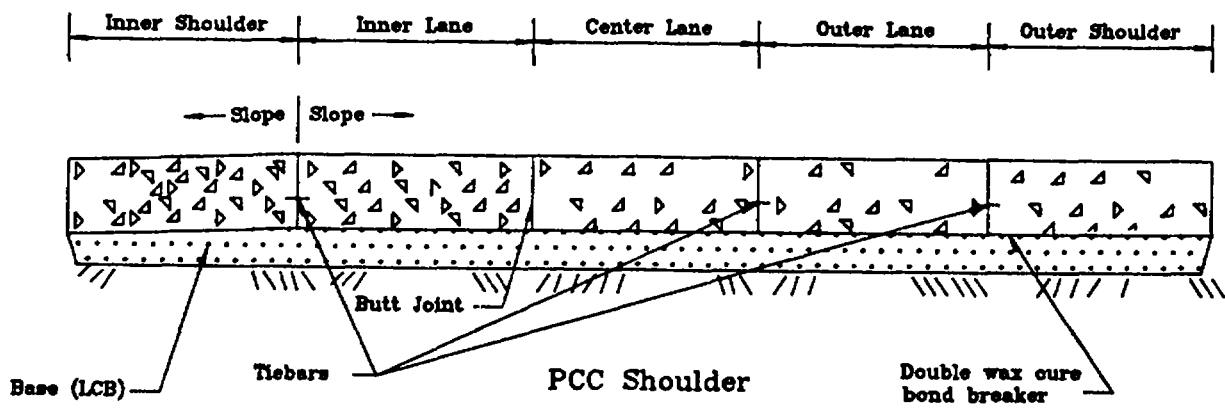
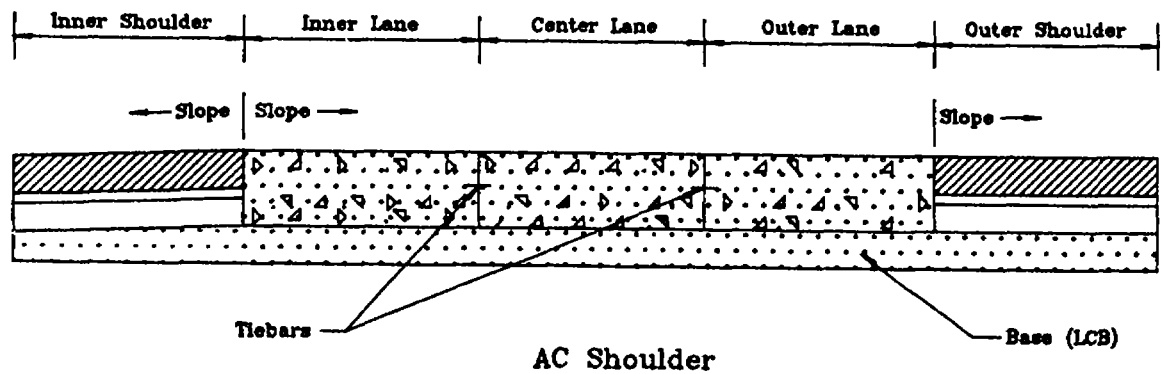
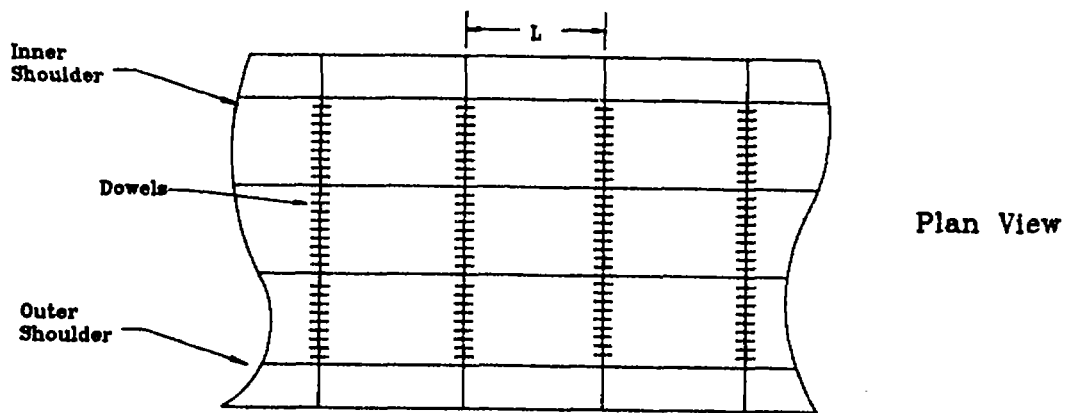


Figure 53. Typical cross-section of JPCP on a stabilized base.

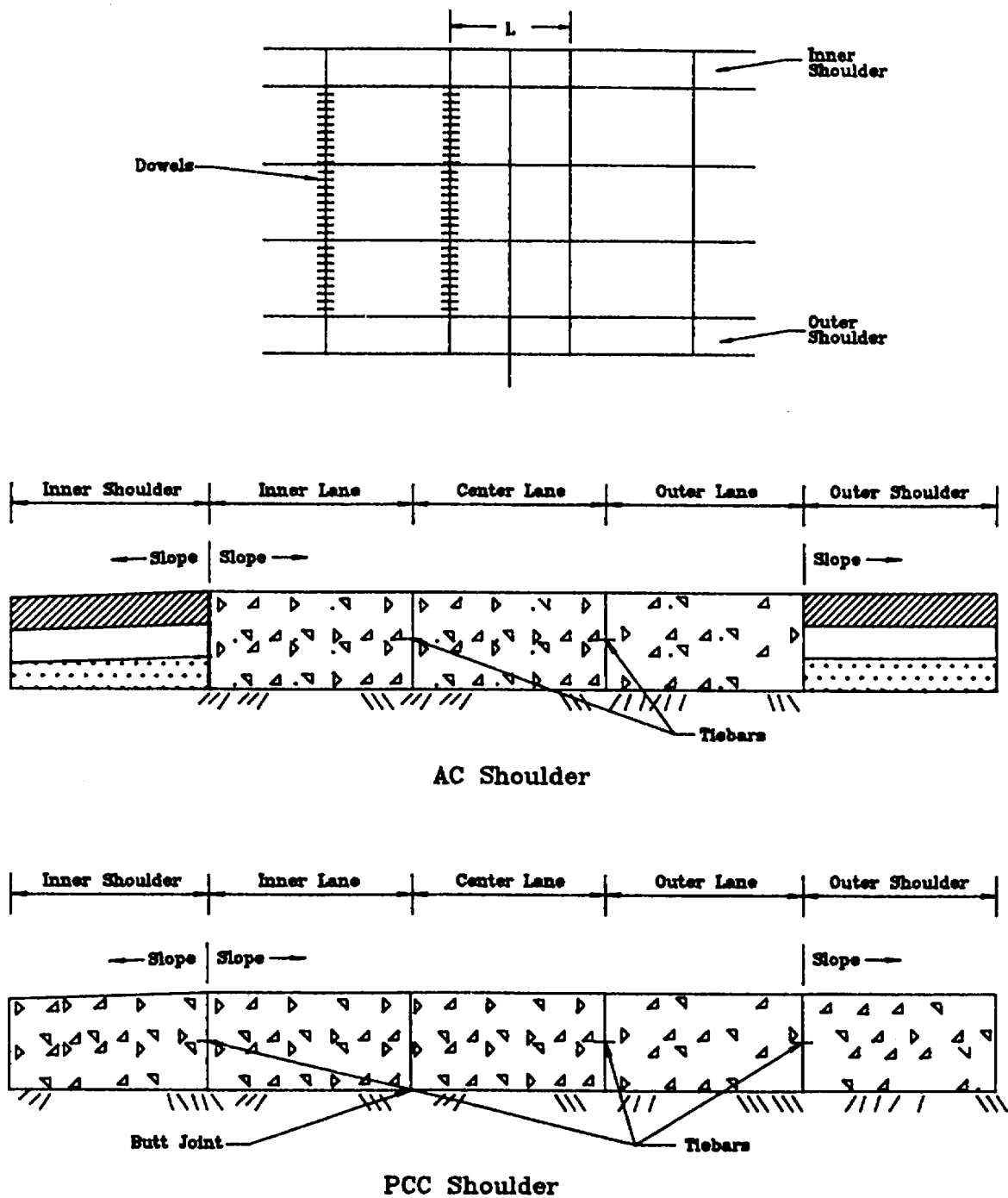


Figure 54. Typical cross-section of full-depth JPCP on subgrade.

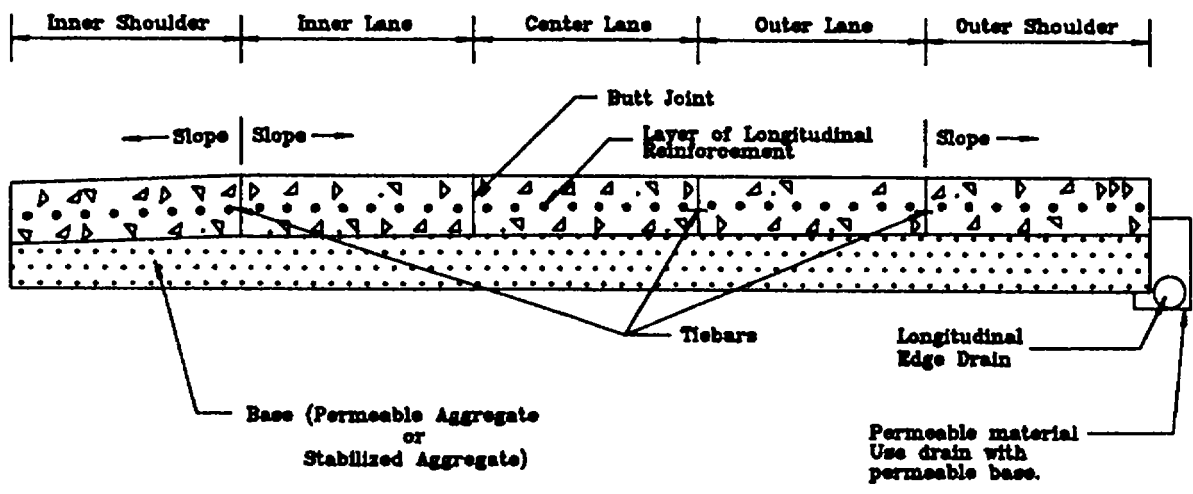
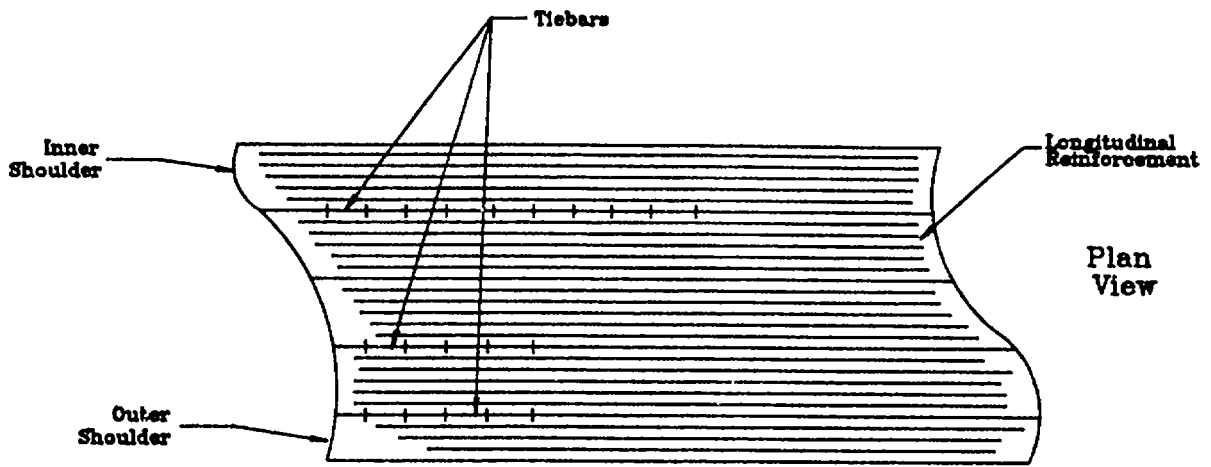


Figure 55. Typical cross-section of CRCP on a base.

certain full-sized Buicks from the faulting of uniformly-spaced transverse joints. Since that time, General Motors has addressed the vehicle design problems and random joint spacing no longer serves a meaningful purpose. In fact, it was shown in chapter 3 that the random-spaced joints appear to influence the faulting of joints between 17- and 15-ft slabs. Thus, it is recommended that a uniform joint spacing be used on all jointed concrete pavement designs in the Phoenix Urban Corridor.

The determination of the spacing to be used is based on slab thickness and base type. A typical rule of thumb is that the transverse joint spacing, in feet, should not exceed 1.5 to 1.75 the slab thickness, in inches.<sup>(32)</sup> In section 4 of the preceding chapter, a discussion of the  $L/l$  concept and its application to pavement performance was presented. This research suggests that the determination of a design transverse joint spacing should be based on a number of parameters, including base type, slab thickness, slab stiffness, the effective modulus of subgrade reaction, and the concrete Poisson's ratio. It is recommended that such an approach be followed to determine transverse joint spacing for concrete pavements in the Phoenix Urban Corridor.

The last aspect of transverse joint design concerns the orientation of the joint. ADOT currently constructs transverse joints at an angle (skewed) to the longitudinal joint. Skewed joints are constructed in order to reduce the load stresses applied to the transverse joint by any given vehicle, since due to the angle of the joint only one wheel of an axle crosses the joint at a time. While skewed joints do theoretically offer this advantage, their benefits in practice have not been substantiated. Research discussed previously did not show any appreciable difference in performance among sections of otherwise similar design in which the joint orientation varied between skewed and perpendicular.<sup>(4)</sup> In addition, there is not expected to be any additional benefits gained from skewing the joints of doweled pavements (which ADOT is currently constructing) because of their positive load transfer capabilities. Furthermore, ADOT (and other highway agencies as well) has had unsatisfactory experiences when the combination of skewed joints and dowels are constructed, due to misalignment of the dowels and the difficulty in properly locating the dowels for joint sawing purposes. Finally, skewed joints cost more to construct, as the transverse joint in a 2:12 skew is 10 percent longer than a perpendicular joint, and will require that much more joint sawing and joint sealing. It is recommended, therefore, that skewed joints not be used.

### **Subdrainage**

In most portions of the United States, the provision of adequate pavement subdrainage is recognized as an important factor affecting the performance of pavement designs. In the Phoenix area, where the average annual rainfall may range from 6 to 8 in, subdrainage does not appear to be quite as important. There are several factors to keep in mind when considering pavement subdrainage for future designs in the Phoenix Urban Corridor. The first is that most of the pavements are in

heavily developed urban areas, where surface run-off is handled by storm drains. Secondly, while there is very little rainfall on an annual average, when it does rain there can be a significant downfall in a very short period of time. Finally, faulting was one of the more notable distresses observed on the jointed concrete pavements. An understanding of the conventional mechanism behind the development of faulting includes the presence of heavy loads and excess subsurface free moisture.

While these factors suggest that excess subsurface moisture has been generated in the past, it is believed that the volume and frequency of such excess is not serious enough to warrant the construction of subsurface drainage or the inclusion of a permeable base layer in the jointed concrete pavement strategies. Rather, it is believed that the amount of rainfall that is typically experienced in this area is better handled through good maintenance practices (sealing of the joints) and by the provision of adequate surface cross-slope.

For the CRCP design strategy, the use of an aggregate base is suggested. An aggregate base will help to minimize friction that can develop between the base and slab and, if designed properly, can promote subsurface drainage. It is suggested that an open gradation, such as that shown in table 26, be used. As an alternative, a stabilized permeable base material may be desired. A gradation for such a material is also shown. Typical binder amounts range from 2 to 4 percent.

Table 26. Recommended gradations for permeable bases.<sup>(39)</sup>

SIEVE SIZE	PERCENT PASSING	
	<i>Aggregate</i>	<i>AC Stabilized</i>
1 1/2-in	100	
1-in	95 - 100	100
3/4-in	---	90 - 100
1/2-in	60 - 80	35 - 65
3/8-in	---	20 - 45
# 4	40 - 55	0 - 10
# 8	5 - 25	0 - 5
# 16	0 - 8	---
# 50	0 - 5	---
#200	---	0 - 2
PERM, ft/day	> 1,000	15,000

## Transverse Joint Design

Transverse joint sealants are used to prevent the intrusion of water and incompressibles into the transverse joint. There are a few important factors to consider in the design of transverse joints. The major parameter of interest is the joint shape factor, or the ratio of the sealant reservoir depth to width. A typical transverse joint configuration is shown in figure 56. The contraction joint is sawed as soon as practical after placement of the concrete. A 1/8-in wide blade should be used to make a sawcut from 1/4 to at most 1/3 of the slab thickness. The concrete should be of adequate strength to withstand the load of the sawing equipment and should not spall when sawed. The sealant reservoir can then be sawed any time before the pavement is opened to traffic, but is best left as long as possible to minimize the potential of spalling.

The dimensions of the transverse joint are a function of several of the design inputs, such as joint spacing, base type, expected temperature range, the coefficient of thermal expansion of the portland cement concrete, and the allowable strain of the type of sealant to be used. Prior to sealing, the sealant reservoir should be cleaned.

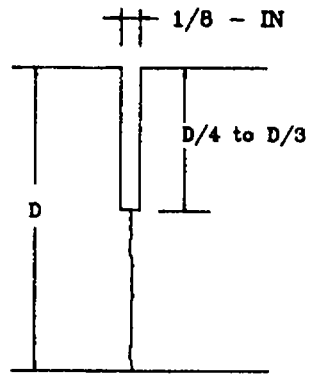
It is recommended that consideration be given to sealing contraction joints at the time of construction and that a sealant be used that has been shown to provide a service life of greater than 5 years. Generally high quality, long life joint seal materials, such as silicone or preformed neoprene sealants, should be specified for heavily traveled urban freeways where maintenance operations would be particularly disruptive to traffic.<sup>(40)</sup> If a silicone sealant is used, a backer rod or backer tape is placed in the reservoir to inhibit three-sided bonding and to assist in obtaining the proper joint shape factor. The observed performance of the original construction sealants used in the Phoenix Urban Corridor indicates that the common asphalt-rubber sealant in use does not provide that performance.

Once a sealant type is selected, the final design of the transverse joint can be completed, according to the following equation:

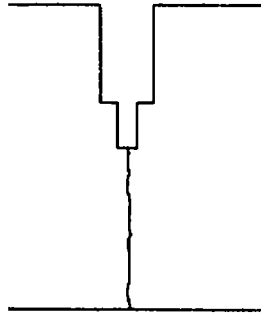
$$\Delta L = C \times L \times [(\alpha_c \times \Delta T) + Z] \quad (25)$$

where:

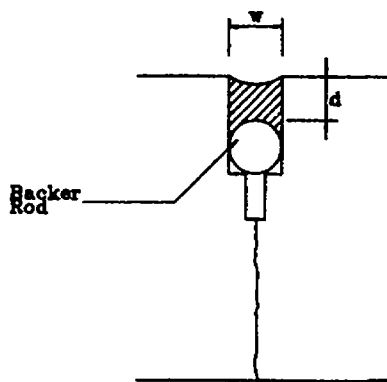
- $\Delta L$  = The joint opening caused by temperature changes and drying shrinkage of the PCC, in.
- $\alpha_c$  = Thermal coefficient of contraction of the PCC slab, °F.
- $\Delta T$  = Temperature range from PCC placement to minimum temperature, °F.



(a) Initial saw cut.



(b) Second saw cut to establish sealant reservoir.



(c) Final transverse joint configuration.

Figure 56. Typical transverse joint details.

- Z = Drying shrinkage coefficient of the PCC slab (neglect for resealing project), in/in.
- L = Joint spacing, in (not ft).
- C = An adjustment factor for friction between slab and subbase, 0.80, for granular untreated subbase 0.65, for stabilized granular subbase (e.g., asphalt, cement).

The required joint design width for the placement of all but the preformed sealants is then computed from the following equation:

$$W = \frac{\Delta L}{S} \tag{26}$$

where:

- W = Design width of transverse contraction joint, in.
- $\Delta L$  = The joint opening caused by temperature changes and drying shrinkage of the PCC, in.
- S = Allowable strain in the joint sealant material. Most asphaltic based sealants allow a maximum tensile strain in the sealant of 25 percent, thus S would be 0.25; whereas silicone sealants require 50 percent (0.50).

Preformed compression seals are selected so that they are compressed 20 to 50 percent of their normal width throughout their life. The determination of the required joint reservoir width and the selection of a proper preformed compression seal is an iterative procedure that should include input from the manufacturer.

### Friction Factor

The friction factor is used to estimate the percent of steel reinforcement required for good CRCP performance. It is a single number that serves as a gross approximation of the very complex interaction between the bottom of a slab and the top of the subbase. Friction factors in the AASHTO Design Guide range from 0.9 for natural subgrade to 2.2 for a surface treatment. Other research suggests that values may actually range from less than 1.0 for slabs on polyethylene sheeting to over 60 for cement-treated bases.

Significant debate continues concerning the estimation of appropriate friction factors for design, and research continues to define and quantify their values and use in design. Stabilized materials have much higher friction factors than nonstabilized materials or bondbreakers. High friction can lead to cracking and the development of significant levels of internal stress in the concrete slab. It is recommended that if concrete is to be placed over a stabilized layer, that stabilized layer be treated with a good bondbreaking treatment, such as a double wax cure.

## **Paving Restrictions**

ADOT specifications state that when daytime ambient temperatures are expected to exceed 100 °F, concrete placement shall be done only between the hours of 8 p.m. and 8 a.m. Hot weather paving can contribute to excessive drying of the mix that can lead to insufficient water available to satisfactorily hydrate the cement. Consideration should also be given to the relative humidity and the wind speed, which can also contribute to rapid drying of the concrete mix.

## **Construction Considerations**

As noted previously, some of the roughness and distresses (spalling from metal insert) observed on the concrete pavements were due to problems during initial construction problems that are actually not related to design. For instance, in discussion with current and former ADOT engineers, it was learned that many problems had been experienced in keeping fresh concrete in front of the paver. The result was excessive stopping and starting of the paving train, which contributed to built-in undulations and roughness. Also, the paving contractors did not have a lot of concrete paving experience nor was good equipment used. These factors likely contributed to some of the pavement roughness.

The Project Engineer should be encouraged to strictly enforce all ADOT policies regarding construction practices, especially if it is observed that practices are being followed that may contribute to a poorly performing pavement. While this is true for all concrete construction, it is of the utmost importance for the construction of CRCP, whose performance is extremely sensitive to the quality of construction.

Smoothness specifications for new concrete pavements have been used by ADOT since about 1986. These specifications require that the contractor meet a certain level of smoothness on a newly-constructed pavement. If the required smoothness is not achieved, corrective grinding by the contractor is usually required at no cost to the agency. Incentives (bonus payments) are also provided to the contractor if an extremely high level of smoothness is achieved. Smoothness specifications have been proven to be an effective means of obtaining a smooth-riding concrete pavement, which was a problem on earlier ADOT concrete designs.

## **Number of Lanes to Tie Together**

Paving equipment currently available are able to pave over 50 ft wide. In order to minimize internal stress development during the curing of the concrete that could lead to shrinkage cracking, it is recommended that no more than three lanes (or 38 ft) be tied together, including any tied concrete shoulders. Although greater lengths have often been recommended in the past, the performance of many concrete pavements across the country has shown that 38 ft is the maximum practical limit.

## **Longitudinal Joint Design**

The design and construction of the longitudinal lane-lane joint can be a critical factor in the development of longitudinal cracking. The establishment of the longitudinal joint as soon as possible after concrete placement will prevent the occurrence of uncontrolled longitudinal cracking.

Several of the projects included in this study had significant longitudinal cracking that is believed to be a result of inadequate longitudinal joint development or late sawing. The need for adequate sawing of the longitudinal joint appears to be more acute for pavements constructed on stabilized base courses. The high stiffness of the stabilized base course, and friction developed between the base and slab, can result in longitudinal cracking during the curing of the concrete slab. Therefore, it is critical that the sawing of longitudinal joints on concrete pavements constructed over stabilized bases be performed in a timely manner. The current practice of sawing the longitudinal joint one-third of the slab thickness appears to be adequate for aggregate bases, but this may need to be increased for pavements placed on stabilized bases.

## **Reinforcement**

The design of longitudinal steel for CRCP is based on mechanistic-empirical equations that account for many of the factors that are believed to be critical for good CRCP performance. These include transverse crack spacing, crack width, and the steel working stress. The equations are incorporated in the AASHTO equations for longitudinal steel design for CRCP and have as their output a percent steel.<sup>(32)</sup> Recent research reported by the University of Texas' Center for Transportation Research demonstrates that "percent steel and bar size, rather than steel reinforcement alone, should be considered in CRCP design."<sup>(41)</sup> Aggregate type and size were also found to have an effect. It is recommended that the bond area of the steel (which is a function of the reinforcement diameter) be considered in the design process and that the constraints recommended in the report not be exceeded. Attention should also be paid to the allowable crack width in this design procedure, as the 0.04 in criterion reported in the literature has since been refuted, with an actual value of between 0.02 and 0.025 in appearing to be more appropriate.

As for transverse steel, it is normally not required unless extensive subsurface movement is expected. From a performance standpoint, therefore, there does not appear to be any reason to include transverse steel in the CRCP design.

## **Shoulder Design**

The major decision to be made in designing the pavement shoulder is the selection of the shoulder type. The JPCP that were surveyed had both AC and PCC shoulders; the other pavement designs had a shoulder of the same type and cross-

section as the mainline pavement. It is a widely held belief that pavement life can be prolonged through the construction of tied concrete shoulders.<sup>(42,43)</sup> Tied concrete shoulders can change edge loads to interior loads, where the stress is lower. They also create a more easily maintained lane-shoulder interface joint, thereby reducing one of the major sources of moisture infiltration in a pavement system. It is also easier to maintain a shoulder of similar type and cross-section design at the same level as the mainline pavement

It was not possible to use the performance data from this research effort to support this conclusion about concrete shoulders, as their effect was confounded by many other factors. Nonetheless, it is recommended that portland cement concrete pavements be constructed of the same material and cross-section as the mainline pavement. This will not only provide the benefits described above, but it will also more readily accommodate shoulder traffic, which is not uncommon in an urban highway setting.

### Load Transfer Design

Transverse joint load transfer is the mechanism by which wheel loads are transmitted from one slab to the adjacent slab. It is generally achieved by one of two methods; aggregate interlock of the two abutting joint faces, or through the use of mechanical load transfer devices, the most common of which are circular dowel bars.

In the past, almost all of the JPCP projects in the dryer Western States did not use dowel bars. This includes many of the pavements that were included in this study. While some of these projects did not develop serious faulting, many have. It is currently recommended that aggregate interlock be used for load transfer only on local roads and streets that carry few trucks, or in areas subjected to only moderate variations in temperature.<sup>(44)</sup> Dowel bars reduce the differential deflection of the joint and increase the load transfer, which in turn decreases the pumping action occurring on the underlying base material, and the resultant faulting and loss of support.

There were insufficient performance data from the sections with doweled transverse joints from which conclusions could be drawn regarding their effectiveness. However, the dowel bars did reduce the magnitude of the corner deflection and also appeared to reduce the development of apparent voids beneath slab corners. Given the extremely high traffic volumes in the Phoenix Urban Corridor and the corresponding need to ensure long-term performance capabilities, the use of epoxy-coated, steel dowel bars, 1/8 of the slab thickness in diameter (up to a maximum of 1.5 in), is strongly recommended for all JPCP designs, including the thick, slab-on-grade design. Dowels have been found to add approximately \$2/yd<sup>2</sup> to the overall cost of a concrete pavement. Since it is extremely difficult to restore load transfer to a concrete pavement once it is lost, the use of dowels can help to ensure a longer life, particularly if actual pavement loadings exceed design values.

## 5. SUMMARY

From a review of the performance of the inservice concrete pavements in the Phoenix Urban Corridor, performance trends reported elsewhere, and the available literature, several concrete pavement design strategies stand out as candidates for future highway construction projects. Two of the designs are jointed plain concrete pavements (doweled JPCP over LCB and thick, slab-on-grade JPCP) and one is a continuously reinforced concrete pavement design. A number of design recommendations and construction considerations are presented that should enhance the performance of these designs.

It has been mentioned in chapters 3 and 4 that the prevailing climatic conditions appear to influence the performance of concrete pavements in the Phoenix Urban Corridor. It was noted that the lack of moisture and the absence of a freezing and thawing period generally appear to aid in the performance of the concrete pavements. However, there are several aspects of the environment that may adversely influence the performance of the pavements, most notably in creating pavement roughness. Specifically, the actions of thermal curling and moisture warping appear to cause some roughness problems in the concrete pavements, so it is essential that any of the proposed designs address that issue. It is believed that all of the proposed designs do so, since it is recommended that both JPCP designs employ dowel bars (which should minimize joint curling and warping), and the CRCP design is constructed without joints, so it should not suffer from any curling and warping problems that can lead to roughness.

One issue that has not been mentioned is the idea of the maintainability of the design strategy. In an urban environment, it is important that the maintenance requirements of a pavement be kept to a minimum (but not ignored) in order to reduce disruptions to traffic. Thus, for the JPCP designs, long-lasting, high-quality joint sealant materials (such as silicone or preformed compression sealants) should be used, and adequately-sized dowel bars are strongly recommended to reduce faulting and joint curling/warping (which can lead to pavement roughness).

The CRCP design holds the promise of providing a smooth riding surface with little maintenance requirements for many years. However, as previously indicated, CRCP designs are very sensitive to the quality of the pavement construction. If not properly constructed, CRCP can create a drain on an agency's maintenance budget, particularly in an urban environment. Therefore, it is important that ADOT carefully consider all construction aspects of CRCP when contemplating its use.

It is recommended that monitoring of ADOT's concrete pavements be continued in order to obtain a better indication of each design's long-term performance capabilities. Modifications to design strategies can be made as more information becomes available.

# CHAPTER 6 RECOMMENDED REHABILITATION MEASURES FOR STUDY SECTIONS

## 1. INTRODUCTION

In this section, a brief description of the design of each of the sections is presented, followed by a summary of the pertinent performance data used to select appropriate rehabilitation techniques. The full summary of the design and performance data is found in appendix A. In appendix B, strip maps of each of the sections can be found. These graphical representations of the sections are quite useful in visualizing the current status of the section.

Based on the assembled information, each of the concrete pavement sections that were studied were also evaluated in terms of identifying the most appropriate rehabilitation scheme for that specific section. That determination was based on the decision trees and matrices presented in appendix E and the interested reader is referred to that section for further enlightenment.

As part of this study, many concrete pavement rehabilitation strategies were evaluated for their appropriateness for use in the Phoenix Urban Corridor. That evaluation is presented in appendix F, and is based on the field performance of existing sections, interviews with knowledgeable ADOT personnel, and information available elsewhere.

## 2. S.R. 360 (SUPERSTITION FREEWAY)

Seventeen sections were surveyed on the Superstition Freeway. The first six were surveyed in 1987 as part of a parallel FHWA study. The rest were surveyed in 1988 under this project. Their ages ranged from 3 to 15 years old and they included both jointed plain, prestressed, and continuously reinforced concrete pavements.

### AZ 1-1, SR 360, WB

This pavement is a 9-in JPCP constructed on a 6-in CTB and a 4-in aggregate subbase. Transverse joints are skewed, nondoweled, and have a random joint spacing of 13-15-17-15 ft. The outer shoulder is 3-in thick asphalt concrete. When surveyed in 1987, the pavement was 15 years old and had carried an estimated 3.3 million ESAL's in the outer lane. At that time, the two-way ADT was estimated at about 110,000 vehicles per day. Approximately 3.1 percent of that traffic volume were heavy trucks (FHWA Classification 5 or greater).

During the survey, an average PSR of 3.4 was recorded for this section. This is one of the lower rated sections in the study. The Mays roughness index was 114 in/mi. The most notable distresses were related to the transverse joints, which exhibited an average of 0.08 in of faulting. In addition, 22 percent of the transverse joints exhibited medium- or high-severity spalling, 21 percent of which had been patched with a cementitious product. The middle lane exhibited similar roughness and serviceability values and slightly more spalling and spall repair. The inner lane had no spalling or repairs at the transverse joints, but did have 15 transverse cracks per mile.

A consideration of the deflection data and an evaluation of the strength data from destructive testing suggests that the pavement is not exhibiting a structural deficiency. The primary distresses are transverse joint faulting and spalling. In order to address these two distresses and improve rideability, it is recommended that the section receive either partial-depth repairs or full-depth repairs at the deteriorated joints. Determination of the appropriate repair method would require further investigation into the depth and extent of the spalling at the transverse joints. It would also be appropriate to grind transverse joints to remove the faulting and restore rideability.

#### **AZ 1-2, SR 360, WB**

This pavement is a 13-in JPCP constructed directly on the subgrade. Transverse joints are skewed, nondoweled, and have a random joint spacing of 13-15-17-15 ft. The outer shoulder is PCC, tapering from 13 in thick at the edge of the pavement to 6-in thick at the shoulder's outer edge. When surveyed in 1987, the pavement was 12 years old and had carried an estimated 2.8 million ESAL's in the outer lane. In 1987, the two-way ADT was estimated at 119,000 vehicles per day, including 3.1 percent trucks.

During the survey, an average PSR of 3.8 was recorded for this section. The Mays roughness index was 65 in/mi, which indicates one of the smoother sections evaluated. There were no serious pavement distresses, although 4 percent of the transverse joints had been patched with a bituminous material. The center lane showed more distress, with a total of 24 percent of the joints exhibiting low- or medium-severity spalling. The inner lane was performing similarly, with almost no distresses and a PSR of 3.8. The outer shoulder was in excellent condition.

A consideration of the deflection data and an evaluation of the strength data from destructive testing suggests that the pavement is not exhibiting a structural deficiency. The average mid-slab deflections were quite low and no voids were identified beneath the slab corners. The condition of the pavement at the time of the survey indicates no need for any rehabilitation. Consideration should be given to keeping the transverse joints sealed with an appropriate sealant material in order to

reduce the development of spalling. As spalls approach medium severity, they should be repaired using partial-depth patching techniques.

#### **AZ 1-4, SR 360, WB**

This pavement is also a 13-in JPCP placed directly on the subgrade. The mainline pavement design is identical to that of AZ 1-3, described above. The outer concrete shoulder is 13-in thick for its full width, however. This pavement section was also constructed four years later than AZ 1-3. When surveyed in 1987, the pavement was 8 years old and had carried an estimated 2.0 million ESAL's in the outer lane. The 1987 two-way ADT was estimated at 94,000 vehicles per day, including 3.1 percent trucks.

From the field survey, an average PSR of 3.6 was recorded for this section. The Mays roughness index was 102 in/mi, which was one of the higher values for the sections on the Superstition Freeway. There was no transverse or longitudinal cracking, negligible spalling, and no spall repair. Transverse joint faulting averaged 0.01 in. The performance data of the center and inner lanes was basically identical to that of the outer lane. The outer shoulder was in excellent condition.

An evaluation of the deflection data suggests that the pavement does not have any structural deficiencies. The average mid-slab deflections were low and no voids were identified beneath the slab corners. The condition of the pavement at the time of the survey indicates no need for any rehabilitation. Routine maintenance should continue to prevent the development of severe deterioration.

#### **AZ 1-5, SR 360, WB**

AZ 1-5 is an 11-in JPCP constructed directly on the subgrade. Transverse joints are skewed, nondoweled, and have a random joint spacing of 13-15-17-15 ft. The outer shoulder is tied PCC, 11-in thick. When surveyed in 1987, the pavement was 8 years old and had carried an estimated 2.3 million ESAL's in the outer lane. In 1987, the two-way ADT was estimated at 106,000 vehicles per day. Approximately 3.1 percent of that traffic volume was heavy trucks.

During the survey, an average PSR of 3.8 was recorded for this section. The Mays roughness index was 85 in/mi, which indicates one of the smoother sections evaluated. There were no serious pavement distresses, although 4 percent of the transverse joints had been patched with a bituminous material. The center lane was performing well, exhibiting no spalling and a PSR of 3.8. The inner lane was performing similarly, with almost no distresses and a PSR of 3.8. The outer shoulder was in excellent condition.

Although 57 percent of the slab corners exhibit voids, the pavement is not showing any signs of a structural deficiency. In fact, the condition of the pavement at the time of the survey is such that it is not in of any rehabilitation. However, consideration should be given to keeping the transverse joints sealed with an appropriate sealant material in order to reduce the development of joint spalling. As the low-severity joint spalls approach medium severity, they should be repaired using partial-depth patching techniques and appropriate spall repair materials.

#### **AZ 1-6, SR 360, WB**

This pavement is a 9-in JPCP constructed on a 4-in LCB. Transverse joints are skewed, nondoweled, and have a random joint spacing of 13-15-17-15 ft. The outer shoulder is 9-in thick JPCP, also placed on the 4-in LCB. When surveyed in 1987, the pavement was 6 years old and had carried an estimated 1.7 million ESAL's in the outer lane. The two-way ADT in 1987 was estimated to be 98,000 vehicles per day, including 3.1 percent trucks.

During the survey, an average PSR of 3.5 was recorded for this section. This is lower than expected for a pavement of this age in this environment. The Mays roughness index was 97 in/mi. The field survey did not identify any distresses of note. The inner lane of the two lanes in the survey was equally free from distresses. The outer shoulder was in excellent condition.

The mid-slab deflections on this section were the lowest of those pavements included in the survey. The absence of significant distresses and the consideration of the nondestructive testing indicates that the pavement is not exhibiting any structural deficiency. According to information provided by ADOT, the transverse joints were sealed with rubberized asphalt in 1986, which is in good condition. At this time, because of the excellent condition of the pavement, no rehabilitation or pavement repair is indicated.

#### **AZ 1-7, SR 360, WB**

Like AZ 1-6, this pavement is a 9-in JPCP constructed on a 4-in LCB. Transverse joints are skewed, nondoweled, and have a random joint spacing of 13-15-17-15 ft. The outer shoulder is 9-in thick JPCP, also placed on the 4-in LCB. At the time of the pavement survey in 1987, the pavement was 6 years old and had carried an estimated 1.3 million ESAL's in the outer lane. At that time, the two-way ADT was estimated to be 75,000 vehicles per day, with 3.1 percent trucks.

During the survey, an average PSR of 3.8 was recorded for this section. The Mays roughness index was 91 in/mi. The field survey did not identify any distresses of note in either the outer lane or inner lane.

The pavement is in excellent structural condition as indicated by the absence of any significant distress and by the results from the nondestructive testing. Information furnished by ADOT indicated that the transverse joints had been sealed with rubberized asphalt in 1986, and that sealant is still in good condition. Due to the excellent overall condition of the pavement, no rehabilitation or pavement repair is recommended at this time.

### **360-01, EB**

This section is a 9-in JPCP constructed on a 4-in LCB. The transverse joints are skewed, nondoweled, and have a random joint spacing of 13-15-17-15 ft. The outer shoulder is constructed of PCC and has the same cross-section as the mainline pavement. The inner lane is paved 16-ft wide and has a 4-ft PCC shoulder. The pavement is one of the newer parts of the Superstition Freeway and, when surveyed in 1988, it was only 3 years old. At that time, it was estimated that the pavement had carried 0.77 million ESAL's in the outer lane and the two-way ADT was estimated to be 46,500 vehicles per day, which included 3.5 percent heavy trucks.

The field survey produced an average PSR of 4.4 for the outer lane, which is very high, but typical for new PCC construction. An average transverse joint faulting of 0.05 in was measured, and 17 percent of the joints showed low severity spalling. The PSR in the inner lane was 4.5, and although faulting was not recorded, the Mays roughness measurement was a low 70 in/mi. There were 13 percent of the transverse joints which were found to exhibit low-severity spalling.

The deflection data suggests that the pavement is structurally sound, but that there is an alarmingly low load transfer efficiency at the transverse joints. The deflection data also suggests the presence of voids beneath 90 percent of the transverse joints. Although there is no single distress that requires the need for rehabilitation at this time, the presence of the faulting, poor load transfer, and void development at the transverse joints are causes of concern. Further evaluation is appropriate to identify the causes of what must be considered premature distress on this 3-year old pavement. If faulting continues at its present rate, diamond grinding and perhaps slab stabilization may be warranted in the near future.

### **360-02, EB**

This section is a 9-in JPCP constructed on a 4-in LCB. The transverse joints are skewed, nondoweled, and have a random joint spacing of 13-15-17-15 ft. The outer shoulder is constructed of PCC and has the same cross-section as the mainline pavement. The inner lane is 16-ft wide and is striped at 12 ft. This pavement is one of the newer parts of the Superstition Freeway and, when surveyed in 1988, it was only 3 years old. At that time, it was estimated that the pavement had carried 0.78

million ESAL's in the outer lane and the two-way ADT was estimated to be 46,500 vehicles per day, including 3.5 percent heavy trucks.

The field survey produced an average PSR of 4.2 for the outer lane, with a Mays roughness measurement of 80 in/mi. An average transverse joint faulting of 0.02 in was recorded, and 5 percent of the transverse joints showed low-severity spalling. The PSR in the inner lane was 4.3, and the Mays roughness measurement was 80 in/mi. There was no transverse joint spalling in the inner lane.

An analysis of the nondestructive testing data suggests that there is not any structural deficiency in the pavement. However, the FWD data indicates that the load transfer efficiency of the transverse joints is only 42 percent, and that voids are present beneath 60 percent of the transverse joints. While this section is not in need of rehabilitation at this time, the low load transfer efficiencies and the presence of the voids beneath the slab corners are abnormally high for a new pavement and should be further investigated.

### 360-03, EB

This section, like 360-01 and 360-02, is a 9-in JPCP constructed on a 4-in LCB. The transverse joints are skewed, nondoweled, and have a random joint spacing of 13-15-17-15 ft. The outer shoulder is constructed of PCC and has the same cross-section as the mainline pavement. The inner lane is paved 16-ft wide. The pavement, when surveyed in 1988, was 5 years old. At that time, it was estimated that the pavement had carried 1.1 million ESAL's in the outer lane; the two-way ADT was estimated to be 46,500 vehicles per day, with 3.5 percent heavy trucks.

The field survey showed an average PSR of 4.1 for the outer lane, with a Mays roughness measurement of 86 in/mi. An average transverse joint faulting of 0.02 in was measured, and 4 percent of the joints showed low-severity spalling. The PSR in the inner lane was also 4.2, and the Mays roughness was 75 in/mi. Transverse joint spalling was observed at 3 percent of the transverse joints in the inner lane. The inner lane also had an average of 55 lin ft/mi of longitudinal cracking.

The deflection testing data suggests that the pavement is structurally sound. However, the load transfer efficiency at the transverse joints was measured to be only 51 percent, and voids were detected at 37 percent of the joints. These values are better than those of the previous two sections, but are not considered good values for such a new pavement. While this section does not require rehabilitation at this time, this section should be subjected to the same investigations as the previous two sections (360-01 and 360-02) to ascertain the reasons for the void development and low load transfer efficiencies.

### **360-04, WB**

This section is an 11-in JPCP placed directly on the subgrade. The transverse joints are skewed and not doweled, with a random joints spacing of 13-15-17-15 ft. The outer concrete shoulder is 11-in thick for its full width. This pavement section was constructed in 1979, and, when surveyed in 1988, the pavement had carried an estimated 2.6 million ESAL's in the outer lane. The 1988 two-way ADT was estimated to be 109,000 vehicles per day, including 3.5 percent heavy trucks.

From the field survey, an average PSR of 4.3 was recorded for this section. The Mays roughness index was 55 in/mi, which was one of the lowest values for any of the sections in the Urban Corridor. Transverse joint faulting averaged 0.04 in and there was negligible spalling. No transverse cracking was recorded, although there was a small amount of longitudinal cracking (18 lin ft/mi) observed. The performance data of the center and inner lanes was similar to that of the outer lane.

The excellent condition of the pavement clearly indicates that the pavement is structurally sound, and the results from the deflection testing evaluation serve to confirm this belief. While there were voids identified beneath 35 percent of the slab corners, the condition of the pavement at the time of the survey indicates no need for any rehabilitation. Routine maintenance should be continued to prevent the development of more severe deterioration.

### **360-05, EB**

This section and the next section, 360-06, are two of the four experimental prestressed concrete pavement sections included in the study. Within that experiment, several other construction variables are found. These two sections were of the standard design, consisting of a 6-in slab on a 4-in LCB. The transverse joints, which are actually 8-ft wide gap slabs where the post-tensioned cables are tied, are spaced at 402 ft intervals. This pavement was 11 years old at the time of its survey in 1988, and had carried an estimated 3.1 million ESAL's in the outer lane. The two-way ADT was 111,000 vehicles per day, including 3.5 percent heavy trucks.

The field survey of this section revealed a PSR of 3.9 and a Mays roughness of 88 in/mi in the outer lane. There was considerable distress occurring at the gap slabs, which had been repaired with either an epoxy or bituminous material.

The type of structural evaluation performed on the other sections was not possible on the prestressed sections. No cores were taken because of the risk of compromising the integrity of the tendons. Deflection data was collected at the mid-slab location, and these average values were almost twice as high as those found on the other PCC pavements in the Urban Corridor.

The major rehabilitation required on this section is at the gap slabs. However, many attempts have been made to repair the spalling at the joints, with very few successes. In any case, the highway in this area is planned for realignment and the prestressed sections are slated for removal. Therefore, rehabilitation options for this pavement are a moot subject.

#### **360-06, EB**

This section is also an experimental prestressed concrete pavement, consisting of a 6-in slab on a 4-in LCB. The 8-ft wide gap slabs are spaced at 402 ft intervals. This pavement was also 11 years old at the time of its survey, and had carried an estimated 3.1 million ESAL's in the outer lane. The two-way ADT in 1988 was 111,000 vehicles per day, with 3.5 percent heavy trucks.

The field survey of this section revealed a PSR of 3.3 in the outer lane and a Mays roughness of 131 in/mi. The middle lane had a PSR of 4.0 and a Mays roughness of 102 in/mi. As with all of the prestressed pavements, there was considerable distress at the gap slabs and had been repaired with a bituminous product.

Deflection data collected from the mid-slab location showed average values that were almost twice as high as those found on the other PCC pavements in the Urban Corridor. The major rehabilitation performed to date and still required on this section is at the gap slabs. The cracking on this pavement is high, but the cracks are tight and there is no clearcut way to repair this condition. One of the best alternatives for rehabilitation is probably a thin overlay, such as the three-layer system. However, the problem at the gap slabs would not be solved by such an approach. As noted above, this section is slated for removal to accommodate new pavement construction.

#### **360-07, EB**

This section and the next section, 360-08, are single lanes that were added as inside lanes to the experimental prestressed concrete pavement sections when those sections required widening to increase highway capacity. The design consisted of a 9-in continuously reinforced concrete slab on a 4-in aggregate base. There is 0.65 percent reinforcing steel in this pavement. This pavement was 4 years old at the time of its survey, and had carried an estimated 0.21 million ESAL's (inner lane). The two-way ADT in 1988 was estimated as 111,000 vehicles per day, with 3.5 percent heavy trucks.

The field survey of this section revealed a PSR of 3.9 in the single lane, with Mays roughness of 86 in/mi. The average transverse crack spacing was 4.35 ft and the cracks were tight. No punchouts or other distresses were noted on this section.

The type of structural evaluation performed on the other sections was not possible on the CRCP. No cores were taken because of the possibility of destroying the integrity of the reinforcing steel. Deflection data was collected at the mid-slab location, and these values were typical of mid-slab deflection data collected on the jointed concrete pavements. Because this pavement is in good condition and not exhibiting any major distresses, at this time there is no need for rehabilitation. If properly constructed, this type of design should require very little maintenance or repair unless it begins to demonstrate structural defects such as widened cracks, pumping, or punchouts.

#### **360-08, EB**

This section is a single lane that was added as an inside lane to the experimental prestressed concrete pavement sections. The design consists of a 9-in continuously reinforced concrete slab on a 4-in aggregate base. There is 0.65 percent reinforcing steel in this pavement. This pavement was 4 years old at the time of its survey, and had carried an estimated 0.21 million ESAL's (inner lane). The two-way ADT in 1988 was 111,000 vehicles per day, including 3.5 percent heavy trucks.

The field survey of this section revealed a PSR of 4.0, with Mays roughness of 80 in/mi. The average transverse crack spacing was 4.65 ft and the cracks were tight. No punchouts, connecting longitudinal cracks between transverse cracks, or other distresses were noted on this section.

Deflection data was collected at the mid-slab location, and these values were typical of mid-slab deflection data collected on the other PCC pavements. This pavement is in good condition and is not exhibiting any major distresses, so no rehabilitation is needed at this time. As previously discussed, this type of design should require very little maintenance or repair unless it begins to demonstrate structural defects such as widened cracks, pumping, or punchouts.

#### **360-09, WB**

This pavement is a 13-in JPCP constructed directly on the subgrade. Transverse joints are skewed, nondoweled, and have a random joint spacing of 13-15-17-15 ft. The outer shoulder is also 13-in thick JPCP. When surveyed in 1988, the pavement was 13 years old and had carried an estimated 3.8 million ESAL's in the outer lane. At that time, the two-way ADT was estimated to be 120,000 vehicles per day, including 3.5 percent trucks.

During the survey, an average PSR of 4.8 was recorded for this section, highest of any of the surveyed sections in this study. The Mays roughness index was 64 in/mi, which is one of the smoother sections evaluated. There were no serious pavement distresses, although there were 35 transverse cracks/mile and 35 lin ft of

longitudinal cracking/mile. These cracks were all low severity and very tight. The transverse joints showed 5 percent low-severity spalling and transverse joint faulting averaged 0.02 in. The center lane showed less distress, with a total of 5 percent of the joints exhibiting low-severity spalling, and a PSR of 4.3. The inner lane had no distress at all, with a PSR of 4.6. The outer shoulder was in fair-poor condition.

The pavement is in good structural condition, as evidenced from the condition data and the deflection and coring data. The average mid-slab deflections were quite low and no voids were identified beneath the slab corners. There was 100 percent load transfer efficiency at the transverse joints.

The condition of the pavement at the time of the survey indicates no need for any rehabilitation. Consideration should be given to keeping the transverse joints sealed with an appropriate sealant material in order to reduce the development of spalling and to resealing of the lane-shoulder joint with an effective sealant material. As the existing joint spalls approach medium severity, they should be repaired using partial-depth patching techniques and appropriate spall repair materials.

### **360-10A, EB**

This section and the next section, 360-10B, are two of the four experimental prestressed concrete pavement sections included in the study. This section varies from the standard design in that the slabs are only 207 ft long. The main line pavement in all of the prestressed sections consists of a 6-in slab on a 4-in LCB. This pavement was 11 years old at the time of its survey, and had carried an estimated 3.1 million ESAL's in the outer lane. The 1988 two-way ADT was 111,000 vehicles per day, including 3.5 percent heavy trucks.

The PSR was 4.0 in the outer lane, with a Mays roughness measurement of 136 in/mi. The PSR in the middle lane was 3.9, but roughness measurements were not recorded for that lane. The gap slabs were not included as part of the surveyed section, so distresses that occurred at the gap slabs are not recorded here.

As previously noted, the type of structural evaluation performed on the other sections was not possible on the prestressed sections. No cores were taken because of the risk of compromising the integrity of the tendons. Deflection data was collected at the mid-slab location, and these averaged values almost twice as high as those found on the other PCC pavements in the Urban Corridor. As for the other prestressed sections, the major rehabilitation required for this section is repair of the gap slabs. However, many attempts have been made to repair the spalling at the joints, with very few successes. In any case, the prestressed sections are to be removed due to the realignment of highways in this area.

### **360-10B, EB**

This section is also an experimental prestressed concrete pavement, consisting of a 6-in slab on a 4-in LCB, with gap slabs spaced at 502 ft intervals. This pavement was also 11 years old at the time of its survey in 1988, and carried an estimated 3.1 million ESAL's in the outer lane. The two-way ADT was 111,000 vehicles per day, including 3.5 percent heavy trucks.

The field survey of this section revealed a PSR of 4.0 in the outer lane; no Mays roughness was obtained. The middle lane had a PSR of 3.9, but no roughness measurements were available.

Deflection data collected from the mid-slab location showed average values that were almost twice as high as those found on the other PCC pavements in the Urban Corridor. The cracking on this pavement is high, but the cracks are tight and there is no clearcut way to repair this condition. One possible method for rehabilitation of this section is probably a thin overlay, such as the three-layer system, although this would not solve the problem at the gap slabs. However, this section will be removed to accommodate new pavement construction.

### **3. INTERSTATE 10**

On Interstate 10 there were eight sections evaluated. Of those, seven were from the 1988 survey and only one was part of the 1987 FHWA survey. While all of the pavements were JPCP, their designs vary considerably.

#### **AZ 2, EB**

This section is a 10-in JPCP constructed on a 5-in LCB. The transverse joints are skewed, doweled (1.25-in diameter, epoxy-coated dowel bars), and have a random joint spacing of 13-15-17-15 ft. The outer shoulder is constructed of PCC and has the same cross-section as the mainline pavement. This pavement was 2 years old when surveyed in 1987. At that time, it was estimated that the pavement had carried 1.7 million ESAL's in the outer lane and the two-way ADT was estimated to be 50,000 vehicles per day, including 9.0 percent heavy trucks.

The field survey produced an average PSR of 3.6 for the outer lane, with a Mays roughness measurement of 71 in/mi. An average transverse joint faulting of 0.01 in was recorded, and 3 percent of the transverse joints showed low-severity spalling. No PSR or Mays roughness data was obtained for the middle or inner lane. There were no distresses observed in those lanes.

The excellent condition of the pavement and the results of the deflection testing suggest that there is not any structural deficiency in the pavement. The

measured load transfer efficiency at the transverse joints was 72 percent, and the presence of voids was indicated beneath 31 percent of the transverse joints. At this time, this section is not in need of rehabilitation. It is recommended that the pavement continue to receive routine maintenance to preserve the transverse joint integrity and to keep the lane-shoulder joint sealed.

#### **10-01, EB**

This section is a 9-in JPCP constructed on a 4-in aggregate base and a 5-in aggregate subbase. The transverse joints are skewed, nondoweled, and have a random joint spacing of 13-15-17-15 ft. The outer shoulder is constructed of AC. This pavement was 20 years old when surveyed in 1988, and along with 10-02 and 10-03, represents the oldest sections surveyed on I-10. At the time of the survey, it was estimated that the pavement had carried 23.1 million ESAL's in the outer lane. The two-way ADT in 1988 was estimated to be 125,000 vehicles per day, including 9.7 percent heavy trucks.

The outer lane had an average PSR of 3.2 and a Mays roughness measurement of 143 in/mi. The outer lane was not accessible for measuring transverse joint faulting; a measure of 0.03 in was obtained from the inner lane, which was the primary lane included in the survey. The PSR in the middle lane was 3.2 with a Mays roughness index of 182 in/mi. The PSR and Mays roughness in the inner lane were 3.8 and 159 in/mi, respectively. No cracking was noted in any of the lanes, but there was excessive transverse joint spalling noted throughout the section. In the outer lane, 35 percent of the joints had medium-severity spalling and 10 percent low-severity spalling. Similar values were obtained for the other two lanes, and over 30 percent of the joints had been repaired with a bituminous patching material.

An analysis of the deflection data suggests that there is not any structural deficiency in the pavement. The measured load transfer efficiency at the transverse joints was 100 percent. The data also indicates the presence of voids beneath 81 percent of the transverse joints.

At this time, this section is in need of rehabilitation to address the joint spalling problems and the poor rideability of each lane. It is recommended that partial- or full-depth repairs be considered at those transverse joints exhibiting medium-severity spalling. The use of appropriate full-depth repair techniques, including dowel bars and base reconstruction as needed, would greatly enhance the rideability of this section. In conjunction with that, it is recommended that either diamond grinding be performed or a thin overlay (such as the three-layer system) be placed to restore the rideability of the section. If diamond grinding is performed, then joint resealing should also be considered.

#### 10-02, EB

This section is also a 9-in JPCP constructed on a 4-in aggregate base and a 5-in aggregate subbase. The transverse joints are skewed, nondoweled, and have a random joint spacing of 13-15-17-15 ft. The outer shoulder is constructed of AC and was not accessible to be surveyed for this project. This pavement was 20 years old when surveyed in 1988. At that time, it was estimated that the pavement had carried 23.7 million ESAL's in the outer lane and the two-way ADT was estimated to be 141,000 vehicles per day, including 9.7 percent heavy trucks.

The field survey produced an average PSR of 3.2 for the outer lane, with a Mays roughness measurement of 155 in/mi. This is one of the roughest pavement sections included in this study. The PSR in the middle lane was 3.2, with a Mays roughness of 174 in/mi, and the PSR in the outer lane was 3.7, with a Mays roughness of 170 in/mi. The primary distress in the outer lane was spalled joints, with 22 percent of the joints showing medium-severity spalling and 16 percent showing low-severity spalling. The joints with medium-severity spalling had been patched with a bituminous material. The condition of the middle lane was very similar, but the spalling in the outer lane was a little more severe.

The overall pavement condition and the results from the nondestructive testing indicate that there is not a structural deficiency in the pavement. The measured load transfer efficiency at the transverse joints was 100 percent. The deflection data did, however, indicate the presence of voids beneath 100 percent of the transverse joints.

The pavement appears to be in need of rehabilitation in all lanes. It is recommended that partial- or full-depth repairs be placed at those transverse joints exhibiting medium- and high-severity spalling. Diamond grinding should be considered to restore the rideability of the pavement. All transverse joints should be resealed to prevent the intrusion of incompressibles. Further investigation should be conducted into the extent of possible voids at the transverse joints to ascertain if slab stabilization is warranted.

Because of the potentially large amount of patching that may be required on this section, it may be more cost effective to reconstruct the pavement. Therefore, consideration should be given to the balance between the cost of rehabilitating this pavement versus the cost of reconstructing it. Inherent in such a consideration should be the large traffic volumes that the pavement carries, including the difficulties and complexities of traffic control and the costs of traffic delays.

#### 10-03, WB

This section is a 9-in JPCP constructed on a 4-in aggregate base and a 5-in aggregate subbase. The transverse joints are skewed, nondoweled, and have a

random joint spacing of 13-15-17-15 ft. The outer shoulder is 3 in of AC on 10 in of aggregate material. This pavement, 20 years old when surveyed in 1988, is estimated to have carried 23.8 million ESAL's in the outer lane. The two-way ADT in 1988 was estimated to be 143,000 vehicles per day, including 9.0 percent heavy trucks.

The field survey showed an average PSR of 3.8 for the outer lane, and a Mays roughness measurement of 144 in/mi. An average transverse joint faulting of 0.03 in was recorded in the outer lane. The transverse joints had extensive spalling, with 39 percent of the joints exhibiting medium-severity spalling and 27 percent exhibiting low-severity spalling. Of those joints exhibiting spalling, 25 percent of the joints had been repaired with a bituminous patching material. In the middle lane, the PSR was 3.8 and the Mays roughness was 122 in/mi. There were 55 percent of the joints with medium-severity spalling, 15 percent with low-severity spalling, and 45 percent of the joints had been repaired. The PSR of the inner lane was 3.4, the Mays roughness was 153 in/mi, and slightly less spalling was noted, although 21 percent of the transverse joints had been patched.

An analysis of the deflection data suggests that there is not any structural deficiency in the pavement. The measured load transfer efficiency at the transverse joints was 94 percent, but the data indicates the presence of voids beneath 100 percent of the transverse joints.

Because of the substantial joint spalling, it is suggested that partial- or full-depth repairs be placed at those joints exhibiting medium- and high-severity spalling (in all lanes). The selection of the preferred repair would depend upon the depth of the spalling and the overall condition of the joint. Full-depth repairs would probably provide a more stable and rideable repair, although they would be far more expensive than partial-depth repairs. Joint resealing should also be performed to prevent the infiltration of incompressibles into the joint. Diamond grinding might be considered for the inner lane only, since its PSR is approaching a marginal value.

If considerable patching is required, the pavement may require diamond grinding or the placement of a thin overlay to restore rideability. Alternatively, if a large amount of patching is needed, reconstruction of the pavement may be the more desirable approach. Further investigation into the extent of possible voids at the transverse joints should be performed to see if full-depth repair would resolve this problem.

#### **10-04, WB**

This section is a 10-in JPCP constructed on a 5-in LCB. The transverse joints are skewed, doweled (1.25-in diameter, epoxy-coated dowel bars), and have a random joint spacing of 13-15-17-15 ft. The outer shoulder is constructed of PCC and has the same cross-section as the mainline pavement. This pavement was 2 years old

when surveyed in 1988. Through 1988, it was estimated that the pavement had carried 2.8 million ESAL's in the outer lane. The two-way ADT in 1988 was estimated to be 51,000 vehicles per day, including 9.0 percent heavy trucks.

The outer lane had an average PSR of 4.1 and a Mays roughness measurement of 88 in/mi. An average transverse joint faulting of 0.03 in was measured. Twenty-five percent of the transverse joints showed low-severity spalling. In the middle lane, the PSR was 4.5 and the Mays roughness was 61 in/mi. There was medium-severity spalling at 3 percent of the joints. In the inner lane, the PSR was 4.3 and the Mays roughness was 59 in/mi. Minimal spalling was noted in the middle lane.

The overall pavement condition and an analysis of the deflection data indicates that this pavement does not have a structural deficiency. The measured load transfer efficiency at the transverse joints was 49 percent and the presence of voids was detected beneath 71 percent of the transverse joints.

At this time, this section is not in need of rehabilitation. However, the percent spalling is fairly high for such a young pavement. Consideration should be given to partial-depth repair at those joints exhibiting medium-severity spalling to keep the rideability high and to provide a uniform reservoir for joint sealing. It is recommended that the pavement also receive routine maintenance to preserve the transverse joint integrity.

Investigations should be made into the possible causes of the spalling (incompressibles, misaligned dowel bars) and into the possible presence of voids beneath the joint. The latter would not be expected to occur on a pavement that is only 2 years old, particularly one that has dowel bars and a lean concrete base.

#### **10-05, EB**

This section, constructed in 1985, is a 10-in JPCP constructed on a 5-in LCB. The transverse joints are skewed, doweled (1.25-in diameter, epoxy-coated dowel bars), and have a random joint spacing of 13-15-17-15 ft. The outer shoulder is constructed of PCC and has the same cross-section as the mainline pavement. When survey in 1988, it was estimated that the pavement had carried 2.4 million ESAL's in the outer lane. The two-way ADT in 1988 was estimated to be 47,000 vehicles per day, including 9.0 percent heavy trucks.

The field survey produced an average PSR of 4.2 for the outer lane, with a Mays roughness measurement of 80 in/mi. An average transverse joint faulting of 0.01 in was recorded. There was no cracking, but over 70 percent of the transverse joints showed low-severity spalling. The PSR and Mays roughness index in the middle lane were 3.8 and 87 in/mi respectively, with negligible spalling. In the inner

lane, the PSR was 4.1 and the Mays roughness was 108 in/mi. There were no other distresses noted in the inner lane.

No structural deficiency in the pavement was noted from the deflection data. The measured load transfer efficiency at the transverse joints was 85 percent and the presence of voids was indicated beneath 64 percent of the transverse joints.

This pavement is performing well and not in need of any immediate rehabilitation. The only problem of note on this pavement is the joint spalling, which for the most part is shallow and does not extend into the pavement very far. Should that joint spalling get progressively worse, it might be appropriate to consider partial-depth repair in some cases. Some investigation into the apparent loss of support also may be warranted to determine the actual extent and severity of the problem.

#### **10-06, WB**

This section is a 10-in JPCP over a 5-in LCB, constructed in 1984. The transverse joints are skewed, doweled (1.25-in diameter, epoxy-coated dowel bars), and have a random joint spacing of 13-15-17-15 ft. The outer shoulder is constructed of PCC and has the same cross-section as the mainline pavement. When surveyed in 1988, it was estimated that the pavement had carried 6.8 million ESAL's in the outer lane; the two-way ADT in 1988 was estimated to be 31,000 vehicles per day, including 3.2 percent heavy trucks.

The field survey produced an average PSR of 4.2 for the outer lane, with a Mays roughness measurement of 64 in/mi. An average transverse joint faulting of 0.02 in was recorded, and 3 percent of the transverse joints showed low-severity spalling. There was 560 lin ft/mi of longitudinal cracking measured. In the middle lane, a PSR of 4.5 and a Mays roughness index of 65 was measured. No other distresses were noted. In the inner lane, the PSR was 4.1 and the Mays was 64 in/mi and no distresses were measured there either.

The pavement is in sound structural condition. The measured load transfer efficiency at the transverse joints was 91 percent, and the presence of voids was detected beneath 15 percent of the transverse joints.

At this time, this section is not in need of rehabilitation. The longitudinal cracking is cause for mild concern, but appears to be related to construction difficulties and not to pavement performance.

#### **10-07, WB**

This section, constructed in 1984, is a 10-in JPCP over a 5-in LCB. The transverse joints are skewed and contain 1.25-in diameter, epoxy-coated dowel bars.

The slabs have a random joint spacing of 13-15-17-15 ft. The outer shoulder is constructed of PCC and has the same cross-section as the mainline pavement. At the time of survey in 1988, it was estimated that the pavement had carried 6.8 million ESAL's in the outer lane. At that time, it was estimated that the two-way ADT was 31,000 vehicles per day, including 3.2 percent heavy trucks.

The outer lane had an average PSR of 4.1 and a Mays roughness measurement of 54 in/mi. An average transverse joint faulting of 0.02 in was recorded, and less than 5 percent of the transverse joints showed any spalling. There was 20 lin ft/mi of longitudinal cracking measured. In the middle lane, a PSR of 4.5 and a Mays roughness index of 51 was measured. No other distresses of note were recorded. In the inner lane, the PSR was 4.1 and the Mays was 65 in/mi.

This pavement section is in sound structural condition. The measured load transfer efficiency at the transverse joints was 100 percent, and the presence of voids was detected beneath 10 percent of the transverse joints.

At this time, this section is not in need of rehabilitation. The longitudinal cracking is not really a cause for concern. The cracks and joints should be kept sealed, and attention should be paid to the possible development of faulting.

#### **4. INTERSTATE 17**

All of the eight sections on Interstate 17 were surveyed in 1988 under this project. These pavements represent the oldest concrete pavement designs in the Urban Corridor, ranging in age from 23 to 27 years old at the time of survey. The designs were fairly similar, with slight variations in layer thicknesses and joint orientation. However, all of the sections on I-17, with the exception of 17-06, had been diamond ground. Thus, the PSR and Mays Roughness data for these sections can not be compared directly to that data for the other sections in this study.

##### **17-01, SB**

Section 17-01 is a 9-in JPCP constructed on a 3-in thick aggregate base and a 6-in thick aggregate subbase. Transverse joints are perpendicular, spaced at 15 ft intervals, and do not contain load transfer devices. The outer shoulder consists of an AC surface on an aggregate base. The pavement, when surveyed in 1988, was 27 years old and had carried an estimated 20.3 million ESAL's in the outer lane. The ADT at that time was 132,000 vehicles per day, including 9.5 percent heavy trucks. The pavement was diamond ground in 1980.

The field survey produced an average PSR of 3.9 for the outer lane, with a Mays roughness measurement of 106 in/mi. The transverse joints showed extensive deterioration; 58 percent had medium-severity spalling and 61 percent of the joints

had been patched with either a bituminous or a cementitious product. In the middle lane, the PSR was 3.9 and the Mays roughness index was 111 in/mi. The transverse joints showed slightly less spalling, with 42 percent having medium-severity spalling and 47 percent of the joints repaired with the same patching materials as in the outer lane. The inner lane had a PSR of 3.6 and a Mays Roughness of 95 in/mi. There was also some spalling in this lane, although the total of low- and medium-severity spalling was just over 30 percent and only 24 percent of the joints had been patched.

Structurally, this pavement appears to be in good condition. The deflection testing indicated low mid slab deflection, 100 percent load transfer at the transverse joints, and apparent voids beneath 20 percent of the joints.

The considerable joint spalling that has occurred on this section in all lanes requires either partial- or full-depth repairs. The selection of the appropriate repair method would depend upon the depth of the joint spalling. Joint resealing should be considered for the transverse joints as well. However, it should be noted that the overall rideability of the pavement is still good.

Depending upon the amount of patching that may be required, consideration should be given to reconstruction of the pavement. If enough of the joints require patching, it may be more cost effective to reconstruct the pavement. However, for reconstruction, it is imperative to consider the costs of traffic control and disruption.

#### **17-02, NB**

Section 17-02 is a 9-in JPCP constructed on a 3-in thick aggregate base and a 6-in thick aggregate subbase. Transverse joints are perpendicular, spaced at 15 ft intervals, and do not contain load transfer devices. The outer shoulder consists of an AC surface on an aggregate base, although this shoulder was not included in the survey. The pavement, when surveyed in 1988, was 27 years old and had carried an estimated 19.4 million ESAL's in the outer lane. The two-way ADT at that time was 126,000 vehicles per day, with 9.5 percent heavy trucks. The pavement was diamond ground in 1980.

Data from the field survey showed an average PSR of 3.9 for the outer lane, with a Mays roughness measurement of 60 in/mi. Like section 17-01, the transverse joints displayed widespread spalling; 43 percent had medium-severity spalling and 17 percent had low-severity spalling. In addition, 36 percent of the joints had been patched with a bituminous patching material. In the middle lane, the PSR was 3.6 and the Mays roughness index was 99 in/mi. The transverse joints showed about the same amount of spalling, and 63 percent of the joints had been repaired with the same bituminous materials. The inner lane had a PSR of 3.7 and a Mays Roughness of 95 in/mi. There was spalling in this lane similar to that found in the other two,

although the total of patched joints was only 35 percent. There was 30 lin ft/mi of longitudinal cracking in the middle and inner lane.

The deflection data indicates that the pavement is structurally sound. Transverse joint load transfer efficiency was 100 percent and the apparent presence of voids detected beneath 15 percent of the joints.

While the overall rideability of the pavement is still good, it appears that this section is in need of some patching. It is recommended that partial- or full-depth repairs be considered at those transverse joints exhibiting medium-severity spalling in all lanes. The sealing of transverse joints is also recommended to prevent the intrusion of incompressibles.

As with the other older sections in the study, consideration should be given to the balance between the cost of rehabilitating this pavement versus the cost of reconstructing it. If enough of the joints require full-depth repair, it may be more cost effective to reconstruct the pavement.

#### **17-03, SB**

This section is a 9-in JPCP constructed on a 3-in thick aggregate base and a 6-in thick aggregate subbase. Transverse joints are skewed, spaced at 15 ft intervals, and do not contain load transfer devices. The outer shoulder consists of an AC surface on an aggregate base. The pavement, when surveyed in 1988, was 23 years old and had carried an estimated 14.4 million ESAL's in the outer lane. The two-way ADT at that time was 112,000 vehicles per day, including 9.5 percent heavy trucks. The pavement was diamond ground in 1986.

The field survey produced an average PSR of 3.9 for the outer lane, with a Mays roughness measurement of 91 in/mi. Medium-severity transverse joint spalling was exhibited by 64 percent of the joints, and 60 percent of those joints had been patched with a cementitious material. There was an average of 134 lin ft/mi of longitudinal cracking in the outer lane. Although the pavement had been ground, faulting still averaged 0.05 in. In the middle lane, the PSR was 3.9 and the Mays roughness index was 92 in/mi. The transverse joints showed about the same amount of deterioration; 64 percent had medium-severity spalling and 67 percent of the joints were repaired with a cementitious patching material. The inner lane had a PSR of 4.2 and a Mays Roughness of 71 in/mi.

The pavement appears to be structurally sound, with 97 percent load transfer at the transverse joints and no voids detected beneath the joints. However, due to the excessive joint spalling, this pavement is in need of partial- or full-depth repairs at the joints. These should be placed in both the outer and middle lanes, the type to be determined by the depth and extent of spalling. It is further recommended that

joint resealing be performed at the transverse joints to prevent the intrusion of incompressibles. No overlay or diamond grinding is recommended at this time since the overall rideability of the pavement is still good.

If enough of the joints require full-depth repair, it may be more cost effective to reconstruct the pavement. Thus, as before, consideration should be given to the balance between the cost of rehabilitating this pavement versus the cost of reconstructing it.

#### **17-04, SB**

Section 17-04, constructed in 1965, is a 9-in JPCP over a 4-in aggregate base and a 6-in aggregate subbase. Transverse joints are skewed, spaced at 15 ft intervals, and do not contain load transfer devices. The outer shoulder consists of an AC surface on an aggregate base. When surveyed in 1988, the pavement had carried an estimated 18 million ESAL's in the outer lane. The two-way ADT at that time was 126,000 vehicles per day, with 9.5 percent heavy trucks. The pavement was diamond ground in 1981.

The field survey produced an average PSR of 3.7 for the outer lane, but with a Mays roughness measurement of 50 in/mi. The transverse joints were showing deterioration, with 17 percent exhibiting medium-severity spalling and 17 percent exhibiting high-severity spalling. Also, 31 percent of the transverse joints had been repaired with a bituminous material. In the middle lane, the PSR was 4.1 and the Mays roughness index was 90 in/mi. The transverse joints showed about the same amount of deterioration; 28 percent had medium-severity spalling and 14 percent had high-severity spalling. There were 33 percent of the joints repaired in the middle lane. The inner lane had a PSR of 3.9 and a Mays Roughness of 61 in/mi. The spalling and spall repairs in the inner lane were similar to that observed in the middle lane.

The pavement appears to be structurally sound, with 100 percent load transfer at the transverse joints. The apparent presence of voids was detected beneath 21 percent of the joints.

The outer and middle lanes of this section are in need of rehabilitation due to the excessive spalling. It is recommended that either partial- or full-depth repairs be considered at those transverse joints exhibiting medium-severity spalling, the type to be determined by the depth and extent of the spalling. Joint resealing should be performed at the transverse joints to prevent further joint deterioration.

Again, it is recommended that the cost of patching this pavement be weighed against the cost of reconstruction. If enough of the joints require full-depth repair, it may be more cost effective to reconstruct the pavement.

### **17-05, NB**

Section 17-05 is a 9-in JPCP constructed on a 4-in aggregate base and a 6-in aggregate subbase. Transverse joints are skewed, spaced at 15 ft intervals, and do not contain load transfer devices. The outer shoulder consists of an AC surface on an aggregate base. The pavement, when surveyed in 1988, was 23 years old and had carried an estimated 14.7 million ESAL's in the outer lane. The two-way ADT at that time was 117,000 vehicles per day, with 9.5 percent heavy trucks. The pavement was diamond ground in 1986.

An average PSR of 4.1 and a Mays roughness measurement of 77 in/mi was obtained for the outer lane. The transverse joints showed the least deterioration of any of the sections on I-17, with only 5 percent exhibiting medium-severity spalling. Twenty-eight percent of the transverse joints had been repaired with a cementitious patching material. In the middle lane, the PSR was 4.2 and the Mays roughness index was 72 in/mi. The PSR in the inner lane was 4.3 with a Mays roughness index of 50 in/mi. There was no spalling in either the middle or the inner lane, although 19 percent of the transverse joints in the middle lane had been repaired.

The pavement appears to be structurally sound, with 99 percent load transfer at the transverse joints. The apparent presence of voids was detected beneath 11 percent of the joints. At this time, this section does not appear to be in need of rehabilitation, although joint resealing is probably advisable. Continued maintenance should be performed as required to repair other spalling and either partial- or full-depth repairs should be considered on these joints as their condition worsens.

### **17-06, NB**

This section, constructed in 1963, is a 9-in JPCP over a 3-in thick aggregate base and a 6-in thick aggregate subbase. Transverse joints are perpendicular, spaced at 15 ft intervals, and do not contain load transfer devices. The outer shoulder consists of an AC surface on an aggregate base. The pavement, when surveyed in 1988, had carried an estimated 19.2 million ESAL's in the outer lane. The two-way ADT at that time was 125,000 vehicles per day, with 9.7 percent heavy trucks.

Section 17-06 is significant in that it is the only section left on I-17 that had not been diamond ground. The field survey showed an average PSR of 2.9 for the outer lane, but Mays roughness data was not available. The average transverse joint faulting was 0.09 in. Medium- and high-severity joint spalling was exhibited by 21 percent of the transverse joints, and 24 percent of the joints had been patched with a bituminous patching product. In the middle lane, the PSR was 2.9 and the Mays roughness index was 232 in/mi. The transverse joints showed more deterioration in the center lane, with 28 percent medium-severity spalling and 10 percent high-severity spalling, and 35 percent of the joints repaired. The inner lane had a PSR of

3.1 and a Mays Roughness of 185 in/mi. There was 11 percent medium-severity spalling and 13 percent of the transverse joints repaired in this lane.

The pavement appears to be structurally sound, with 100 percent load transfer at the transverse joints. The apparent presence of voids was detected beneath 77 percent of the transverse joints.

It appears that all lanes of this section are in need of rehabilitation, due to the spalling and faulting and overall poor serviceability of the pavement. Partial- or full-depth repairs should be performed at those joints exhibiting medium- or high-severity spalling, followed by either diamond grinding or the placement of a thin overlay (such as the three-layer system) to restore rideability. If diamond grinding is to be performed, the transverse joints should be resealed. The probability that there are voids beneath the transverse joints should also be further explored, and, if so, slab stabilization should be considered.

Reconstruction might be an option to consider if extensive patching is required. The cost of the proposed patching and grinding should be weighed against the cost for total reconstruction.

#### **17-10, NB**

Section 17-10 is a 9-in JPCP constructed on a 4-in aggregate base and a 6-in aggregate subbase. Transverse joints are perpendicular, spaced at 15 ft intervals, and do not contain load transfer devices. The outer shoulder consists of an AC surface on an aggregate base. The pavement was constructed in 1961. When surveyed in 1988, it had carried an estimated 19.3 million ESAL's in the outer lane. The two-way ADT in 1988 was 132,000 vehicles per day, with an estimated 9.5 percent heavy trucks. The pavement was diamond ground in 1979.

Data from the field survey indicated an average PSR of 4.1 for the outer lane, with a Mays roughness measurement of 103 in/mi. There was negligible longitudinal cracking. Spall repair had been performed at 30 percent of the transverse joints, while transverse joint spalling, ranging from low to high severity, inflicted 28 percent of the joints. In the middle lane, the PSR was 4.1 and the Mays roughness index was 101 in/mi. There was less spalling in the middle lane, but more high-severity spalling; 23 percent of transverse joints had been repaired. The PSR in the inner lane was 4.3 with a Mays roughness index of 85 in/mi. There was 32 percent spalling in the medium-severity spalling and 33 percent of the transverse joints had been repaired.

The pavement appears to be structurally sound, with 100 percent load transfer at the transverse joints. The apparent presence of voids was detected beneath 63 percent of the joints.

This section is probably in need of rehabilitation due to the spalling and potential presence of voids. However, the overall serviceability of the pavement is still good. For all lanes, it is recommended that partial- or full-depth repair be considered at the transverse joints with medium-severity spalling. Resealing of the transverse joints should also be considered. If the presence of voids are verified, slab stabilization should be considered as well.

#### **17-11, NB**

This section is a 9-in JPCP constructed on a 4-in aggregate base and a 6-in aggregate subbase. Transverse joints are skewed, spaced at 15 ft intervals, and do not contain load transfer devices. The outer shoulder consists of an AC surface on an aggregate base. The pavement, when surveyed in 1988, was 23 years old and had carried an estimated 15.6 million ESAL's in the outer lane. The two-way ADT at that time was 126,000 vehicles per day, including 9.5 percent heavy trucks. The pavement was diamond ground in 1986.

The field survey produced an average PSR of 4.1 for the outer lane, and a Mays roughness index of 83 in/mi. The transverse joints were severely deteriorated, with 57 percent exhibiting medium-severity spalling and 33 percent exhibiting high-severity spalling. Also, 54 percent of the transverse joints had been repaired with a cementitious patching material. There was 200 lin ft/mi of longitudinal cracking in this lane. In the middle lane, the PSR was 4.3 and the Mays roughness index was 87 in/mi. The transverse joints showed less deterioration; 46 percent had medium-severity spalling and 47 percent had been patched. The inner lane had a PSR of 4.5 and a Mays Roughness of 44 in/mi. The spalling and spall repairs in the inner lane were similar to that observed in the middle lane.

The pavement appears to be structurally sound, with 89 percent load transfer at the transverse joints. The apparent presence of voids was detected beneath 15 percent of the joints.

This section appears to be in need of further rehabilitation due to the excessive spalling. Partial- or full-depth repairs should be placed in all lanes at those joints exhibiting medium- and high-severity spalling. Resealing of the transverse joints should also be considered to prevent the continual spalling of the joints. Due to the excellent serviceability of the pavement, diamond grinding or a thin overlay are not needed.

## **5. SUMMARY**

Recommended rehabilitation actions for the various sections in the Phoenix Urban Corridor have been discussed. These recommendations are summarized in tables 27 through 29.

Table 27. Summary of recommended rehabilitation actions for pavement sections on S.R. 360.

SECTION ID	RECOMMENDED REHABILITATION	FURTHER INVESTIGATIONS
AZ 1-1	Partial- or full-depth repairs; diamond grinding to restore ride	Depth and extent of areas for repair
AZ 1-2	No major rehab at this time; continue maintenance	None
AZ 1-4	No major rehab at this time; continue maintenance	None
AZ 1-5	No major rehab at this time; continue maintenance	None
AZ 1-6	No major rehab at this time; continue maintenance	None
AZ 1-7	No major rehab at this time; continue maintenance	None
360-01	No major rehab at this time; continue maintenance	Reasons for low load transfer and verification of voids
360-02	No major rehab at this time; continue maintenance	Reasons for low load transfer and verification of voids
360-03	No major rehab at this time; continue maintenance	Reasons for low load transfer and verification of voids
360-04	No major rehab at this time; continue maintenance	None
360-05	None (section to be removed)	None
360-06	None (section to be removed)	None
360-07	No major rehab at this time; continue maintenance	None
360-08	No major rehab at this time; continue maintenance	None
360-09	No major rehab at this time; continue maintenance	None
360-10A	None (section to be removed)	None
360-10B	None (section to be removed)	None

Table 28. Summary of recommended rehabilitation actions for pavement sections on I-10.

SECTION ID	RECOMMENDED REHABILITATION	FURTHER INVESTIGATIONS
AZ 2	Partial- and full-depth repair; Diamond grinding (with joint resealing) or thin overlay to restore ride	Depth and extent of areas for repair
10-01	Partial- and full-depth repair; diamond grinding (or thin overlay); slab stabilization; joint resealing	Depth and extent of areas for repair; verification of voids; costs of repair vs. reconstruction
10-02	Partial- and full-depth repair; diamond grinding; slab stabilization; joint resealing	Depth and extent of areas for repair; verification of voids, costs of repair vs. reconstruction
10-03	Partial- and full-depth repair; diamond grinding (inner lane only), slab stabilization, joint resealing	Depth and extent of areas for repair; verification of voids, costs of repair vs. reconstruction
10-04	No major rehab at this time; continue maintenance	Causes of spalling and verification of voids
10-05	No major rehab at this time; continue maintenance	Causes of spalling and verification of voids
10-06	No major rehab at this time; continue maintenance	None
10-07	No major rehab at this time; continue maintenance	None

Table 29. Summary of recommended rehabilitation actions for pavement sections on I-17.

SECTION ID	RECOMMENDED REHABILITATION	FURTHER INVESTIGATIONS
17-01	Partial- and full-depth repair; joint resealing	Depth and extent of areas for repair; costs of repair vs. reconstruction
17-02	Partial- or full-depth repair; joint resealing	Depth and extent of areas for repair; costs of repair vs. reconstruction
17-03	Partial- or full-depth repair; joint resealing	Depth and extent of areas for repair; costs of repair vs. reconstruction
17-04	Partial- or full-depth repair; joint resealing	Depth and extent of areas for repair; costs of repair vs. reconstruction
17-05	No major rehab at this time; continue maintenance	None
17-06	Partial- or full-depth repair; diamond grinding (or thin overlay), slab stabilization; joint resealing	Depth and extent of areas for repair; verification of voids; costs of repair vs. reconstruction
17-10	Partial- or full-depth repair; slab stabilization; joint resealing	Depth and extent of areas for repair; verification of voids
17-11	Partial- or full-depth repair; joint resealing	Depth and extent of areas for repair

The recommendations provided in tables 27 through 29 should be considered advisory. In many instances, further data is required and these are indicated by the type of further investigations that are suggested. In addition, comparisons between various alternatives may be required to determine if any one alternative is more appealing than the others in terms of costs, performance period, traffic control requirements, etc. Also, the recommendations are based on 1000-ft surveys of each section, which in some cases may not be of sufficient length to reflect the actual condition of the entire construction section. Before a major rehabilitation project is undertaken, a project-long survey should be conducted. This is also recommended because field surveys upon which these recommendations were based were conducted over 3 years ago.

It is of interest to note that none of the sections exhibited any structural deficiencies. The major problems on the pavement sections were joint spalling, joint faulting (on a few pavements), and overall pavement roughness. Partial-depth repairs are probably the most cost-effective means of addressing the joint spalling problem, provided the spalling is not too deep or too extensive along the joint. If the joint spalling is over one-half of the slab depth or extends over most of the slab length, full-depth repairs may be required.

One method of partial-depth spall repair that has proven to be effective and highly-productive is the use of milling machines for the partial-depth removal of concrete material.<sup>(45)</sup> The machine can be used to remove up to a full-lane width, and produces a rough face for which the repair material to adhere. This procedure may be effective in Arizona for those joints that were formed using the metal insert.

For those sections exhibiting poor rideability, diamond grinding or a thin overlay (such as the three-layer system) may be appropriate. However, attention must be paid to the causes of the roughness. For example, if the roughness was caused by joint faulting, it is expected that the faulting will develop shortly after treatment unless the cause of the joint faulting is treated (generally, loss of support or voids). Thus, if substantial voids are located beneath slab corners, treatment such as slab stabilization may be appropriate to prevent the redevelopment of faulting.

If the number of repairs for a given section become substantial, reconstruction may be worth considering as an alternative. While it is believed that performing pavement restoration (in the form of partial-depth repairs, full-depth repairs, joint resealing and diamond grinding) for as long as possible is an effective rehabilitation alternative for the pavements in the Phoenix Urban Corridor, the costs of such an approach may be exorbitant if repair quantities become too great.

A brief description of the various rehabilitation techniques considered here is provided in appendix E. Additional information on the procedures to follow for each rehabilitation technique is provided in references 46 and 47.

## CHAPTER 7 SUMMARY AND CONCLUSIONS

Over the next 20 years, ADOT plans to build several hundred lane miles of new portland cement concrete pavements in the Phoenix urban area. Prior to embarking on such an ambitious construction effort, ADOT wants to document the performance of their existing PCCP and use that information to assist in the selection of optimum design strategies for the new concrete construction. As portions of the existing concrete pavement system are approaching 30 years of service, it was also desired to identify optimum rehabilitation methods for these concrete pavements.

A total of 35 concrete pavement sections were selected for evaluation, representing every concrete pavement construction project that ADOT has undertaken in the Phoenix Urban Corridor (PUC) from 1961 to the early 1980's. In order to complete the objectives of the contract, an intensive office and field data collection effort was undertaken. This process involved the identification of candidate sections, the selection of specific sections for evaluation, extensive field testing, interviews with knowledgeable ADOT personnel, and data storage and data analysis procedures.

To assist in the evaluation of current designs and in the projection of realistic design lives for pavement design strategies, the capabilities of several existing pavement analysis models were assessed. Performance prediction models were also considered for their applicability to conditions in the Phoenix area. The analytical models evaluated and judged useful were the CMS model and the ILLI-SLAB program. The CMS model enables the design engineer the ability to determine the effects of the environment on that pavement. The CMS model may be used in conjunction with ILLI-SLAB to determine the stresses and deflections resulting from the environment and the combination of load and environment. These stresses and deflections can, with the use of a fatigue equation or transfer function, be translated into the number of repetitions that a pavement slab can sustain before failing in fatigue. This is the basis of a mechanistic-empirical design procedure.

The concrete pavement performance prediction models evaluated included AASHTO, PEARDARP, COPEs, PFAULT, and the recently-developed FHWA models. With one exception, none of the models were able to accurately predict the distress (faulting, cracking, joint deterioration, pumping), serviceability, or roughness measured on the pavements included in the study.

The one prediction model that was shown to be acceptable for Arizona conditions was the new FHWA PSR model. That model uses pavement distress to provide an indication of the overall riding quality of a pavement (on a scale of 0 to 5) and can be useful in determining how the traveling public may view the

serviceability of a roadway that is exhibiting certain levels of distress. It could be used in programming rehabilitation or maintenance activities.

Attempts at the development of new models for faulting and roughness were not successful. The limited nature of the data base, the confounding of various design factors, and the absence of time-sequence data made this task impossible. Much more performance data, distributed over time (i.e., time-sequence data for each section) and space (i.e., more sections added), are needed to permit the development of acceptable faulting and roughness models.

Two-variable linear regressions, relating the ESAL applications sustained by a specific pavement section to the roughness, were performed using the historical roughness data. These regressions were successful for a selected number of sections and provide a means of estimating future roughness for the specific pavement section. However, these relations are only for those pavements for which they were developed and *could not* be extended to other pavements.

Based upon the results of the performance evaluation of the various concrete pavement designs in the Phoenix Urban Corridor and without the benefit of usable performance prediction models, it appears that there are two designs that perform better than the others. These designs are:

- 9- or 10-in JPCP over LCB (with dowels).
- Thickened JPCP placed directly on grade.

The JPCP over LCB exhibited a good rideability, had low faulting, and had fewer voids developing beneath the corners. The slab-on-grade design was extremely resistant to joint faulting and displayed an ability to maintain pavement smoothness over time. The good performance of the several CRCP designs in use in the Phoenix Urban Corridor and their overall success in similar climates prompted their addition to a group of three design strategies recommended for future concrete pavement construction. A number of design and construction considerations are presented that should enhance the performance of these designs.

It is readily admitted that there were too few sections of each design type to make a complete and statistically valid analysis. It is further acknowledged that some data was missing and some of the sections are neither very old nor have they sustained significant levels of traffic loading.

Each of the concrete pavement sections that were studied were also evaluated in terms of the most appropriate rehabilitation scheme for that specific section. Decision trees and matrices were developed and used in the evaluation. Recommendations for rehabilitation are provided, but should be considered advisory. In many instances, further data is required and these are indicated by the type of

further investigations that are suggested. In addition, comparisons between various alternatives may be required to determine if any one alternative is more appealing than the others in terms of costs, performance period, traffic control requirements, etc. The recommendations are based on 1000-ft surveys of each section, which in some cases may not be of sufficient length to reflect the actual condition of the entire construction section. Before a major rehabilitation project is undertaken, a project-long survey should be conducted. This is also recommended because field surveys upon which these recommendations were based were performed over 3 years ago.

# REFERENCES

1. Delton, J. P., "Non-conventional vs. Conventional Concrete Pavements in Arizona," Proceedings, Second International Conference on Concrete Pavement Design, Purdue University, April 1981.
2. Mueller, P. E. and L. A. Scofield, "An Expanded Evaluation of Arizona's Ten Mile Concrete Test Roadway," Proceedings, Fourth International Conference on Concrete Pavement Design and Rehabilitation, Purdue University, April 1989.
3. Scofield, L. A., C. Y. Lin, A. S. M. Mustaque Hossain, "A Ten Year Evaluation of the Superstition Freeway Experimental Sections," Arizona Department of Transportation, AZ-SP-8901, February 1989.
4. Smith, K. D., D. G. Peshkin, M. I. Darter, A. L. Mueller, and S. H. Carpenter, "Performance of Jointed Concrete Pavements, Volume I—Evaluation of Concrete Pavement Performance and Design Features," Federal Highway Administration, FHWA-RD-89-136, March 1990.
5. Smith, K. D., D. G. Peshkin, M. I. Darter, A. L. Mueller, and S. H. Carpenter, "Performance of Jointed Concrete Pavements, Volume IV—Appendix A, Project Summary Reports and Summary Tables," Federal Highway Administration, FHWA-RD-89-139, March 1990.
6. Smith, K. D., D. G. Peshkin, M. I. Darter, A. L. Mueller, and S. H. Carpenter, "Performance of Jointed Concrete Pavements, Volume V—Appendix B, Data Collection and Analysis Procedures," Federal Highway Administration, FHWA-RD-89-140, March 1990.
7. Rauhut, J. B., M. I. Darter, R. L. Lytton, P. R. Jordahl, M. P. Gardner, G. L. Fitts, and K. D. Smith, "Data Collection Guide for Long-Term Pavement Performance Studies," Draft document prepared for the Strategic Highway Research Program (SHRP), December 1987.
8. Smith, K. D., M. I. Darter, J. B. Rauhut, and K. T. Hall, "Distress Identification Manual for the Long-Term Pavement Performance (LTPP) Studies," Draft document prepared for the Strategic Highway Research Program (SHRP), December 1987.
9. Carpenter, S. H., "Selecting AASHTO Drainage Coefficients," paper presented at the 68<sup>th</sup> Annual Meeting of the Transportation Research Board, January 1989.

10. UNIFY Relational Database Management System, Version 3.2, UNIFY Corporation, 1985.
11. Statistical Analysis System (SAS), Version 6.03, SAS Institute Inc., Cary, North Carolina, 1987.
12. Smith, K. D., A. L. Mueller, M. I. Darter, and D. G. Peshkin, "Performance of Jointed Concrete Pavements, Volume II—Evaluation and Modification of Concrete Pavement Design and Analysis Models," Federal Highway Administration, FHWA-RD-89-137, July 1990.
13. Mueller, A. L., D. G. Peshkin, K. D. Smith, and M. I. Darter, "Performance of Jointed Concrete Pavements, Volume VI—Appendix C, Synthesis of Concrete Pavement Design Methods and Analysis Models; and Appendix D, Summary of the Analysis Data for the Evaluation of Predictive Models," Federal Highway Administration, FHWA-RD-89-141, July 1990.
14. Dempsey, B. J., W. A. Herlache, and A. J. Patel, "The Climatic-Materials-Structural Pavement Analysis Program User's Manual," FHWA/RD-86/085, 1986.
15. Dempsey, B. J., W. A. Herlache, and A. J. Patel, "Environmental Effects on Pavements—Volume III, Theory Manual," Federal Highway Administration, FHWA/RD-84/115, 1986.
16. Liu, S. J., and R. L. Lytton, "Environmental Effects on Pavements—Volume IV, Drainage Manual," Federal Highway Administration, FHWA/RD-86/116, 1986.
17. Kopperman, S., G. Tiller, and M. Tseng, "TTI Pavement Drainage Model: TTIDRN and TTIINF Interactive Microcomputer Version, User's Manual: IBM-PC and Compatible Version," Federal Highway Administration, FHWA Contract No. DTFH61-85-C-00051, Final Report, January 1986.
18. Tabatabaie, A. M., E. J. Barenberg, and R. E. Smith, "Longitudinal Joint Systems in Slip-Formed Rigid Pavements, Volume II—Analysis of Load Transfer Systems for Concrete Pavements," Federal Aviation Administration, Report No. FAA-RD-79-4, November 1979.
19. Ioannides, A. M., "Analysis of Slab-on-Grade for a Variety of Loading and Support Conditions," Ph.D. Dissertation, 1984.
20. Ioannides, A. M., E. J. Barenberg, and M. R. Thompson, "Finite Element Model with Stress Dependent Support," Transportation Research Board, Transportation Research Record No. 954, 1984.

21. Tayabji, S. D., and B. E. Colley, "Analysis of Jointed Concrete Pavements," Federal Highway Administration, FHWA Report FHWA/RD-86/041, February 1986.
22. Tayabji, S. D., and B. E. Colley, "Improved Rigid Pavement Joints," Federal Highway Administration, FHWA Report No. FHWA/RD-86/040, February 1986.
23. Darter, M. I., "Design of Zero-Maintenance Plain Jointed Concrete Pavement, Volume I—Development of Design Procedures," Federal Highway Administration, FHWA-RD-77-111, April 1977.
24. Kopperman, S., G. Tiller, and M. Tseng, "JCP-1: Interactive Microcomputer Version, User's Manual: IBM-PC and Compatible Version," Federal Highway Administration, FHWA-TS-87-205, January 1986.
25. Sawan, J. S., M. I. Darter, and B. J. Dempsey, "Structural Analysis and Design of Portland Cement Concrete Highway Shoulders," Federal Highway Administration, FHWA/RD-81/122, April 1982.
26. Majidzadeh, K., and G. J. Ilves, "Structural Design of Roadway Shoulders—Final Report," Federal Highway Administration, FHWA/RD-86/089, May 1986.
27. Thompson, M. R., and Q. L. Robnett, "Final Report: Resilient Properties of Subgrade Soils," Civil Engineering Studies, Transportation Engineering Series No. 14, Illinois Cooperative Highway and Transportation Series No. 160, June 1976.
28. Johnson, T. C., D. M. Cole, and E. J. Chamberlain, "Influence of Freezing and Thawing on the Resilient Properties of a Silt Soil Beneath an Asphalt Concrete Pavement," CRREL Report 78-23, September 1978.
29. Bergan, A. T., and C. L. Monismith, "Characterization of Subgrade Soils in Cold Regions for Pavement Design Purposes," Highway Research Record No. 431, 1973.
30. Dowe, D. S., "A Finite Element Approach to Plate Vibration Problems," Journal of Mechanical Engineering Science, Volume 7, Number 1, 1965.
31. Ioannides, A. M., and R. A. Salsilli-Murua, "Slab Length, Slab Width, and Widened Lane Effects in Rigid Pavements," Technical Document, prepared under contract DTFH61-85-C-00103, December 1988.

32. "AASHTO Guide for Design of Pavement Structures—1986," American Association of State Highway and Transportation Officials, Washington, D.C., 1986.
33. van Wijk, A. J., "Rigid Pavement Pumping: 1. Subbase Erosion, 2. Economic Modeling," Federal Highway Administration, FHWA Contract Number DTFH61-82-C-00035, Final Report, September 1985.
34. van Wijk, A. J., J. Larralde, C. W. Lovell, and W. F. Chen, "Pumping Prediction Model for Highway Concrete Pavements," American Society of Civil Engineers, Journal of Transportation Engineering, Volume 115, Number 2, March 1989.
35. van Wijk, A. J., "Purdue Economic Analysis of Rehabilitation and Design Alternatives for Rigid Pavements: A User's Manual for PEARDARP," Federal Highway Administration, FHWA Contract No. DTFH61-82-C-00035, Final Report, September 1985.
36. Darter, M. I., J. M. Becker, M. B. Snyder, and R. E. Smith, "Portland Cement Concrete Pavement Evaluation System—COPEs," National Cooperative Highway Research Program, Report No. 277, September 1985.
37. Heinrichs, K. W., M. J. Liu, M. I. Darter, S. H. Carpenter, and A. M. Ioannides, "Rigid Pavement Analysis and Design," Federal Highway Administration, FHWA-RD-88-068, July 1989.
38. Ioannides, A. M., M. R. Thompson, and E. J. Barenberg, "Westergaard Solutions Reconsidered," Transportation Research Record 1043, Transportation Research Board, 1985.
39. "Technical Guide Paper on Subsurface Pavement Drainage," Technical Paper 90-01, Federal Highway Administration, October 1990.
40. "Highway Design Manual of Instructions," Fourth Edition, California Department of Transportation, January 1987.
41. Won, M., McCullough, B. F., and W. R. Hudson, "Evaluation of Proposed Texas SDHPT Design Standards for CRCP," Research Report Number 472-1, University of Texas Center for Transportation Research, April 1988.
42. Tayabji, S. D., C. G. Ball, and P. A. Okamoto, "Effect of Concrete Shoulders on Concrete Pavement Performance," Transportation Research Board, Transportation Research Record 954, 1984.

43. Ray, G. K., "Concrete Shoulders and Lane Widening—Structural Benefits and Improved Pavement Performance," paper presented to the 1985 Missouri/Kansas PCC Paving Workshop, Kansas City, Missouri, November 5, 1985.
44. "Concrete Pavement Joints," Draft Technical Advisory, Federal Highway Administration, 1990.
45. Zoller, T., J. Williams, and D. Frentress, "Pavement Rehabilitation in an Urban Environment: Minnesota Repair Standards Rehabilitate Twin Cities Freeways," Proceedings, Fourth International Conference on Concrete Pavement Design and Rehabilitation, Purdue University, April 18-20, 1989.
46. "Pavement Rehabilitation Manual," FHWA-ED-88-025, Federal Highway Administration, September 1985 (supplemented April 1986, July 1987, March 1988, February 1989, and October 1990).
47. Darter, M. I., S. H. Carpenter, K. T. Hall, M. B. Snyder, R. E. Smith, A. L. Mueller, K. D. Smith, M. Herrin, R. P. Elliott, R. J. Roman, W. E. Poston, B. J. Dempsey, E. J. Barenberg, D. J. Janssen, and S. M. Stoffels, "Techniques for Pavement Rehabilitation," FHWA-HI-90-022, Federal Highway Administration/National Highway Institute, October 1987.